

Universidade de Lisboa  
Faculdade de Farmácia



**Continuous feeding and mixing in continuous  
tablet manufacturing: measuring system  
responses to parameter and material changes  
and implementation of NIR sphere**

André João Nascimento Canas

Dissertation to obtain the Master of Science Degree in  
**Pharmaceutical Engineering**

Work supervised by:

Professor João Almeida Lopes (Supervisor)

Professor Ossi Korhonen (Co-Supervisor)

2016

Universidade de Lisboa

Faculdade de Farmácia



**Continuous feeding and mixing in continuous  
tablet manufacturing: measuring system  
responses to parameter and material changes  
and implementation of NIR sphere**

André João Nascimento Canas

Dissertation to obtain the Master of Science Degree in  
**Pharmaceutical Engineering**

Work supervised by:

Professor João Almeida Lopes (Supervisor)

Professor Ossi Korhonen (Co-Supervisor)

2016

The experimental work was performed in PROMIS continuous tablet manufacturing line (University of Eastern Finland, School of Pharmacy, Kuopio, Finland). All the facilities, equipments, materials and support were gently provided by



UNIVERSITY OF  
EASTERN FINLAND

## Abstract

Continuous manufacturing is an advantageous choice in many industries, including the pharmaceutical. Its main advantages are better controllability, and, for sufficiently large volumes, lower manufacturing costs by decreased footprint and labor. Since the inception of the process analytical technology initiative (PAT), and more recently, the quality-by-design (QbD) initiative, significant efforts in designing new manufacturing strategies for the pharma industry are underway.

Continuous mixing is important in many processes in pharmaceutical manufacturing, including some obvious ones such as API and lubricant mixing, and some less apparent, such as wet granulation, coating, extrusion, and drying, where mixing often plays a critical role.

In this study, NIR spectroscopy is used to further understand a novel continuous mixing process. This new method is used to monitor the concentration of paracetamol blends that range from 30 to 70% (w/w). An experimental design was performed to define a set of runs in order to identify the critical process parameters and evaluate their impact on the critical quality attributes such as the homogeneity of the powder blend produced in the in-line mixer. The in-line mixer used was the Hosokawa Modulomix. The mixing process was monitored by an near infrared spectral camera aided by an integration sphere with an innovative design, attached to the mixer's outlet port.

The process parameters evaluated and their respective range were: mixer speed (300-1500 rpm), total feed rate (5-15 kg/h), inlet port (A or B) and excipient type (dibasic calcium phosphate or paracetamol). All process variables were kept constant throughout the experiments, and whilst maintaining the total feed rate constant, step changes to the paracetamol concentration were introduced at different time points. These were meant to stimulate the system and allowed for monitoring of system mixing performance with alternating setpoints for a wide range of settings, and for determination of the mixer's mean residence time.

The NIR spectral camera was able to operate, through the integration sphere's innovative design, with multi-point signal acquisition for a good representative analysis of the flowing powder. The mixer speed was revealed to be the most important critical process parameter. Mixture performance was determined via the powder blend's relative standard deviation (RSD), and results revealed that powder homogeneity was very good under all experimental conditions, having the RSD values always remained under 5% RSD.

**Key words: Chemometrics; Continuous manufacturing; Continuous mixing; Near-infrared spectroscopy; Powder blending**

## Resumo

A produção contínua tem sido frequentemente adotada em muitas indústrias, incluindo a química, alimentar, micro-eletrónica, entre outras. As suas principais vantagens são um maior controlo, e para volumes suficientemente grandes, menores custos de fabrico através de menor necessidade em mão de obra e possibilidade de uso de equipamento de menores dimensões. A indústria farmacêutica contudo, devido à natureza rígida da sua estrutura regulamentar, tem permanecido focada em larga medida no método de produção por “lote”.

Não obstante, desde a iniciativa de tecnologia analítica de processo lançada pela Food and Drug Administration, e mais recentemente, da iniciativa Quality-by-design, (que visam não só o desenvolvimento integrado do produto desde a sua conceção até a sua entrada no mercado mas também a otimização de recursos, matérias primas e instalações), que esforços significativos têm sido levados a cabo de forma a desenvolver novas estratégias de produção.

A produção contínua de formas farmacêuticas sólidas de dose individual tem pois, como um dos seus objetivos, melhorar a qualidade do medicamento a partir da origem, reduzindo o seu custo de fabrico, e ao mesmo tempo permitir aos doentes o acesso a medicamentos mais seguros. Para isso, realizam-se delineamentos experimentais para perceber de que forma os parâmetros do processo influenciam as respostas do mesmo. As tecnologias analíticas de processo são ferramentas fundamentais de monitorização porque fornecem dados do produto e do processo em tempo real. Esses dados são utilizados em modelos de análise multivariada que por sua vez devolvem informação sobre o processo. Esses modelos são em grande medida, ferramentas que contribuem para a construção de mecanismos de controlo do próprio processo. Estes mecanismos de controlo garantem que perturbações no processo são corrigidas de forma a obter os atributos críticos de qualidade desejados conforme as especificações.

A produção contínua aplicada à produção farmacêutica secundária é atrativa visto que processos como compressão, compactação por rolos, e enchimento de cápsulas já são efetuados de forma contínua, enquanto que a mistura, granulação por via húmida, secagem e revestimento são efetuados em “lote”. Esta combinação de operações “lote” com operações contínuas torna-se frequentemente uma fonte de ineficiência. Para além disso, os processos contínuos podem ser aumentados em escala simplesmente por

extensão do tempo de operação, ao contrário dos processos tipo “lote”, que invariavelmente requerem um aumento de escala físico que muitas vezes não é fácil de fazer nem eficaz.

A produção contínua possui outras vantagens em relação à produção por “lote”, nomeadamente o tamanho de equipamento reduzido, menor inventário para o processo, menos manuseamento sólido como por exemplo o enchimento e esvaziamento de misturadores (reduzindo assim efeitos potencialmente indesejados como a segregação), um controlo mais preciso em torno de um estado estacionário bem definido, e uma maior uniformidade na aplicação de tensões de corte. Contudo, a produção contínua tem algumas limitações, como o custo inicial mais elevado, dificuldade de implementação para produtos com baixo volume de produção, e flexibilidade reduzida do processo. Apesar da produção contínua ter sido fortemente implementada na indústria química, o conhecimento relativamente à mistura de pós por via de processos contínuos ainda é limitado e relativamente poucos artigos têm sido publicados nesta área.

A mistura é uma operação unitária extremamente importante em muitos processos de produção farmacêutica, incluindo alguns bastante óbvios como a mistura de substâncias ativas e lubrificantes, e alguns menos aparentes, tais como a granulação por via húmida, revestimento, extrusão, e secagem, onde a mistura tem um papel crucial. O desenvolvimento de operações de mistura contínua requer uma avaliação de um amplo espaço paramétrico, que inclui a seleção e conceção dos equipamentos de mistura e alimentação, avaliação dos parâmetros de operação tais como velocidade de rotação das pás do misturador e taxa de alimentação, caracterização dos efeitos de propriedades físicas como distribuição do tamanho de partícula e coesão dos pós, e o controlo de variáveis ambientais tais como a temperatura e humidade relativa. Este grande número de variáveis, e as suas interações entre si, torna extremamente difícil a implementação do processo para uma nova entidade sem estudos detalhados. Tendo tudo isto em conta, a identificação de parâmetros críticos de processo é um passo essencial em direcção à implementação da produção contínua.

O processo de mistura em contínuo inicia-se pelo enchimento e calibração dos alimentadores que irão debitar as matérias primas em pó a serem misturadas. Estes alimentadores estão assentes em balanças extremamente sensíveis que pesam continuamente a quantidade de massa de pó existente dentro da tremonha, tendo um modo gravimétrico como princípio de funcionamento. O sensor gravimétrico das

balanças regula assim automaticamente o débito com que os pós são alimentados para o misturador. Com o misturador ligado as partículas de pó ao entrarem no misturador cilíndrico pela porta de alimentação sofrem agitação pelas pás fixas ao rotor que se encontra no eixo central do misturador. Estas pás podem ter várias configurações e orientações e portanto originam diversos tipos de fluxos de matéria dentro do misturador. Ao atingir a porta de descarga do misturador a mistura de pós homogênea é libertada para um recipiente ou para um transportador para a próxima operação unitária.

Este trabalho experimental foi realizado utilizando a linha de produção contínua de comprimidos do PROMIS Centre, na University of Eastern Finland, School of Pharmacy, em Kuopio, na Finlândia. Neste trabalho, recorreu-se a alimentadores gravimétricos (K-Tron K-ML-D5-KT20) de duplo parafuso e a um misturador contínuo (Hosokawa Modulomix). O processo de mistura consistia em homogeneizar uma mistura de pós composta pelo princípio ativo (paracetamol) e um excipiente (fosfato de cálcio ou celulose microcristalina). A monitorização do processo foi seguida em tempo real por um sistema de infravermelhos próximos com uma câmara espectral SPECIM e um sensor ImSpector (SPECIM, Finland). Este sistema encontra-se associado a um acessório inovador que permitiu a aquisição de seis sinais simultâneos em locais diferentes da zona de amostragem de forma a melhor representar o fluxo de pó que saia do misturador. Este acessório denominado de “esfera de integração” utiliza seis fibras óticas para recolher informação do fluxo de pó e foi desenhado especialmente para este processo.

A relação entre os possíveis parâmetros de processo e os atributos de qualidade da mistura de pós foi estabelecida através de ensaios definidos de acordo com um delineamento experimental fazendo variar: a velocidade do misturador de 300 rpm a 1500 rpm; a taxa de alimentação total entre 5 kg/h e 15 kg/h; a porta de alimentação (A e B) e dois excipientes (fosfato de cálcio e celulose microcristalina). Considerou-se o desvio padrão relativo entre o teor de paracetamol nas amostras determinado com UV-Vis e o teor de paracetamol calculado a partir dos dados de registo dos alimentadores, como atributo de qualidade.

A análise de componentes principais foi usada como método de análise exploratória dos espectros obtidos assim como para identificar medições atípicas.



Todas variáveis do processo foram mantidas constantes ao longo das experiências. Apesar da taxa de alimentação total ter sido mantida constante ao longo das experiências, a taxa de alimentação do paracetamol e do excipiente foi variada sob forma de níveis de concentração (40%, 50%, 60% e 70%) . Estas variações tiveram como objetivo estimular o sistema, observar a sua resposta e monitorizar de que forma isso afetava a homogeneidade da mistura resultante nesses instantes.

A câmara espectral de infravermelho próximo operou através da esfera de integração, com aquisição de sinal em múltiplos pontos de forma a obter uma análise representativa do fluxo de pós. Isto permitiu que os modelos de análise de componentes principais identificassem claramente as perturbações aos níveis de concentração das matérias primas causadas no sistema, e detetar o tempo necessário para que o processo atingisse o estado estacionário. Os modelos baseados nos espetros obtidos foram capazes de capturar as concentrações de paracetamol e excipiente ao longo do tempo. Estes resultados foram confirmados através de análise por resolução multivariada de curvas onde foi possível quantificar de forma precisa os teores de substância ativa e excipiente (no caso da celulose microcristalina) impondo os espetros dos compostos puros. Verificou-se também que após cerca de três minutos do início das experiências, o sistema atingia o estado estacionário.

O sistema revelou óptimo desempenho de mistura, pois os valores do desvio padrão relativo revelaram ser inferiores a 5% em todas as experiências independentemente das definições do processo. Os modelos de regressão entre os parâmetros do processo e os atributos de qualidade indicaram que a velocidade do misturador era o parâmetro crítico de processo mais relevante.

***Palavras-chave: Espectroscopia de infravermelho próximo; Mistura contínua; Produção contínua; Quimiometria; Tecnologia analítica de processo.***

## Acknowledgements

I would very much like to thank Prof. Ossi Korhonen, for the mentorship, patience and clarity with which he supervised my work. That, along with all his patience and great personality, made the experience of doing my internship abroad much more pleasant and enriching. Also a word of appreciation and thanks to Prof. Jarkko Ketolainen for the opportunity of being able to do my internship at the School of Pharmacy, University of Eastern Finland.

I would like to thank Anssi-Pekka Karttunen for being an excellent colleague and also tutor, for his dedication to our work and for the good mood we were able to share while doing the experimental work. Thanks for all the support.

I am very grateful to Prof. João Almeida Lopes for also allowing me the opportunity to develop my experimental work at University of Eastern Finland. I would also like to thank him for giving me tireless support during the writing of this thesis, and for all I have learned from him, in and out of the classroom.

A very special thanks to Rute Dias, for embarking in this journey with me since the beginning. Thank you for all your friendship and support, this would not have been possible without it.

I would also like to acknowledge my friends Sara Ramos, Pedro Januário, Marisa Lopes, Valter Marques, Eloísa Silva, Joana Valadas and Gonçalo Grazina for the constant support and continuous encouragement throughout this internship.

Last but not the least, I would like to thank my parents and my family for the unconditional support and encouragement throughout my years of study and through the process of researching and writing this thesis.

This accomplishment would not have been possible without any of them. Thank you.

# Contents

Abstract .....	i
Resumo .....	iii
List of Figures .....	ix
List of Tables.....	xii
List of Abbreviations.....	xiii
Chapter 1.....	1
Motivation .....	1
Chapter 2.....	2
Objectives.....	2
Chapter 3.....	3
Introduction .....	3
3.1 Continuous manufacturing .....	5
3.2 Continuous mixing.....	7
3.3 Monitoring of continuous mixing with near-infrared spectroscopy .....	10
3.4 Continuous manufacturing line.....	12
Chapter 4.....	16
Materials and methods .....	16
4.1 Raw-materials .....	16
4.2 Equipment .....	22
4.3 Methods .....	32
Chapter 5.....	39
Results and discussion.....	39
5.1 Exploratory data analysis .....	39
5.2 Residence time distribution calculation.....	52
5.3 UV-Vis measurements.....	54
5.4 System variables influence over response parameters.....	62
Chapter 6.....	66
Conclusions.....	66
Future Perspectives .....	68

References.....69

## List of Figures

Figure 1 - Full line configuration schematic (adapted from (25)).....12

Figure 2 - "Rat-hole" example.....13

Figure 3 - Labview control software interface. On the left: monitoring of the powder mixture. On the right: monitoring of the compaction force.....14

Figure 4 – Full production line .....15

Figure 5 - Dibasic calcium phosphate molecular structure.....16

Figure 6 - Spectrum of EMCOMPRESS in the NIR region encompassing the region 1000–2500 nm .....17

Figure 7 - MCC molecular structure.....18

Figure 8 - Spectrum of EMCOCEL 90M in the NIR region encompassing the region 1000–2500 nm .....19

Figure 9 - Molecular structure of paracetamol .....20

Figure 10 - Spectrum of Paracetamol in the NIR region encompassing the region or 1000–2500 nm .....21

Figure 11 - Experimental configuration setup.....22

Figure 12 - K-Tron LIW powder feeders.....23

Figure 13 - Gain-in-weight versus loss-in-weight batching schematic (adapted from (57)) .....24

Figure 14 - Loss-in-weight powder feeder schematic (adapted from (58)) .....25

Figure 15 - Modulomix in-line mixer with inlet ports A and B, and outlet port C.26

Figure 16 - Modulomix in-line mixer. On the left: With the side panel removed, exposing the mixing chamber. On the right: Before cleaning with the external casing removed .....27

Figure 17 - Example of Modulomix cascade setup (adapted from (59)) .....28

Figure 18 - Belt conveyor .....29

Figure 19 - NIR spectral camera. On the left: fiber receiving and merging accessory. On the upper right: profile of the cased camera. On the lower right: profile of the camera with no casing. ....30

Figure 20 - The integration sphere.....31

Figure 21 - Shimadzu UV-1800 spectrophotometer.....31

Figure 22 - Paracetamol step changes along the duration of each experimental run.....34

Figure 23 - Raw NIR spectra obtained for run N6 .....39

Figure 24 - Pre-processed NIR spectra for run N6.....40

Figure 25 - Score plot for the PCA model obtained from run N6 spectra. ....41

Figure 26 - Q residuals vs Hotelling  $T^2$  from a PCA model from run N6 spectra .....41

Figure 27 - Evolution of the first PC over time for run N6.....42

Figure 28 - Raw and preprocessed (first derivative) NIR spectra of paracetamol. ....43

Figure 29 - Preprocessed (first derivative) and PCA PC1 loadings NIR spectra of paracetamol .....	43
Figure 30 - Raw and preprocessed (first derivative) NIR spectra of MCC.....	44
Figure 31 - Preprocessed (first derivative) and PCA PC2 loadings NIR spectra of MCC.....	44
Figure 32 – Preprocessed (first derivative) paracetamol and MCC NIR spectra. ....	45
Figure 33 - Scores (first and second component) obtained from the MCR model for the eight runs containing MCC. ....	46
Figure 34 - Corrected scores (first and second component) obtained from the MCR model for the eight runs containing MCC.....	48
Figure 35 - Overlay of the first component profiles obtained for the PCA (blue) and MCR (orange) models for experiment N6. ....	48
Figure 36 - Overlay of the first component profiles obtained for the PCA (blue) and MCR (orange) models for experiment N12. ....	49
Figure 37 - Overlay of the first component profiles obtained for the PCA (blue) and MCR (orange) models for experiment N13. ....	49
Figure 38 - Overlay of the first component profiles obtained for the PCA (blue) and MCR (orange) models for experiment N14. ....	50
Figure 39 - DCP and paracetamol raw NIR spectra encompassing the region 1000–2500 nm .....	51
Figure 40 - Weibull Sigmoid function fitting for the 50% to 60% step change for experiment N6.....	52
Figure 41 – Function E(t) representing the residence time distribution for experiment N6.....	53
Figure 42 - UV-Vis Calibration Curve .....	55
Figure 43 – Overlay of paracetamol feeder setpoint, real fed paracetamol concentration and UV-Vis measured results for experiment N1.....	56
Figure 44 - Overlay of paracetamol feeder setpoint, real fed paracetamol concentration and UV-Vis measured results for experiment N2.....	56
Figure 45 - Overlay of paracetamol feeder setpoint, real fed paracetamol concentration and UV-Vis measured results for experiment N3.....	56
Figure 46 - Overlay of paracetamol feeder setpoint, real fed paracetamol concentration and UV-Vis measured results for experiment N4.....	57
Figure 47 - Overlay of paracetamol feeder setpoint, real fed paracetamol concentration and UV-Vis measured results for experiment N5.....	57
Figure 48 - Overlay of paracetamol feeder setpoint, real fed paracetamol concentration and UV-Vis measured results for experiment N6.....	57
Figure 49 - Overlay of paracetamol feeder setpoint, real fed paracetamol concentration and UV-Vis measured results for experiment N7.....	58
Figure 50 - Overlay of paracetamol feeder setpoint, real fed paracetamol concentration and UV-Vis measured results for experiment N8.....	58
Figure 51 - Overlay of paracetamol feeder setpoint, real fed paracetamol concentration and UV-Vis measured results for experiment N9.....	58
Figure 52 - Overlay of paracetamol feeder setpoint, real fed paracetamol concentration and UV-Vis measured results for experiment N10 .....	59
Figure 53 - Overlay of paracetamol feeder setpoint, real fed paracetamol concentration and UV-Vis measured results for experiment N11 .....	59

Figure 54 - Overlay of paracetamol feeder setpoint, real fed paracetamol concentration and UV-Vis measured results for experiment N12 .....	59
Figure 55 - Overlay of paracetamol feeder setpoint, real fed paracetamol concentration and UV-Vis measured results for experiment N13 .....	60
Figure 56 - Overlay of paracetamol feeder setpoint, real fed paracetamol concentration and UV-Vis measured results for experiment N14 .....	60
Figure 57 - RSD according to experiment number and concentration step.....	61
Figure 58 - Regression coefficients for the bulk residence time model developed including error bars for assessing coefficients significance. ....	63
Figure 59 - Regression coefficients for the mass hold at the end of the run model developed including error bars for assessing coefficients significance.....	63
Figure 60 - Regression coefficients for the mass hold at 180s model developed including error bars for assessing coefficients significance. ....	64
Figure 61 - Regression coefficients for the relative standard deviation developed model including error bars for assessing coefficients significance.....	65

## List of Tables

Table 1 - Complete continuous line equipment description .....	14
Table 2 - Experimental design used to define the runs' conditions according to four process parameters.....	32
Table 3 - LIW feeders step changes.....	33
Table 4 - Mass hold and residence time for the produced experiments. ....	53
Table 5 - UV-Vis calibration curve measurement results .....	54
Table 6 - Relative standard deviation between UV-Vis results and feeder registry data.....	61
Table 7 – Data introduced into the Modde worksheet to build the PLS models. The input variables were: feed rate, mixer speed, port and excipient; and the responses were: bulk residence time, mass hold at the end of run, mass hold at 180s and RSD. ....	62

## List of Abbreviations

API, Active Pharmaceutical Ingredient

BRT, Bulk Residence Time

CM, Continuous Manufacturing

CMP, Critical Material Properties

CPP, Critical Process Parameters

CQA, Critical Quality Attributes

DoE, Design of Experiment

FDA, Food and Drug Administration

NIR, Near-Infrared

NIRS, Near-Infrared Spectroscopy

PC 1, Principal Component 1

PC 2, Principal Component 2

PCA, Principal Component Analysis

PAT, Process Analytical Technology

PLS, Partial Least Square

PSD, Particle Size Distribution

QbD, Quality by Design

RSD, Relative Standard Deviation

RTD, Residence Time Distribution

Sav-Gol, Savitzky-Golay



# Chapter 1

## Motivation

The ongoing paradigm shift in the pharmaceutical industry with the introduction of new legislation and guidelines supporting continuous manufacturing, represents a huge opportunity for process optimization, lower manufacturing costs, and higher quality products.

The push for continuous manufacturing has focused on solid dosage forms. A continuous manufacturing line built to produce tablets with real time release has been one of the most sought after objectives. Mixing, being the first unit operation of a continuous tableting line, is involved in the production of several pharmaceutical dosage forms (e.g., tablets, granules, powders), and represents a critical operation to the process.

The CM approach for the manufacturing of drug products lays on top of the quality-by-design (QbD) principles, which demand the implementation of process understanding methodologies and require full adoption of process analytical technologies (PAT). In this context, the widely adopted near-infrared spectroscopy method, as a PAT tool, enables real-time monitoring of the process, feeding process models with frequent and high quality data.

Statistical models can be adjusted to deal with these data to monitor and to estimate in real-time drug product properties. Thus, this work aims at providing knowledge on powder blending as a continuous process, to support its future implementation in the pharmaceutical industry.

The experimental work was performed in the research and development continuous tableting line (PROMIS-line), constructed at the School of Pharmacy of the University of Eastern Finland.

## Chapter 2

### Objectives

This written thesis is the result of the experimental work performed in the PROMIS-line (School of Pharmacy of the University of Eastern Finland).

The main objectives of this work are to gain knowledge on how to operate the feeding and blending equipment part of the continuous production line, and to study and monitor the following mixing process parameters:

- Total feed rate (ranging from 5 kg/h to 15 kg/h).
- Composition/formulation ratio
- Mixer speed
- Mixing residence time

Capture real-time near-infrared spectra of the output blend in order to:

- implement a process analytical method to monitor in real-time the quality of the blend after the continuous in-line mixer;
- better understand the design and technical characteristics of a newly developed near infrared probe including an integration sphere and several monitoring ports;
- assess blend homogeneity from a spectral time series.

## Chapter 3

### Introduction

Pharmaceutical companies, during their product development process, undergo long and expensive research efforts with the objective of optimizing and understanding the production of homogeneous powder blends. These solid mixtures, comprised of several substances including active pharmaceutical ingredients (API) and excipients (like lubricants and diluents), constitute the base material for several pharmaceutical unitary operations and pharmaceutical forms. Minimizing variability in solid mixtures is essential to the pharmaceutical industry, because mixture uniformity has direct impact on the performance and quality of the product. Bearing that in mind, it becomes clear that when significant divergence from the desired mixing performance happens, it generally leads to batch rejection, triggers costly process investigations, and corrective actions are often required to maintain regulatory compliance (1).

Although some strides and efforts have been made in the field recently, powder flow and powder mixing are processes that are far from being well understood. It is not uncommon for powder mixing processes to be designed ad-hoc, with little experimental data available to support them. The need to further understand blending processes has thus become a priority for regulatory bodies in the last 15 years, and rightfully remains the central focus point of quality-by-design (QbD) and process analytical technology (PAT) efforts.

Over the last decade, the International Conference on Harmonization (ICH) and the Food and Drug Administration (FDA) have issued a series of guidelines for drug manufacturing. In the ICH Guidelines Q7, Q8, Q9, Q10 and Q11 and FDA Guidance for Industry — PAT in which the FDA has published their current thinking on using QbD methods to identify critical quality attributes (CQA), and state the need for a systematic approach to process development through the implementation of engineering modeling and optimization techniques.(2)(3)(4) This will allow the manufacturing of safe and effective products with their quality built into the process.(5) This philosophy of QbD has been applied in other industries to reliably create products with the desired quality attributes. Quality is assured through the development of reliable and robust processes, designed based on the knowledge of process principles.(4) The transition from batch to continuous pharmaceutical operations can facilitate the development of processes within the QbD framework. Continuous processing allows real-time control, lesser need for scale-up studies and can help to reduce product variability.(6)

The pharmaceutical regulatory environment has recognized that in CM processes the major challenges are the coordination of equipment input/output properties, and the formulation of predictive process control strategies. In order to achieve equipment coordination and predictive capabilities, the relationships between critical quality attributes (CQA), critical material properties (CMP) and critical process parameters (CPP) need to be correlated sequentially between the multiple unit operations in product manufacturing, through the use of mathematical models characterizing individual unit operation performance as a function of CPPs (e.g., screw speed, residence time) and CMPs (e.g., particle size distribution).(4) In addition, multi-unit processes can be characterized with respect to the temporal-space location of particles in the system.(7)

These guidelines are intended to motivate manufacturers to enhance their processes for better quality, apply CM to drugs and to gain a deeper insight in pharmaceutical manufacturing processes, replacing empirical approaches by knowledge-based procedures.

The objective of “building in quality” requires a very fine comprehension of the key parameters of a process, and in order to avoid having to “test into the final product” it is vital to understand their impact on the product quality. With this in mind, PAT needs to be understood in a much broader sense: in addition to the implementation of sensors for real-time measurement of CPP, understanding of the process based on mathematical models is essential to guarantee and control product quality.(3) PAT requires, based on mechanistic process understanding, the:

- (1) identification of the key parameters;
- (2) continuous and real-time measurement of the selected parameters and
- (3) development of a control strategy based on the relevant multivariate real-time measurements

Before developing process control models, it is also important to consider environmental data and information regarding raw materials. For powder-blending processes the ultimate goal is to obtain a uniform blend with a blend quality close to optimal (in typical applications the relative standard deviation (RSD) should be below 5%). Today, powder homogeneity is obtained through predetermined and established processes, i.e., a constant fill level and a fixed mixing time. This approach, remains as the standard in current pharmaceutical manufacturing, and does not compensate for variability of the raw material's specifications such as particle size or crystallinity, which may significantly

affect segregation behavior and mixture quality, or the environmental conditions, such as temperature and moisture. Of even greater importance is the fact that since blender performance and mixing kinetics are unpredictable when switching between different mixer types, it becomes impossible to scale-up in a reliable way. This has led to a growing interest and study of this field by the scientific community in recent years, with the goal of exploring and comprehending the fine details of particle and powder mixing, using both experimental (8)(9) and computational approaches.(10–15)

Interestingly, continuous processing has been utilized extensively by petrochemical, food, and chemical manufacturing but has yet to reach the pharmaceutical industry to a meaningful extent. Recent research efforts indicate that a well controlled continuous mixing process illustrates the capability of scale-up and ability to integrate on-line control ultimately enhancing productivity significantly.(16,17)

The FDA's PAT initiative has encouraged the development of new technology to improve upon the current manufacturing paradigm.(3) As a result, substantial attention has recently focused on continuous processing due to the ability to control disturbances online, avoiding the loss of processing materials and enabling effective process scale-up.

### **3.1 Continuous manufacturing**

Continuous processing has numerous known advantages, over the past few years, CM of solid dose pharmaceutical products has been an area of high interest. CM can be defined as a process where starting materials are manufactured into the final product as a constant flow with an integrated set of equipment, and equipment is controlled to produce required product quality. The scale of continuous production is defined by time rather than dimension of equipment as in batch production.(18) Some pharmaceutical equipments operate inherently continuously, like tableting machines and roller compactors. Others, such as wet granulators and coaters, have to be modified for continuous production. A typical continuous process for pharmaceutical manufacturing consists of unit operations such as powder feeding, blending, granulation, compaction and capsule filling. Powder transfer between unit operations can be performed with the aid of gravity or conveyers. In vertical configuration, pieces of equipment are placed on top of each other and powder is transferred between unit operations by gravity. This configuration requires a footprint of only a few square meters, but the height of the room has to be two to three stories high. In horizontal configuration, continuous line can fit in

normal room height but conveyers (pneumatic or screw) are required to transfer powder between unit operations. Feeding and blending are among the most critical parts in the manufacturing process, affecting directly the homogeneity of the powder mixture and thus the uniformity of the end product. For this reason, feeding accuracy and monitoring as well as ensuring proper blender settings are essential.(17)(19–23)

In a continuous process, monitoring and ensuring blend uniformity in real time at the blender discharge point is critical. Unlike batch manufacturing, it is difficult to rework a blend in a CM scenario. Nevertheless it has numerous known advantages, including reduced cost, increased capacity, facilitated scale up, mitigated segregation, and more easily applied and controlled shear.(24) To set up continuous line into operation, the primary task is to synchronize the yield of each piece of equipment in regard to mass balance. If the line is not balanced adequately, material can start accumulating at a point of operation, or a unit of operation can run out of material if it functions at a faster rate than the previous unit. Thus, reliable mass flowmeters are of great importance. Process monitoring and process controls are integral parts of CM.(25) Another important aspect is the understanding of process disturbances and how they are dampened or accumulated in subsequent unit operations. A key parameter for that is the residence time distribution (RTD) of each piece of equipment.

The residence time is a critical equipment and process parameter that characterizes the period of time a particle stays in one or more unit operations in a continuous system. The RTD is defined as the probability of particles exiting the equipment at a given time period based on the flow patterns inside of the unit.(26) Mathematical models for the RTD have previously been developed for chemical engineering applications in order to characterize the influence of operating conditions, material properties and unit geometry on the degree of non-ideal behavior (i.e., back-mixing). Pharmaceutical unit operations for which the RTD has been experimentally studied include feeding, blending, and granulation processes.(27) RTD can be used to characterize the propagation of transient disturbances across sequential unit operations in flowsheet simulations. The RTD can provide traceability along the continuous line and delineate continuous products based on the feed strategy. Manufactured products created using different batches of starting material can be traced in order to comply with process validation. This will facilitate the prediction and rejection of out-of-spec products by tracing disturbances along the process. Overall, RTD models can add significant value to the transition from batch to continuous operations by providing reliable predictive tool for behavior of unit operations based on their residence time.(27)

In manufacturing processes involving large capacities, continuous processing is considered a viable choice although the pharmaceutical industry has so far relied on batch manufacturing. CM offers several advantages over batch manufacturing as: smaller footprint of manufacturing sites, no or limited scale-up, better process understanding with PAT, higher quality of products with the aid of PAT and faster production to market time.(28) The biggest gain for the pharmaceutical industry is that while batch processes are dependent on time and do not scale-up well, continuous processes only need an extension of time to scale up, and the same equipment can be used for the production of phases I–III clinical products (short runs) and final production (continuous run) (29). This eliminates problems related to site and equipment change. A second advantage is the reduction of waste as optimized continuous processes can operate in a much more efficient way than batch and are easy to control. When looking at CM with an integral perspective we see that these advantages ultimately decrease production costs and increase the quality of pharmaceutical products.(30) The advantages of CM cannot be realized without overcoming several challenges prior to its adoption in the pharmaceutical industry.(29) And continuous mixing is one of the most important.

## **3.2 Continuous mixing**

Among emerging technologies for improving the performance of blending operations, continuous mixing (as continuous processing in general) currently commands enormous interest at pharmaceutical companies. However, development of a continuous powder blending process requires venturing into a process that has a large and unfamiliar parametric space. While continuous blending processes have been used in other industries, in general such applications operate at much larger flow rates and have less demanding homogeneity requirements than typical pharmaceutical applications.(31)

Powder mixing is widely used in pharmaceutical, cosmetic, chemical, cement, food, agricultural, and other industries in which product mixtures need to satisfy typical performance criteria. It is a process in which two or more than two solid substances are intermingled in a mixer by continuous movement of the particles. Mainly, the object of mixing operation is to produce a bulk mixture which when divided into different doses, every unit of dose must contain the correct proportion of each ingredient. The degree of mixing will increase with the length of time for which mixing is done.(31) The pharmaceutical industry, mainly produces tablets, capsules or packets that are usually mixtures of 5 to 15 ingredients, and which may contain several API. Standards have

been developed to estimate the quality of the mixtures with respect to each of the actives and thus authorise the release of the products on the market.

The process is complex as it depends on many factors operating at various scales: single particle properties, bulk particle properties, general mixer design and operation, combination of operating conditions, mixture formulation, etc. In batch mixture operation, all ingredients are loaded into the mixer together or in a pre-defined sequence, and mixed until a homogenous material is produced and discharged from the mixer in a single lot. The output of a batch mixer is measured in kg/batch. The continuous mixer on the other hand is generally dedicated to a single high volume product. Ingredients are continuously charged into the mixer in accordance with the formulation. The mixing takes place as the material travels from the charging port to the discharge nozzle, from where it is continuously discharged. The output of a continuous mixer is measured in kg/h.

Experimental work in continuous mixing published so far has focused on operating conditions such as rotation rate, mixer inclination angle, and flow rate.(21) While several types of continuous mixers have been built, and many more can easily be conceived, only a few geometric designs have been examined in the literature.(32) However, many more conditions remain to be examined, and for many interesting designs, performance has never been quantitatively examined in the literature.

Studies have been mainly focused on the influence of operating conditions (feed rate, impeller speed, etc.) and geometric designs (mixer size, impeller types, etc.) on the efficiency and throughput of mixers.(19) The performance of several continuous mixers has been investigated for materials with different flow properties.(33) The effects of different types of stirrer on the hold-up and quality of mixtures have been examined.(34) The quality of a mixture, which may be the degree of homogeneity of loose material at the outlet of a mixer, is important for end-user properties as perceived by customers or for in-process properties used by manufacturers for normative procedures. In addition, mixing process optimisation is a matter of reducing mixing time and saving energy, especially for low added-value products.

Chemical and process engineers working with powders are currently faced with problems associated with mixture quality. There is a need to overcome such difficult barriers as sampling, use more or less advanced statistical analysis, cope with different standards and practices, but also understand a wide range of available technologies. Most of the time, when considering the insertion of a new mixer in an existing process, costly pilot or full scale tests need to be performed. As a consequence, the general tendency in the industry is to avoid any change, and to concentrate on the way to validate the actual process. This is illustrated by a certain elasticity in sampling recommendations and practices.(35,36)



In the pharmaceutical industry, the above general picture is magnified. This is especially due to traceability needs and quality insurance that requires step-by-step validation, unit operation by unit operation. It also means that a single change in a single operation requires resetting the validation of the following steps, and sometimes of the previous ones. Furthermore, since reprocessing is generally not allowed in such processes, if a mixture is found to be inhomogeneous, the whole related production must be destroyed. Even if there is clearly no problem of product contamination by an external source, it is not permitted to mix the powders again. That of course increases the prices of products and indirectly induces a social cost.

Basic advantages of continuous mixers with respect to batch mixers are currently: Lower size of the mixing vessel for a same production level; less segregation risk due to the absence of handling operations, such as filling and emptying; lower running costs; better definition of mixture homogeneity, at the outlet of the apparatus.

In the pharmaceutical context, it is even possible to add and emphasize:

- The possibility to include an on-line analysis set-up at the outlet of the mixer to measure the quality of the mixtures, but also to implement process control. This point is exactly in the direct line of the PAT recommendations.
- The fact that practically all the final steps, such as tableting and conditioning, in a drug fabrication scheme are already continuous operations.
- The elimination of scale-up problems during process development.

This last point is undoubtedly a very serious advantage for continuous mixers enhanced by the PAT initiative from the FDA. The qualification of a full-scale pharmaceutical “batch” during process development is actually done at a scale of one-tenth of the industrial scale. This means that if one wants to produce 100 kg at industrial scale in a batch mixer, the validation can be done with a mixer containing 10 kg of mixture. This is a serious problem as there is no guarantee that what has been proved with a 100L mixer will still hold good for a 1m<sup>3</sup> batch vessel. In contrast, continuous mixer qualification, will simply require a full-scale validation of, for example, 1h if the industrial production time of a certain product is 10h. The risk of error is undoubtedly much easier to estimate for a continuous process rather than for a batch process that has to “cross the scales”.

### 3.3 Monitoring of continuous mixing with near-infrared spectroscopy

Different spectroscopic methods, mostly NIR and Raman, are among the PAT [ methods recently introduced by the FDA for process monitoring and building predictive understanding of pharmaceutical manufacturing processes.(3)(37–41) Examples of PAT applied to powder blending processes are abundant in literature. They typically include NIR spectroscopy, Raman spectroscopy and laser induced fluorescence (LIF).(39,40,42) Also laser diffraction, image analysis and machine vision are used.(43) Preferably all of these PAT tools run in-line. NIR spectroscopy is currently one of the principal analytical techniques for monitoring pharmaceutical processes.(44)

The NIR spectral region extends from 780 to 2500nm, and NIR spectra consist of absorbance bands corresponding to overtone and combination of fundamental C–H, N–H, S–H and O–H molecular vibrations. NIR methods have been developed to monitor a number of pharmaceutical unit operations including granulation, drying and crystallization.(45–47) Both chemical and physical information are obtained from NIR spectra after properly processing following an adequate method of analysis. For process control, the first principle model-based controls are the most obvious choices, but also gray or black-box models are used due to the lack of first principle models. Continuous monitoring of blend uniformity is the first step towards implementing process control for continuous blending operations, or to facilitate rejection of out-of-specification powder from the manufacturing stream.

NIR spectroscopy has been applied extensively to batch pharmaceutical blending processes to identify the time at which a mixture is homogeneous and stopping the process. Most of the PAT work for blend uniformity monitoring exists for batch blending, which includes commonly used blenders such as the V-blender, the bin blender, the Y-mixer and the Nauta mixer.(41,48–50) Methods reported in the literature to monitor blend uniformity are mostly generic, and include quantitative methods such as a partial least squares (PLS) modeling, or qualitative methods such as principal component analysis (PCA) of the spectra acquired during the blending process, monitoring the pooled standard deviation between spectra, and monitoring the dissimilarity between the process spectra and spectrum of a uniform mixture or individual components. PAT for blending has been reported primarily as a tool for monitoring evolution of RSD during the blending process and for detecting blending end-point. The final blend uniformity measured using PAT methods and the blend uniformity measured using an off-line method are often not related, and the methods to link off-line and on-line blend uniformity measurements are not well established in literature. In order to directly relate the off-line

and on-line measurements, it is necessary to quantify the sample size being analyzed in the in-line measurements and relate that with the offline measurements. In the continuous blending process, powder is typically in a state of motion and, inherently, there is a certain degree of spectral averaging involved in the measurement. Blend uniformity, quantified by the relative standard deviation (RSD) between the in-line measurements, is dependent on the degree of averaging.

### 3.4 Continuous manufacturing line

The work presented in this thesis was performed at the University of Eastern Finland, School of Pharmacy's PROMIS-line. It used a continuous tableting line that is modular and can produce tablets via dry granulation or direct compression (Figure 1).

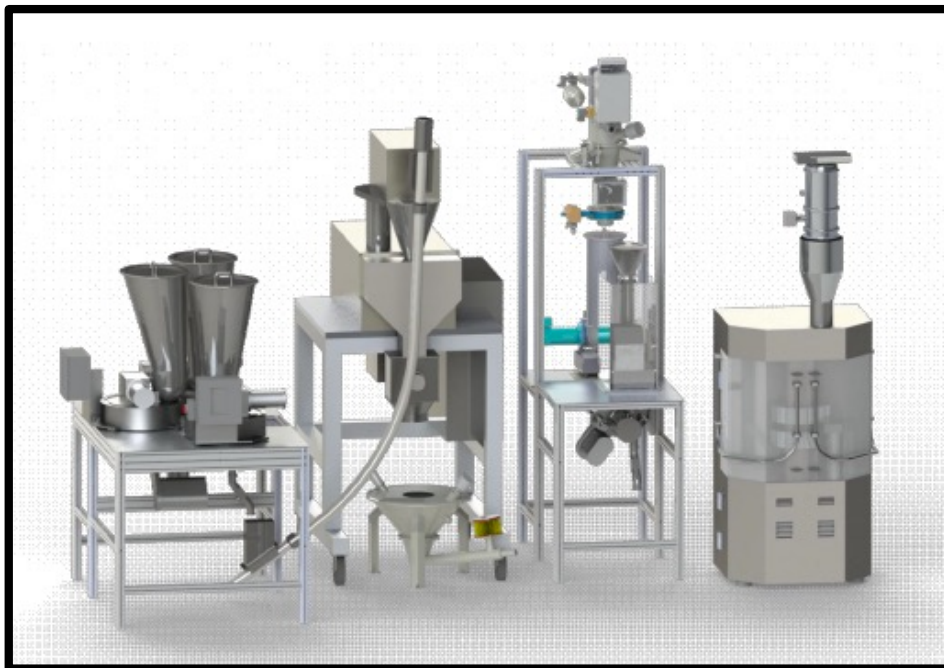


Figure 1 - Full line configuration schematic (adapted from (25))

Being a standard continuous tableting line, the PROMIS-line comprises a set of unit operations and equipment (Table 1) such as loss-in-weight or loss-in-volume feeders that weight and feed the powder substances (API and excipients) into the mixer. These feeders run at specific feed rates that are determined by the formulation specifications, and provide real time data via a computer regarding both the feed rate and the total mass still held inside the hopper. A few difficulties are observed at this stage when working with low feed rates and with cohesive materials. These type of conditions may frequently generate “rat-holes” (Figure 2) that occur when, due to the cohesive nature of the material a “dome” of air is created inside the hopper above the feeding screws, stopping the flow of powder at the feeder exit, affecting the overall performance of the line and limiting its throughput. Inserting a metal rod into the powder in the hopper normally caused the colapse of the “rat-hole”.



*Figure 2 - "Rat-hole" example*

Next the formulation components are blended inside the mixer resulting in a homogenous powder blend. These mixers are typically tubular blenders, consisting of a horizontal cylinder with a bladed shaft which rotates around a central axis. Powder is fed through the entrance port at one end of the mixer, and exits through another port on the other end. The impeller that rotates along the axis of the continuous mixer has the double purpose of both blending and transporting the material, thus an optimal amount of radial and axial movement of particles in the blender is required in order to achieve ideal mixing.

If the desired manufacturing process for tableting is direct compression, then the powder blend is directly fed to the tableting machine. If granulation is necessary prior to the tableting it can be performed via wet or dry granulation which can both be achieved continuously through modern equipment and roller compaction respectively. Of all the equipment in the line, the tableting machine holds the bottleneck being the equipment with the lowest throughput.

Table 1 - Complete continuous line equipment description

Equipment	Brand and manufacturer	Specifications (in continuous operation mode)
3 Loss-In-Weight powder feeders	K-Tron, K-ML-D5-KT20	500 g/h - 24 kg/h
Loss-In-Weight granule feeder	K-Tron, K-CL-24-KT24	300 g/h - 40 kg/h
Loss-In-Weight micro feeder	K-Tron, K-CL-SFS-MT12	32 g/h - 300 g/h
Two continuous blenders	Hosokawa, Modulomix	300 - 1450 rpm
Roller compactor	Hosokawa, Pharmapaktor L200/30P, with flake crusher FC 200	Screw speed: 0 - 53 rpm; Roll speed: 0 - 19 rpm; Roll pressure: 0 - 50 kN; Flake crusher: 32 - 313 rpm
Tableting machine	PTK, PT-100 with PISCon	96 000 tablets/h
Screw conveyer	Entecon Spiral Screw	Constant speed
Vacuum conveyer	K-Tron, P10-BV-100-VE	Constant speed
Vacuum conveyer	Volkman, VS200 Eco	Constant speed

Transfer of powder between unit operations is done either with the aid of gravity or with screw conveyers, depending on the configuration or setup of the equipment. Throughout the continuous process, feeding and mixing are the most important steps, because of their direct impact on homogeneity of the powder mixture and consequently on the final product's uniformity. It is therefore essential to guarantee precise feeding and mixing, as well as real-time monitoring of the equipment. By integrating all the equipment used in the continuous line (except the tablet press) with a control software (built on top of Labview (National Instruments Corporation, Austin, TX)) (Figure 3), it is possible to not only monitor and control in real-time, but to collect and store information onto a data server. That data can also be graphically represented in real time.

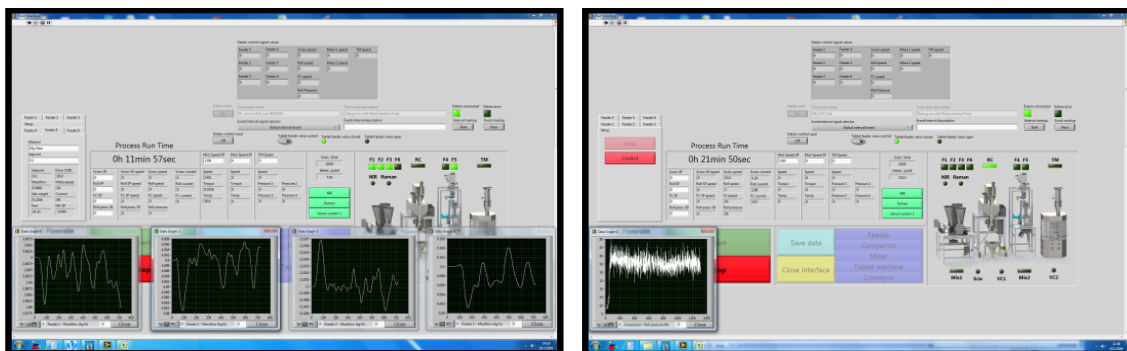


Figure 3 - Labview control software interface. On the left: monitoring of the powder mixture. On the right: monitoring of the compaction force



*Figure 4 – Full production line*



## Chapter 4

### Materials and methods

#### 4.1 Raw-materials

##### Dibasic calcium phosphate

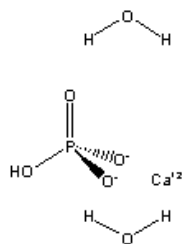


Figure 5 - Dibasic calcium phosphate molecular structure

Dibasic calcium phosphate dihydrate (DCP) (Figure 5) is a white, odorless, tasteless, free-flowing powder or crystalline solid. It occurs as monoclinic crystals and is used in the production of tablets and capsules as an inorganic binder and also as a flowing agent in high speed tablet production.(51) Good material flow is crucial for the manufacturing process and helps ensure the final product will have a consistent composition. DCP is directly compressible and the pharmaceutical industry uses it in two main mesh sizes. The milled material is typically used in wet-granulation, roller-compaction or slugged formulations. The ‘unmilled’ or coarse-grade material is typically used in direct-compression formulations. The coarser grades flow well and have excellent compressibility.

It works synergistically with microcrystalline cellulose (MCC) and other excipients that exhibit plastic deformation to improve powder flow and increase compaction, leading to more robust tablets and less loss in production and packaging. Additionally, because DCP is composed of calcium and phosphorous, it offers nutritional benefits to dietary supplements, being also used in breakfast cereals, flour and animal feed. It is one of the more widely used materials, particularly in the nutritional/health food sectors. Phosphorus or phosphate cannot be detected directly with near-infrared spectroscopy (NIRS) because of the low di-pole moment between P and O. However, P can be quantified via NIRS if it is bound organically or is tightly associated with other soil properties.(52) Therefore, it is not surprising that only few NIRS models are available to



predict concentrations of phosphate or different phosphorus fractions in soil.(53–55) The selected DCP for the experimental work was EMCOMPRESS<sup>®</sup> produced by JRS Pharma, (Rosenberg, Germany). This DCP is a coarse-grade material suitable for direct compression and high speed tableting with an advertised average particle size of 190 $\mu\text{m}$ . A particle size D50 of 124 $\mu\text{m}$  was experimentally determined by laser diffraction, bulk density was measured at 0.74 g/mL, and the angle of repose was determined to be 44 $^\circ$  with a Hosokawa Micron Powder Tester model PT-X.

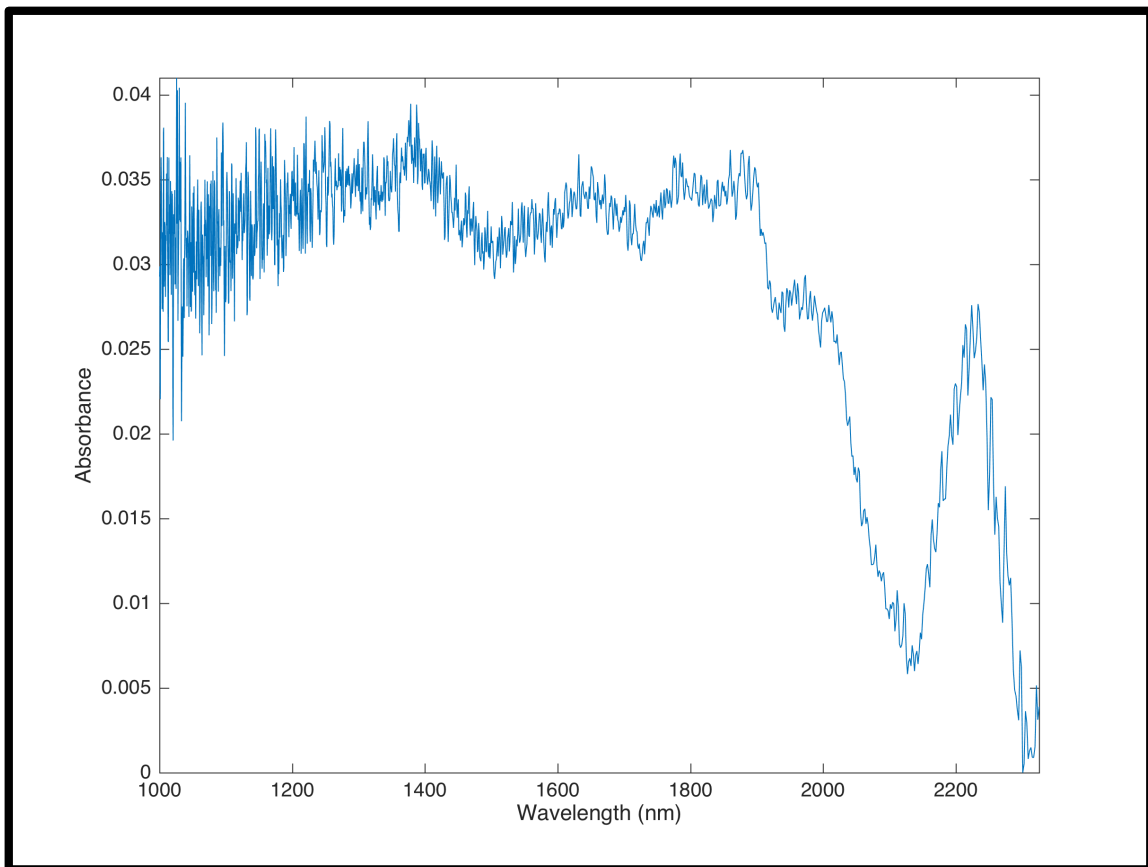


Figure 6 - Spectrum of EMCOMPRESS in the NIR region encompassing the region 1000–2500 nm

## Microcrystalline cellulose

Cellulose is the most abundant natural polymer on earth with an annual biomass production of 50 billion tons. Microcrystalline cellulose (MCC) (Figure 7) is a purified, odorless, tasteless, partially depolymerized cellulose that occurs as a white, crystalline powder composed of porous particles.<sup>(51)</sup> The most common source of pharmaceutical MCC is wood, in which cellulose chains are packed in layers held together by a cross-linking polymer (lignin) and strong hydrogen bonds.

MCC was discovered in 1955 by Battista and Smith and was first commercialized under the brand name Avicel<sup>1</sup> (FMC, 2013). In 1964 FMC Corporation introduced Avicel<sup>1</sup> PH to the pharmaceutical industry as an ingredient for direct compression tableting. MCC was first registered in the supplement to the British National Formulary, twelfth edition, in 1966 and more than 60 years later, MCC is manufactured globally by more than 10 suppliers with several commercial brands (Avicel PH; Emcocel; Tabulose; Vivapur; etc).

It is commercially available in different particle sizes and moisture grades that have different properties and applications.

MCC is widely used in pharmaceuticals, primarily as a binder and diluent in oral tablet and capsule formulations where it is used between 20% and 90% of the final formulation in both wet-granulation and direct-compression processes.<sup>(51)</sup> It is physiologically inert, non toxic, flows relatively well and is produced virtually free of organic or inorganic contaminants. In addition to its use as a binder/diluent MCC also has some lubricant (8) and disintegrant properties when used between 5% and 15% of the final formulation, that make it useful in tableting, and offers other advantages including broad compatibility with APIs, ease of handling, and security of supply. MCC is also used in cosmetics and food products.

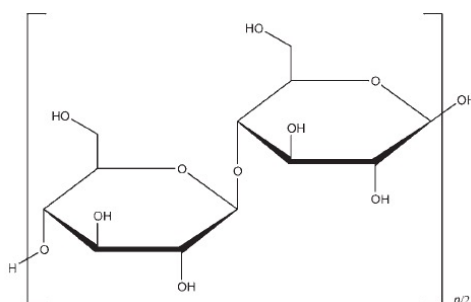


Figure 7 - MCC molecular structure

MCC is commonly manufactured by spray drying a neutralized aqueous slurry or pulp

that results from the hydrolysis of vegetable cellulose with dilute mineral acid solutions. Most commercial grades are formed by varying and controlling the spray drying conditions in order to manipulate the degree of agglomeration (particle size distribution) and moisture content (loss on drying). MCC is generally considered as the diluent having the best binding properties and is recognized as one of the preferred DC binders.

The selected MCC for the experimental work was EMCOCEL 90M<sup>®</sup> produced by JRS Pharma, (Rosenberg, Germany). This MCC is a medium size standard grade, suited for the majority of directly compressible actives, and combines good flow and high compactibility. According to the manufacturer's specifications EMCOCEL 90M has a particle size distribution between 90 and 150  $\mu\text{m}$ , a particle size D50 of 130 $\mu\text{m}$ , moisture content below 6%, bulk density between 0.25 and 0.37  $\text{g}/\text{cm}^3$ , and a Carr Index of 21. A particle size D50 of 124 $\mu\text{m}$  was experimentally determined by laser diffraction, bulk density was measured at 0.36  $\text{g}/\text{mL}$ , and the angle of repose was determined to be 43° with a Hosokawa Micron Powder Tester model PT-X.

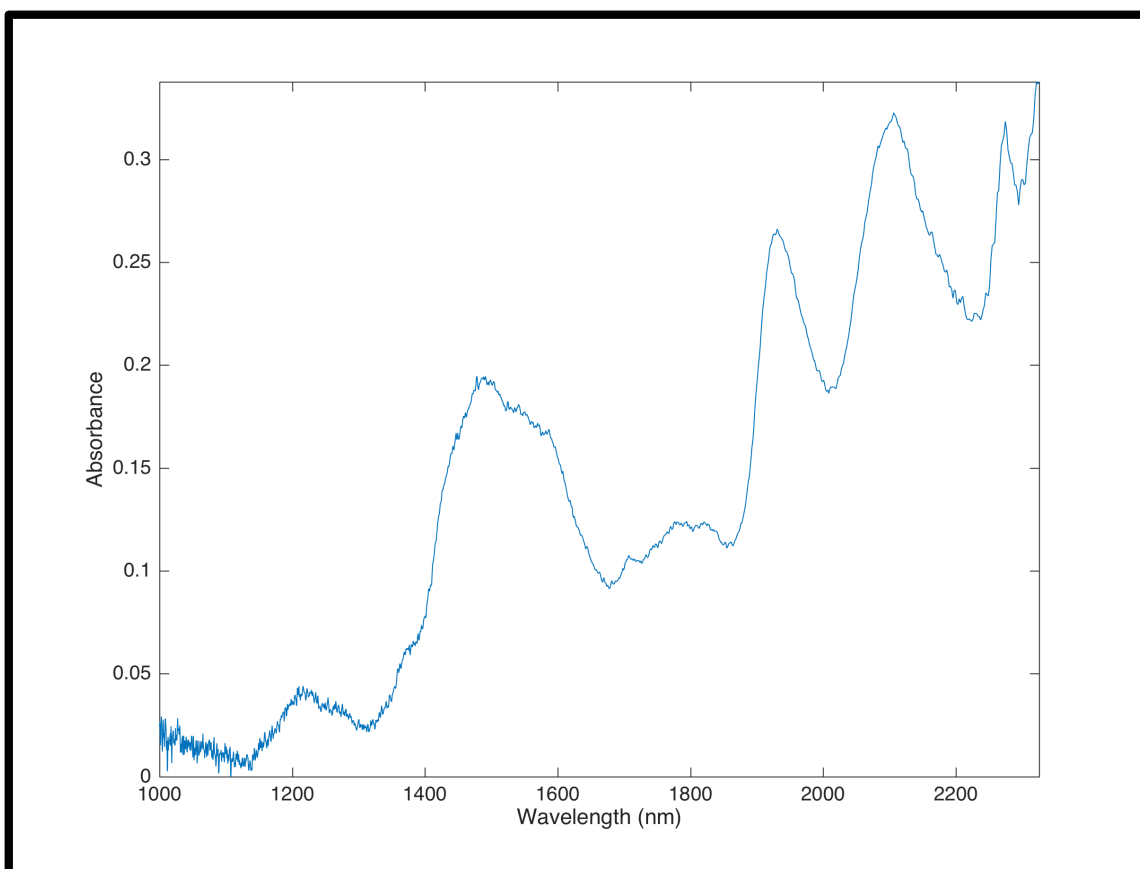


Figure 8 - Spectrum of EMCOCEL 90M in the NIR region encompassing the region 1000–2500 nm

## Paracetamol

Paracetamol (common international denomination) (Figure 9) also called acetaminophen, was synthesized by Morse in 1878, and appears as an odorless, slightly bitter white crystalline powder. Paracetamol is a nonprescription analgesic and antipyretic drug, but it is not an NSAID (Nonsteroidal Anti-inflammatory Drug) as it doesn't participate in the inflammatory response. The analgesic and antipyretic properties of paracetamol were first discovered in the late nineteenth century and clinically used by Von Mering in 1887. Two molecules were already in use for the treatment of mild to moderate pain, acetanilide and phenacetin, but studies later conducted by Brodie and Axelrod in 1948 established that paracetamol was the major metabolite of both these molecules and that resulted in the rediscovery of paracetamol as substitute analgesic for phenacetin due to its nephrotoxicity. Phenacetin disappeared from the market as paracetamol's popularity grew, and since then it has become one of the most popular and widely used drugs in the world for pain and fever treatment, and probably the most prescribed drug for children.(56)

The paracetamol used for the experimental work was purchased from Xiamen Forever Green Source Biochem Tech. Co., Ltd (Xiamen, China). A particle size D50 of 87 $\mu$ m was experimentally determined by laser diffraction, bulk density was measured at 0,35 g/mL, and the angle of repose was determined to be 58° with a Hosokawa Micron Powder Tester model PT-X. For UV-Vis quantification paracetamol's characteristic 242nm absorbance peak was considered.

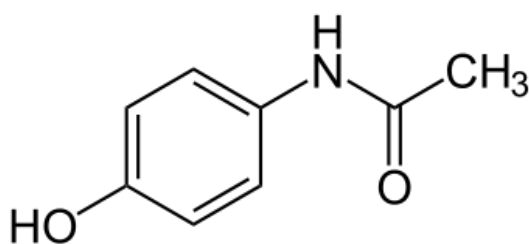
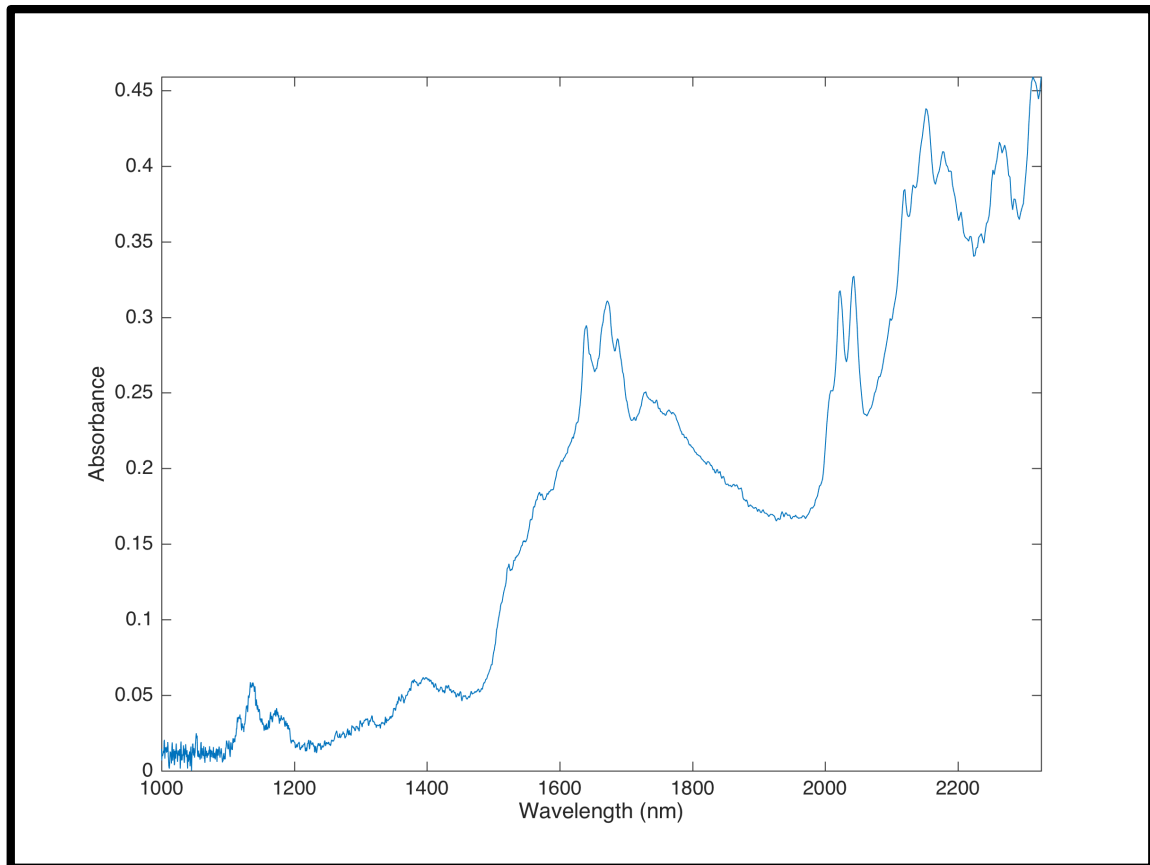


Figure 9 - Molecular structure of paracetamol



*Figure 10 - Spectrum of Paracetamol in the NIR region encompassing the region or 1000–2500 nm*

The raw materials were characterized according to the physical properties described in the and. Paracetamol has the worst flowability (Carr Index 28). MCC is the material that flows better (Carr Index 16.7).

## 4.2 Equipment

The system used consists of two loss-in-weight feeders (K-Tron), a continuous in-line mixer (Modulomix, Hosokawa Micron) with a NIR spectral camera (Specim, Finland) and integration sphere (VTT, Finland) attached to its outlet port and a conveyor belt under the sphere's discharge (Figure 11).

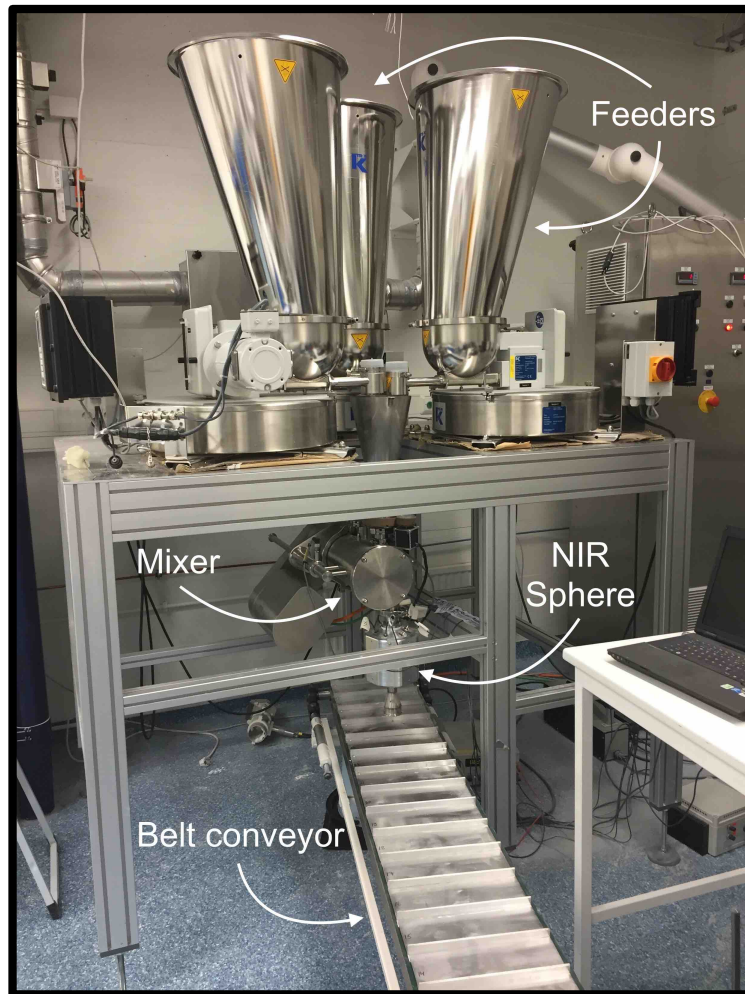


Figure 11 - Experimental configuration setup

### 4.2.1 Powder blending

- |   |
|---|
| a) Three LIW powder feeders K-Tron, K-ML-D5-KT20 (for excipients and API) |
| b) One in-line continuous mixer, Hosokawa Modulomix                       |

## a) LIW Twin Screw Feeders

All three of the K-Tron K-ML-D5-KT20 twin screw feeders (Figure 12) used in the experimental work were able to operate either in volumetric mode or gravimetric mode. It is important to know the operating differences between each mode in order to understand which was better for this experiment.



*Figure 12 - K-Tron LIW powder feeders*

### **Volumetric feeding principle**

Bulk material is discharged from a hopper with a constant volume per unit of time by regulating the speed of the feeding device. The actual volume of material fed is determined through calibration. The feeding accuracy is dependent on the uniformity of the material flow characteristics and the bulk density.

Gain-in-weight (GIW) batches employ volumetric feeders to feed each ingredient sequentially, while loss-in-weight (LIW) feeders feed multiple ingredients simultaneously into a collection hopper (Figure 13). Instead of the layering of ingredients that you get with GIW feeding, in LIW feeding all the ingredients are metered at the same time, eliminating the layering effect and the time and cost for further processing downstream.

It is relevant to state that in continuous mixing, due to time constraints and to the several simultaneous feeding flows, GIW operation is generally not possible and thus

LIW provides the more reliable feeding mechanism.

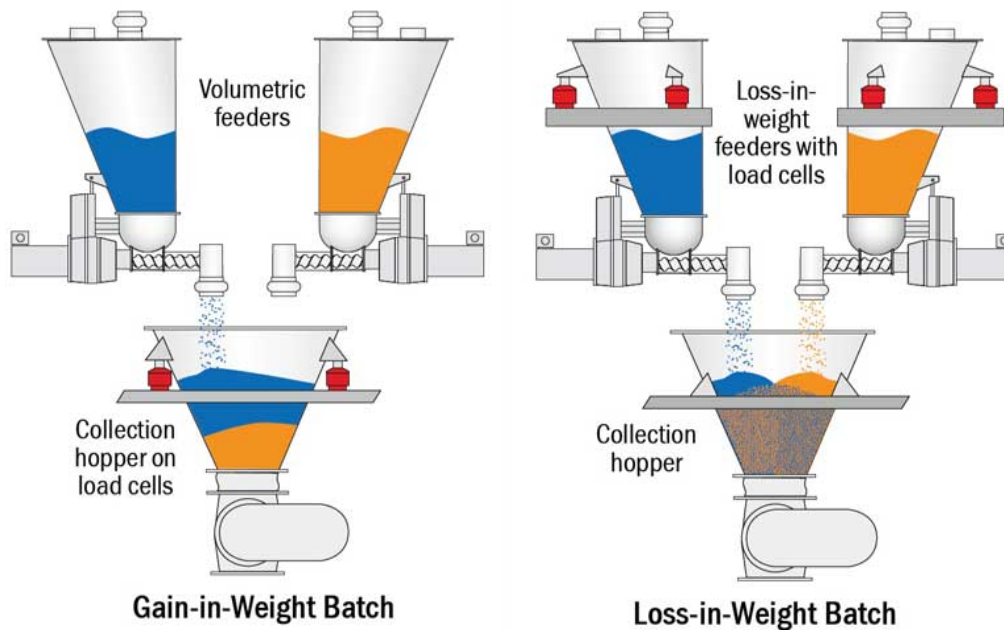


Figure 13 - Gain-in-weight versus loss-in-weight batching schematic (adapted from (57))

### LIW gravimetric feeding principle

Bulk material is discharged from the hopper with a constant weight per unit of time by weighting the hopper/feeder assembly and regulating the speed of the feeding device depending on the rate of weight loss. The weighting control system compensates for non-uniform material flow characteristics and variations in bulk density, an advantage over volumetric feeding, therefore providing a high degree of feeding accuracy.

When the hopper reaches a predetermined minimum weight level, the LIW control can be briefly interrupted and the hopper refilled. During the refill period the controller regulates the speed of the feeding device based upon the historic weight and speed information that was accumulated during the previous weight loss cycle, or switches to a default volumetric mode. The LIW feeding principle is most accurate when using a high resolution, fast responding, vibration immune weighing systems such as the D5 platform scale or load cells combined with self-tuning controls such as the compact Coperion K-Tron Control Module (KCM).



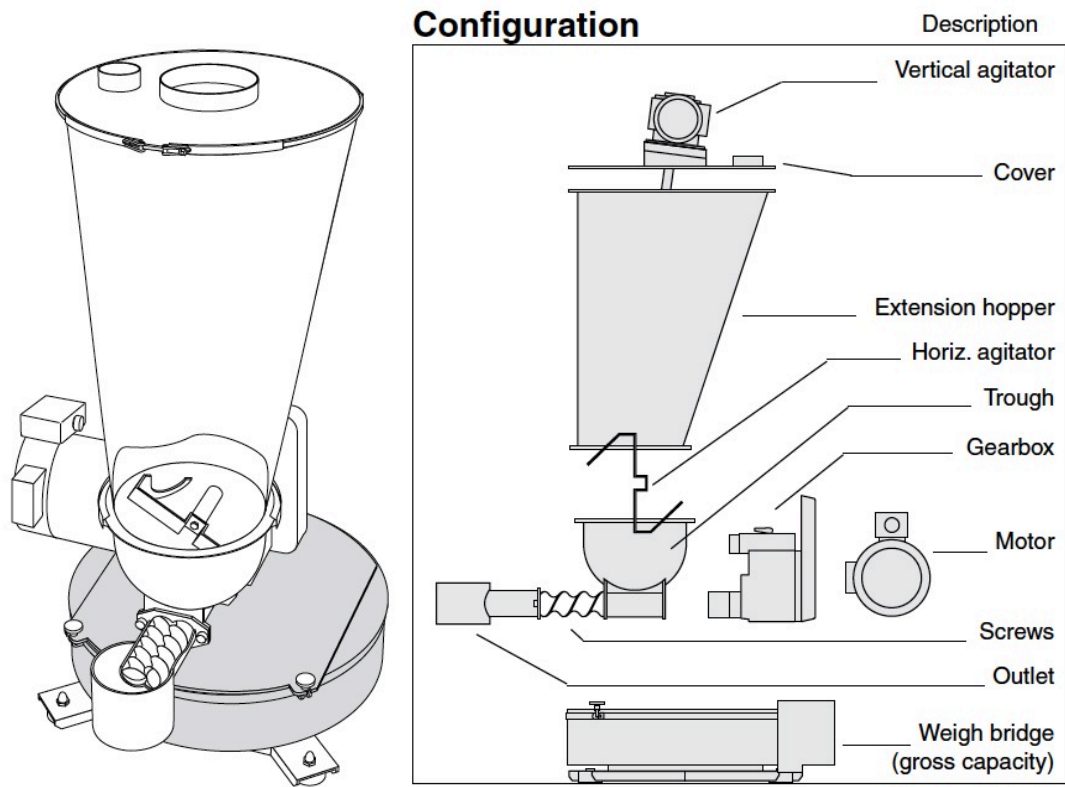


Figure 14 - Loss-in-weight powder feeder schematic (adapted from (58))

LIW feeders (Figure 14) are the best at providing fast and accurate measurement and control of individual ingredients fed into a batch or continuous process. When the weighing accuracy of each ingredient in a process is crucial to maintain the formulation within specification, when a formulation includes micro ingredients that are usually expensive, when cycle times must be kept short, or there is a big gap in the ratio of a major ingredient to a minor ingredient, LIW feeders are the best solution.

In very specific situations, if additional verification of delivered batch weight is required, a dual weighing scenario may be used, with the combination of a LIW feeding into a GIW system.

Batch size and accuracy requirements will often determine whether GIW or LIW feeders are the best for the process. In general, GIW feeding can be used in batch manufacturing when the response time and resolution of a platform scale is sufficient to guarantee batch accuracy requirements. Even though most floor scales do not have sufficient speed and resolution to measure small amounts of product into a large volume container.

Achieving an accuracy of  $< \pm 0,03 \%$ , the K-Tron system employed uses a hopper with twin screw LIW feeders mounted on a D5 Platform Scale that provides 1 part in 4 million resolution, controlled by a compact KCM. The LIW KCM controller monitors

material weight loss from the hopper and controls the start/stop functions of the feeder. With each feeder possessing its own dedicated weighing system, the K-Tron LIW Twin Screw Feeder system delivers each ingredient with great accuracy, in less time, and was the best solution for this experimental setup.

## b) In-line continuous mixer

The in-line continuous mixer used was a Hosokawa Modulomix (Figure 15). It has a small footprint with good reactivity, holds a relatively small residue at the end of mixing and has rapid start-up and shutdown protocols. It produces a homogeneous mix in a blending chamber, with little change to PSD or temperature. It can operate at a range of 300 to 1460 rpm, has a maximum capacity of 130 kg/h and can be used with different mixing conditions due to its in-process variable rotor speed as well as several designs of its agitator blades.

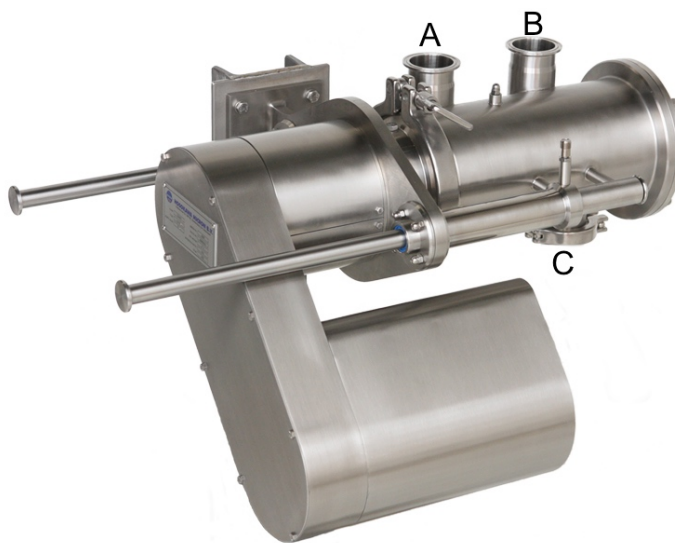


Figure 15 - Modulomix in-line mixer with inlet ports A and B, and outlet port C

Inlet ports A and B are connected to the feeding systems and can be used for separate feeding of API and excipients to the mixer. Inside the mixing chamber there is a rotating axis on which the agitator blades are placed at different angles (Figure 16). On the axis there is also a partitioning disc separating almost completely the mixing chamber between the inlet port zone and outlet port zone. This helps prevent powder from exiting the mixer through outlet port C without having been properly blended.



*Figure 16 - Modulomix in-line mixer. On the left: With the side panel removed, exposing the mixing chamber. On the right: Before cleaning with the external casing removed*

If necessary, due to formulation requirements, multiple Modulomix mixers can be cascaded in series to allow for multiple stage mixing processes. As seen in Figure 17 up to three different formulation components (API, binder, diluent, etc) can be fed through the first inlet port at the same time and, if needed, additional components may also be added through the second inlet port.

All of these components are blended efficiently within the mixer under high shear conditions. If the formulation requires the addition of a lubricant this can be done through the third inlet port that directly connects to the second mixer where the blending occurs at low shear conditions (needed for the lubricant).

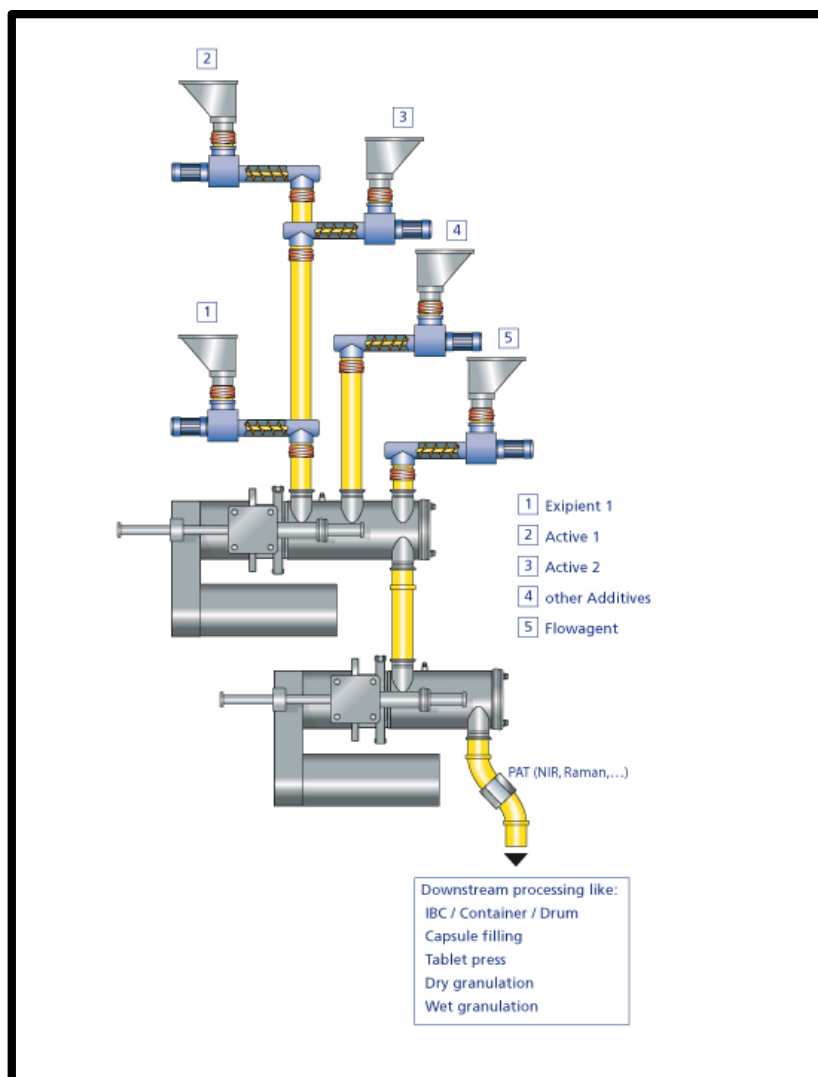


Figure 17 - Example of Modulomix cascade setup (adapted from (59))

The Hosokawa Modulomix was integrated in a PAT environment as the final mixture left the mixing system via a specially-designed PAT chute/integration sphere. Different PAT devices like Raman or NIR spectrometers can be used for continuous control of the quality of the mix. In this experimental work, NIR spectroscopy was the selected PAT device used.

### c) Belt conveyor

To ensure that the collection of the powder mixture and its samples was done in the most coherent and regular way possible, a belt conveyor (Figure 18) was devised and placed under the in-line mixer / NIR sphere chute where it would collect the powder mixture during the experiments. The conveyor had an electric motor with a voltage control which could be regulated, resulting in higher or lower belt speed. All of the powder that fell onto the belt was divided into several rotating metallic trays that delivered the powder into

manually placed plastic bags at the end of the conveyor. This system was regulated for a sampling time of 10 seconds and allowed for timed and regular sampling to be assured through all the experiments.



Figure 18 - Belt conveyor

## 4.2.2 Monitoring of API content/homogeneity

- |   |
|---|
| a) NIR Spectral Camera and Integration Sphere |
| b) Shimadzu UV-1800 UV-Vis Spectrophotometer  |

### a) NIR spectral camera and integration sphere

The NIR spectral camera used for the acquisition of spectra was a SPECIM Spectral Camera (Specim, Finland), an integrated combination of an ImSpector imaging spectrograph and an area monochrome camera. It works as a push-broom type line scan camera providing full, contiguous spectral information for each pixel in the line.

This SPECIM NIR camera provides 320 pixel spatial resolution and image rate from 50 to 350 Hz. The NIR Spectral Camera model consists of an ImSpector N17E imaging spectrograph for the wavelength region 900 - 1700 nm and a temperature stabilized InGaAs detector. The transmission diffraction grating and lens optics included in the spectrograph provide high light throughput and distortionless image which is designed to meet the requirements of the associated detector.

The cooling unit is maintenance free and keeps the detector temperature stable throughout a wide ambient temperature range. The camera is also equipped with an



electro-mechanical shutter for dark image acquisition integrated in its housing.

For setting up the NIR instrument, spectra do not originate from only one image or source, but from six overlapping signals from six separate fiber optic probes. Therefore an accessory shown in Figure 19 is attached to the spectral camera in order to receive and merge all six fiber optic signals.

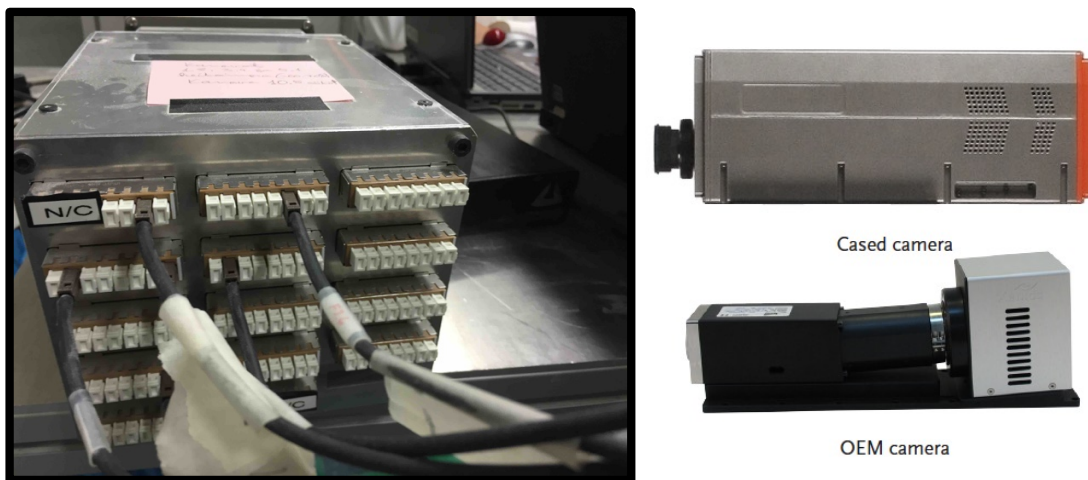


*Figure 19 - NIR spectral camera. On the left: fiber receiving and merging accessory. On the upper right: profile of the cased camera. On the lower right: profile of the camera with no casing.*

The purpose of using six fibers for signal acquisition relates to the challenge of in-line continuous monitoring of production material. In order for the signal that reaches the spectral camera to be representative of the flowing material exiting the chute, only one measuring point is insufficient, due to the small area illuminated and to the large quantity that is being processed at each moment. Thus a special accessory called an integration sphere was used as a setup that allows multi-point signal acquisition for a more representative analysis.

The accessory designed by the VTT Technical Research Centre of Finland Ltd (VTT) in Finland (Figure 20), consists of a metal box with a glass tube that spans across a hollow white teflon sphere inside of it. The tube is open at both ends and serves as a chute where the material flows through as it exits the in-line continuous mixer at its outlet port. On the surface of the white teflon sphere are six fiber optic probes pointed at different angles at different points of the glass tube, these fiber optic probes are mounted and secured on the sphere's metal casing. There is also a halogen lamp that can be replaced when needed that acts as a light source inside of the sphere.

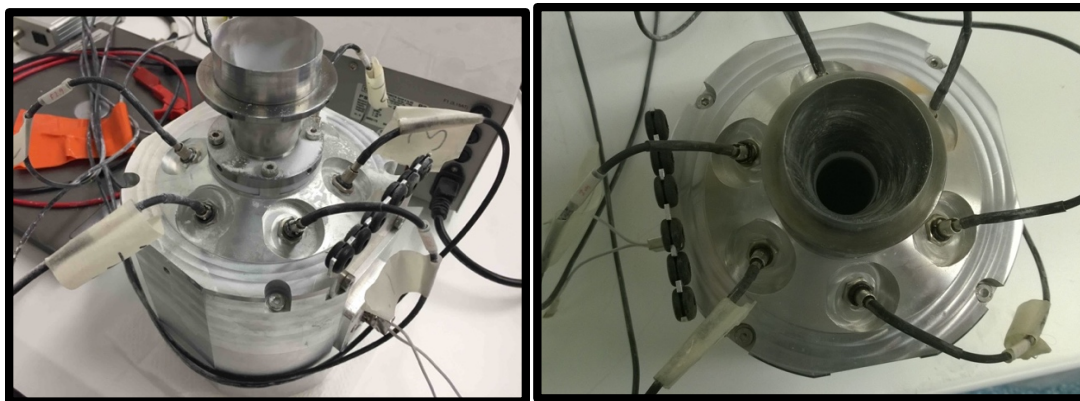


Figure 20 - The integration sphere.

As mentioned before, NIR spectra for all runs were obtained through the merging of the signal of the six fibers into one through the optical accessory attached to the spectral camera. This solution allows for a much better integration of PAT tools in general, and NIR specifically into continuous pharmaceutical processing. It avoids the need of taking several samples of the flowing material, avoiding potential contamination, allowing for continuous in-line multi-point monitoring of the blend quality.

#### b) Shimadzu UV-1800 UV-Vis spectrophotometer

A UV-VIS spectrophotometer was used to quantify the paracetamol present in the collected samples. The equipment was a Shimadzu UV-1800 (Figure 21) using a spectroscopy with a Czerny-Turner mounting and a 1 nm resolution capability.



Figure 21 - Shimadzu UV-1800 spectrophotometer.

## 4.3 Methods

### 4.3.1 Experimental design

In order to evaluate how mixing performance is affected by process parameters, a set of 14 experiments was defined using Modde (MKS, Malmö, Sweden ) as seen in Table 2. The design of experiments (DoE) included three centre points spaced throughout the run order, allowing for the best characterization of the system whilst doing a small number of experiments. Process parameters varied were: mixer speed (300, 900 and 1500 rpm), feed rate (5, 10 and 15 kg/h), inlet port (A or B) and excipient type (MCC or DCP).

Table 2 - Experimental design used to define the runs' conditions according to four process parameters.

Experiment Name	Run Order	Total Feed Rate (kg/h)	Mixer Speed (rpm)	Port	Excipient	Run Time Aprox (min)
N1	2	5	300	A	MCC	15
N2	4	5	1500	B	DCP	15
N3	9	15	300	B	DCP	15
N4	12	15	1500	A	DCP	15
N5	7	15	1500	B	MCC	15
N6	11	15	1500	A	MCC	15
N7	8	15	300	B	MCC	15
N8	13	15	300	A	DCP	15
N9	6	5	1500	B	MCC	15
N10	3	5	1500	A	DCP	15
N11	5	5	300	B	DCP	15
N12	1	10	900	A	MCC	15
N13	10	10	900	A	MCC	15
N14	14	10	900	A	MCC	15

### 4.3.2 Preparation of the mixtures

Before conducting a run of an experiment, both LIW feeders (API + excipient) were filled with enough raw material so that the experiment could run without any interruption during the intended time (at least 15 min). When there was already enough raw material in the feeders left from a previous run it was necessary to check if no “rat-holing” had occurred stirring the raw material inside the feeder with a metal rod. Although the LIW feeders could be operated through the attached KCM, they were mainly software controlled through the desktop computer running Labview.

When the mixing process was ready to start, the rotating hopper mounted onto the inlet port of the mixer was turned on (to ensure better flow of raw material into the



mixer), and then the LIW feeders and the continuous mixer. At the start of each run, the settings for the feeders and mixer were constant for that experiment's specific values (mixing speed, total feed rate, inlet port and excipient type).

Even though there was a fixed total feed rate for each experiment, specific API and excipient feed rate step changes were introduced at different times in each run by varying the relative feed rate of each LIW feeder (API and excipient) as seen in Table 3. This way it was possible, while maintaining the total feed rate constant, to achieve the desired step changes.

Table 3 - LIW feeders step changes

Step %		Total Feed Rate 5 kg/h		Total Feed Rate 10 kg/h		Total Feed Rate 15 kg/h	
API	Excipient	API feed	Excip feed	API feed	Excip feed	API feed	Excip feed
50	50	2,5	2,5	5	5	7,5	7,5
40	60	2	3	4	6	6	9
60	40	3	2	6	4	9	6
70	30	3,5	1,5	7	3	10,5	4,5

These step changes have been introduced throughout the run in order to better understand system responses to changing API feed rates, mixing performance with different formulation ratios, mean residence time and particle RTD. In the latter, the method utilized was the step input, and the region selected for the calculations was the first step change from 50% API to 60% API (%w/w) around the 3 minute mark. These step change settings were done for every experiment with the step changes having the same duration and time points as seen in Figure 22.

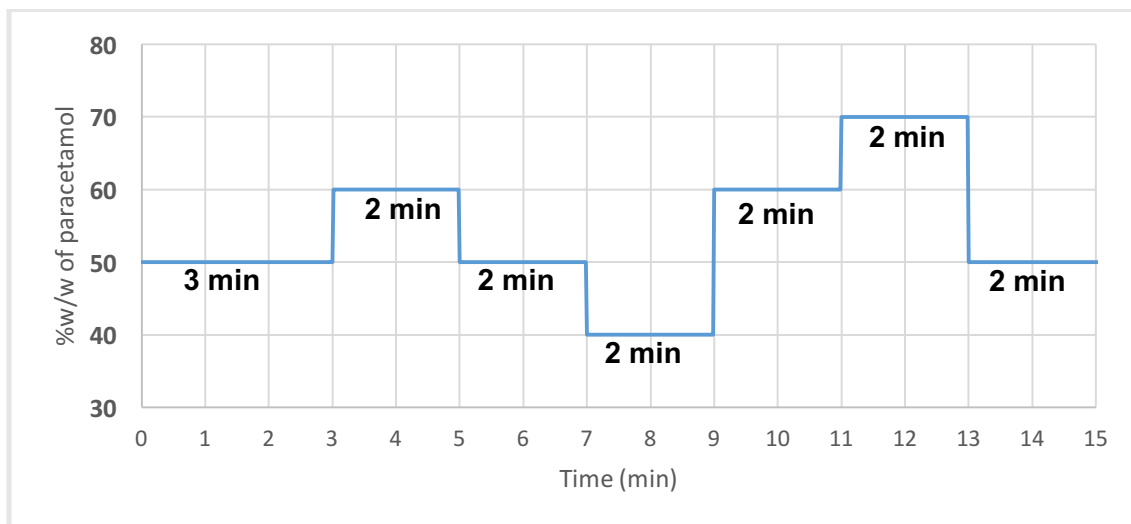


Figure 22 - Paracetamol step changes along the duration of each experimental run

The only parameter that varies throughout the run is the relative feed rate of each feeder (API and excipient) in order to achieve the desired step changes while maintaining the total feed rate constant. The initial 50% step lasts 3 minutes and is the only step that lasts more than the others, since it is necessary to guarantee that when we reach the first step change to 60% the mixing process, as well as the powder accumulation that occurs inside the clean mixer, have stabilized and that the resulting blend is as homogenous as it can be. Without this guarantee it would not be feasible to calculate the RTD from the step change data. For this reason one extra minute was added to this step. The resulting blend that poured from the mixer outlet was collected into several plastic bags in 10 second intervals with the help of the belt conveyor.

### 4.3.3 Powder blend monitoring with NIR spectroscopy

Powder blend API content and mixture homogeneity were monitored with a NIR spectrometer connected to an in-line integration sphere that was attached to the continuous mixer outlet. The NIR data collected from the start until the end of each run was processed and stored by the acquisition software. That data was further analysed in Matlab using PLS Toolbox.

### **4.3.4 Mass hold**

#### **Mass hold at 180 seconds**

By subtracting the cumulative collected powder mass in the sample bags from the known fed powder mass in the first 180 seconds, it was possible to determine the mass hold at the end of the first steady state step of 3 minutes.

#### **Mass hold at the end of the run**

After stopping the feeders and the mixer at the end of each experimental run, the powder still left inside of the mixer was collected onto a tray placed under the exit port. In order to force the powder out, the mixer's rotating axis was turned on to 1500 rpm and the powder collected until no more was flowing. The powder mass was weighted in an analytical scale and registered.

### **4.3.5 Paracetamol quantification with UV-VIS**

Upon running all fourteen experiments it was necessary to determine the real amount of paracetamol in the binary mixture samples, and cross-check that against the feeder data in order to verify blend homogeneity. Therefore an analytical method had to be chosen that adequately detected the desired substance. Apart from the reference high performance liquid chromatography (HPLC) which is a fairly expensive, time consuming and laboratory "busy" equipment, one other method was available that allowed for the quantification of paracetamol in the collected samples in an easier and less expensive way. That method was UV-Vis spectroscopy using the Shimadzu UV-1800 spectrophotometer to measure paracetamol's characteristic 242 nm absorbance peak. In order to achieve this, diluted solutions were made from each powder sample. Since producing diluted solutions for every sample would be nearly impossible in the time available, key samples taken right before each step change (where mixture homogeneity is theoretically higher) were selected and analysed. The procedure to obtain these solutions from the respective powder samples was the same for every run of experiments. A calibration curve was built with several paracetamol standard solutions in order to verify measurement linearity in the desired absorbance range. Paracetamol standard solutions were made with both milli-Q water and tap water to test for potential solvent interference. It was determined that using tap water had no interference in the UV-Vis measurements and so, due to the high savings in laboratory costs, that was the selected solvent.

Each sample was weighted in an analytical scale inside the plastic bag. The plastic bag weight was taken into account as tare weight and 20% of the real powder sample weight was used to make a “mother” solution in a 0.5 L volumetric flask with tap water at room temperature. From that “mother” solution, a dilution to a 50 mL volumetric flask was made in order to achieve a theoretical target concentration of 15 µg/mL.

This theoretical target concentration was chosen because it represents the center point in the range of measured concentrations for the calibration curve which presented good linearity, it is the final solution concentration of a 50/50 sample, and it has an adequate absorbance signal value.

The decision of using 20% of the total powder sample to produce the mother solution and then to dilute that same solution was based on the concern of accurately representing the sample. If not, in the case of a non ideally mixed sample or if segregation of the powder had occurred inside the bag, it would be possible that the smaller amount of powder taken to make the solution would have had much higher proportions of one substance than the other, biasing the results. The only exception to this rule was experiment N9 in which, due to the smaller amount of powder collected in each bag (about 11g), 50% of the total powder sample was used. All solutions were filtered with 45 µm Porvair syringe filters before UV-Vis measurement.

All the UV-Vis measurements of each sample were acquired in triplicate, averaged and registered on the Shimadzu proprietary software. Later, they were exported to Microsoft Excel for further data analysis.

#### **4.3.6 Particle size measurement**

The size distribution of powder particles was measured off-line by light scattering in the Scirocco unit of the Malvern Mastersizer 2000 equipment.

#### **4.3.7 Exploratory data analysis**

All data obtained with the NIR spectrometer were extracted from the acquisition software and ported to Matlab (The Mathworks Inc. Natick, MA). Principal component analysis (PCA) was applied to data of each experiment (before PCA the dataset encompassing the spectra was scaled by mean-centring). Multivariate curve resolution (MCR) was additionally tested to analyse the experiments where the excipient was MCC. PCA and MCR were performed on the PLS Toolbox (Eigenvector Research, Inc., Manson, WA) for Matlab. Spectra were preprocessed with Savitzky-Golay (first derivative, second

order polynomial and 15 points) for PCA and multiplicative scatter correction (MSC) for MCR using the PLS Toolbox.

#### 4.3.8 Residence time calculation

Residence time is a very important parameter since it can be used to characterize the propagation of transient disturbances across sequential unit operations in a system, and therefore an effort was made to try and determine it in this experimental work.

There are two ways to stimulate the system in order to calculate the particles residence time. Through a very short pulse input and through a continuous step change. Naturally due to the configuration of our experimental setup the chosen method was the step change, and the best time to perform such a change is during steady-state when we can guarantee that there are no disturbances affecting the system. We need to guarantee that the only disturbance or stimulation to the system is done by us, by performing the step change.

Having this in mind, the selected step change for this part of the study was the very first from 50% to 60%, 3 minutes after the start of the run. The dataset used for this calculation started after 150 seconds (30 seconds before the step change) until 300 seconds (2 minutes after the step change), since the point is to focus on the sigmoid portion of the dataset.

The method for obtaining the RTD and residence time for each experimental run, starts with fitting a curve to the sigmoid dataset in the SigmaPlot software (Systat Software Inc. San Jose, CA). The type of equation selected was a sigmoidal Weibull 5 parameter equation because it presented the best overall fit and shape for our process step change. Then the Weibull equation had to be normalized so that when plotted, the bottom and top section values would be 0 and 1 respectively. After that, the differential equation had to be calculated, and from it can be obtained the probability distribution function  $E(t)$ , which in this case is the RTD. For the residence time value it is necessary to calculate the integral for  $t \cdot E(t)$ , and thus obtain the mean residence time  $\tau$ . The Variance  $\sigma^2$  can be calculated through the integration of  $(t-\tau)^2 \cdot E(t)$  consequently also obtaining the standard deviation  $\sigma$ .

### **4.3.9 Bulk residence time**

The bulk residence times were obtained dividing the mass hold at the end of the run by the corresponding feed rate of those experiments.

$$\text{Bulk Residence Time (h}^{-1}\text{)} = \frac{\text{Mass hold (kg)}}{\text{Feed rate (kg/h)}}$$

### **4.3.10 System variables influence over response parameters**

Linear models between process variables and system responses were developed in Modde. The selected variables were: feed rate, mixer speed, inlet port and excipient. The selected responses were: bulk residence time, mass hold and UV-Vis versus feeders RSD. The value of each response was determined by the aforementioned methods. The variables' setpoints and their corresponding responses were introduced in Modde and a PLS model was built, in order to analyse the resulting coefficients.

## Chapter 5

### Results and discussion

#### 5.1 Exploratory data analysis

After having collected all the NIR data from the acquisition software we were left with 14 .bin files of 275 Mb each with 100 spectra per second. In order for the obtained NIR data to be introduced into Matlab there was the need to use a custom script written by the VTT, that extracted the data from the original .bin file into Matlab and at the same time reduced the file size into a more manageable one by averaging those 100 spectra per second into 1 spectrum per second. After that, the resulting spectra were plotted against the wavelengths and the spectral region that contained the poorest information, namely from 865 to 1300 nm was removed, leaving the 1300 to 1689 nm region to be analysed (Figure 23). For practical purposes the experimental run of the DoE that will be used as an example will be the N6 which uses MCC as the excipient.

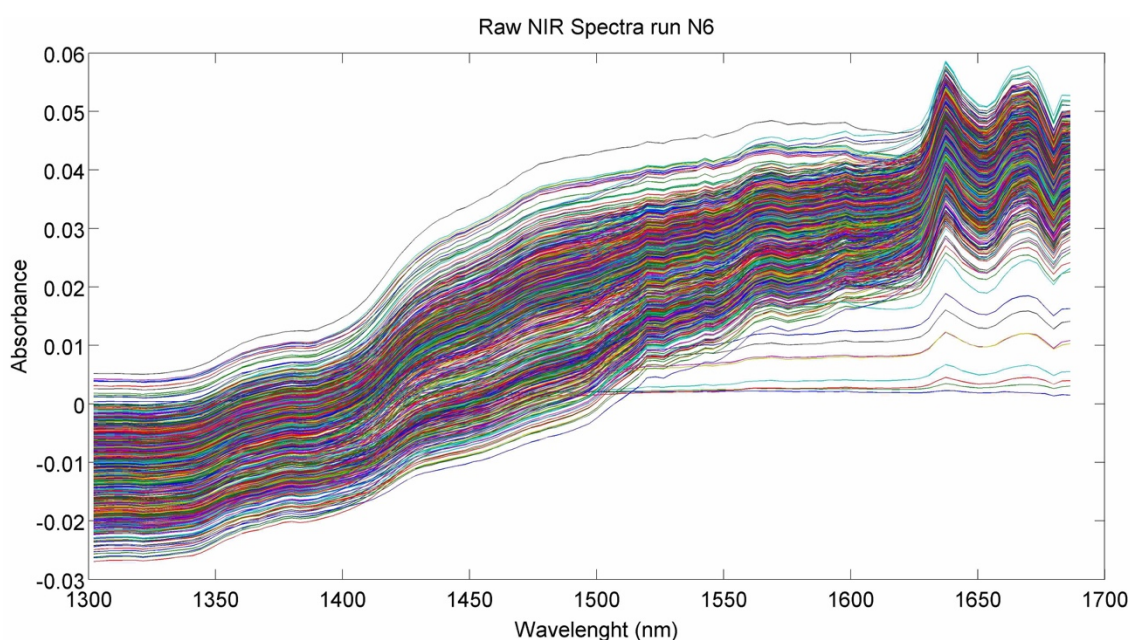


Figure 23 - Raw NIR spectra obtained for run N6

The spectra were then pre-processed with a first derivative Savitzky-Golay algorithm in order to emphasize and maximize the physical and chemical information contained (Figure 24). This pre-processing method also tends to accentuate the noise because of

the derivative calculation implied, and because of that a smoothing effect is also applied to remove high frequency noise on each row of the matrix. The smoothing effect is applied to a variable subset number of points and fits a “n” order polynomial on those points, therefore it is up to the user to select the best settings. In this experimental work each subset “window” contained 15 points and a second order polynomial smoothing effect was applied.

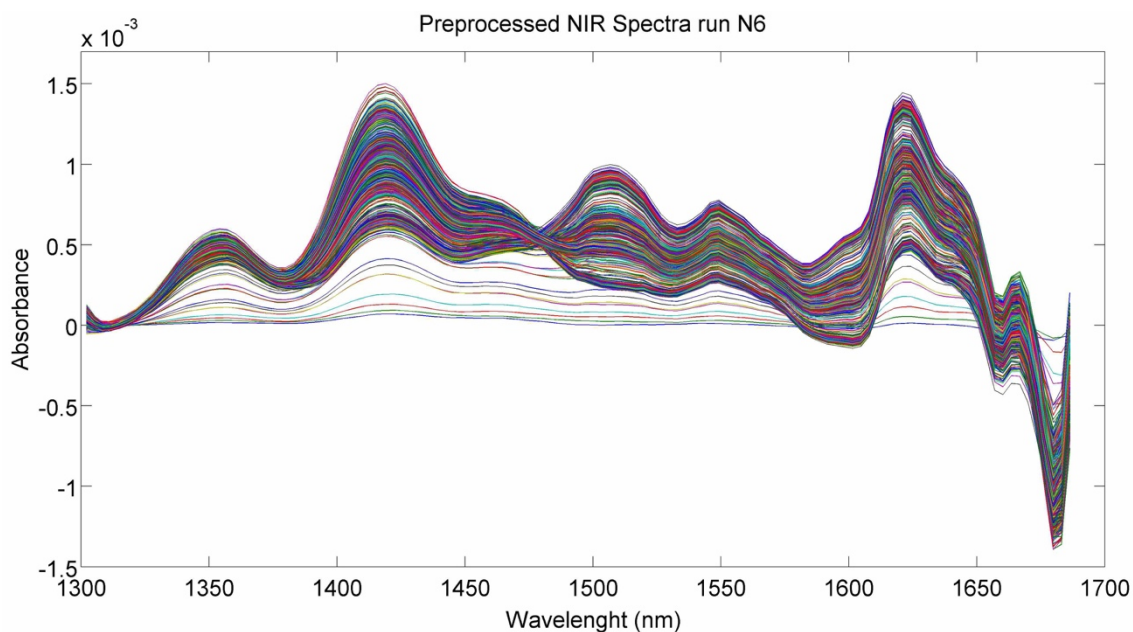


Figure 24 - Pre-processed NIR spectra for run N6

### 5.1.1 Principal component analysis

After the spectra were mean-centred, the PCA model was built. This was repeated for all runs. In Figure 25 we can observe the score plot where the first principal component (PC1) captured 82.1% variance, against the second principal component (PC2) that captured 11.2% variance. The first principal component describes the direction of the major variation in the data set, which is the greatest axis of the ellipse. The scores were coloured according their PC1 information in order to evidenciate how, through the score plot, it is easily identifiable that there are four main score clusters. These four main clusters are undoubtedly correlated to the four different mixture proportion steps (40%w/w, 50%w/w, 60%w/w and 70%w/w) that are achieved throughout each experiment.



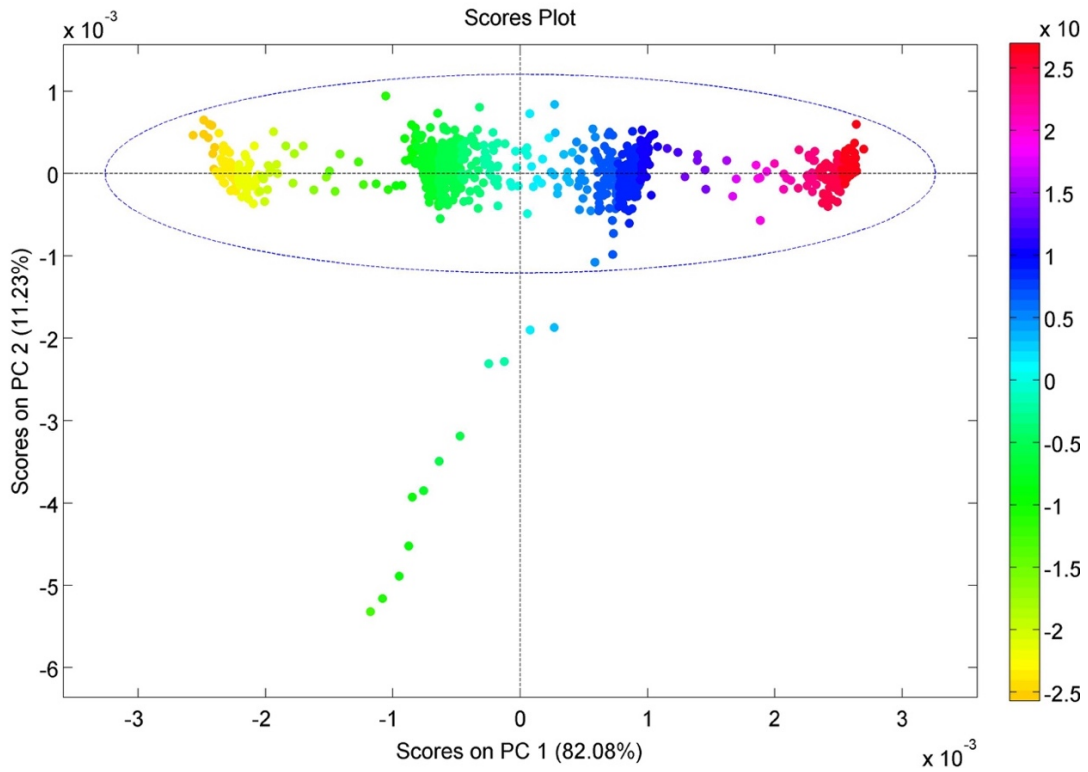


Figure 25 - Score plot for the PCA model obtained from run N6 spectra.

The light green and light blue scores found outside of the 95% confidence ellipse make up for the first few seconds of the mixing process. In those instants, the system has not yet stabilized and that explains why those particular scores don't belong to any of the four identifiable clusters. That can be corroborated by looking at the model squared residuals versus the Hotelling's  $T^2$  statistic plot in Figure 26 in which each point has been time labeled.

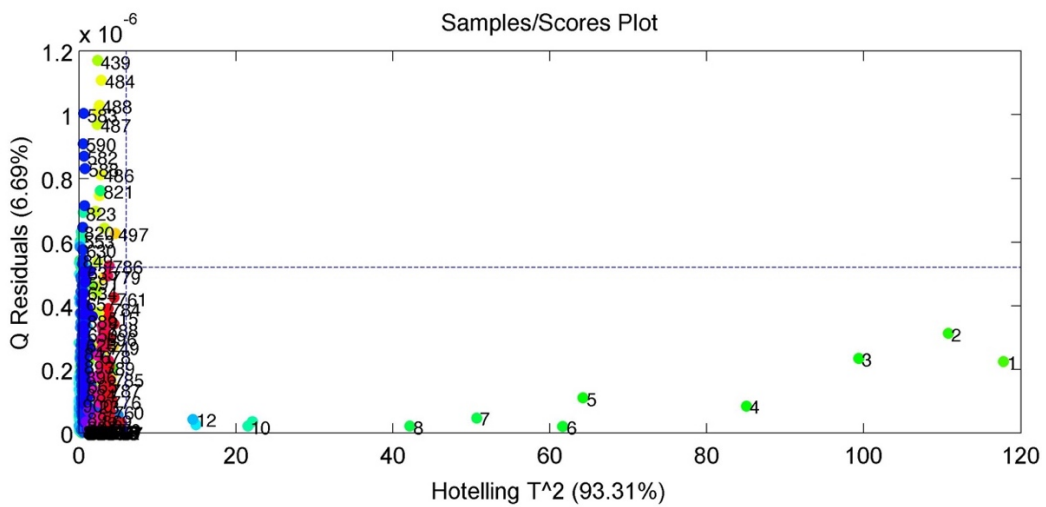


Figure 26 - Q residuals vs Hotelling  $T^2$  from a PCA model from run N6 spectra

The Hotelling's  $T^2$  statistic is the sum of normalized squared scores and a measure of the variation in each sample inside the PCA model. Q residuals is the sum of squares of each row in the error matrix E that is obtained by calculating the difference between the original data and the model predictions (e.g., the residuals). The Q statistic points out how well each sample conforms to the modelled part of the PCA model. The blue dotted lines represent their respective 95% confidence limits and therefore also exclude the scores representing the first few instants of the run.

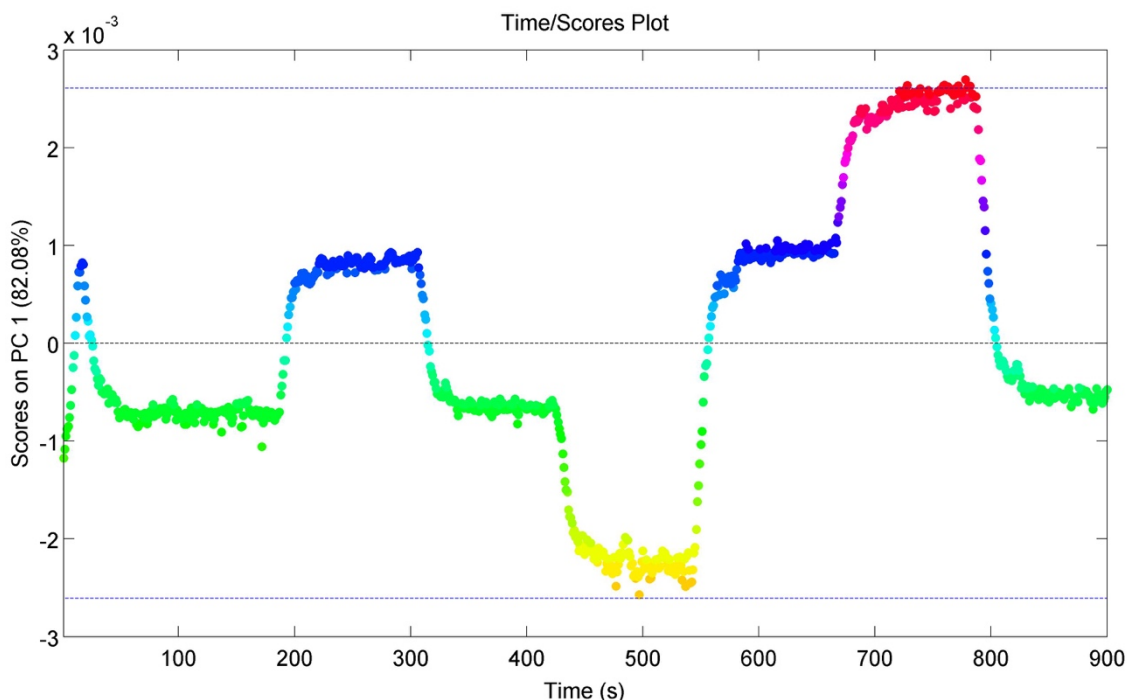


Figure 27 - Evolution of the first PC over time for run N6.

Finally, by plotting the scores versus the run time in Figure 27, we obtain an almost identical profile as in Figure 22 and are able to identify the already mentioned instability in the early moments of the experiment. Furthermore it is possible to verify that the four main score clusters identified in Figure 25 fit quite perfectly with the defined steps of the experiment. It is possible to affirm that the yellow cluster corresponds to the 40% step, the green cluster to the 50%, the blue cluster to the 60% and the red cluster to the 70%. Looking at these results it is possible to infer that the PC1 of the PCA is very directly related to the mixture content of one of the substances (paracetamol).

In order to confirm if the PC1 loadings do indeed represent paracetamol, and if the PCA is indeed measuring the API content of the blend and not MCC content (in binary mixtures this is plausible to happen), we must compare the PC1 loadings with the preprocessed pure spectra of the desired substance and check if there is a match.



Figure 28 - Raw and preprocessed (first derivative) NIR spectra of paracetamol.

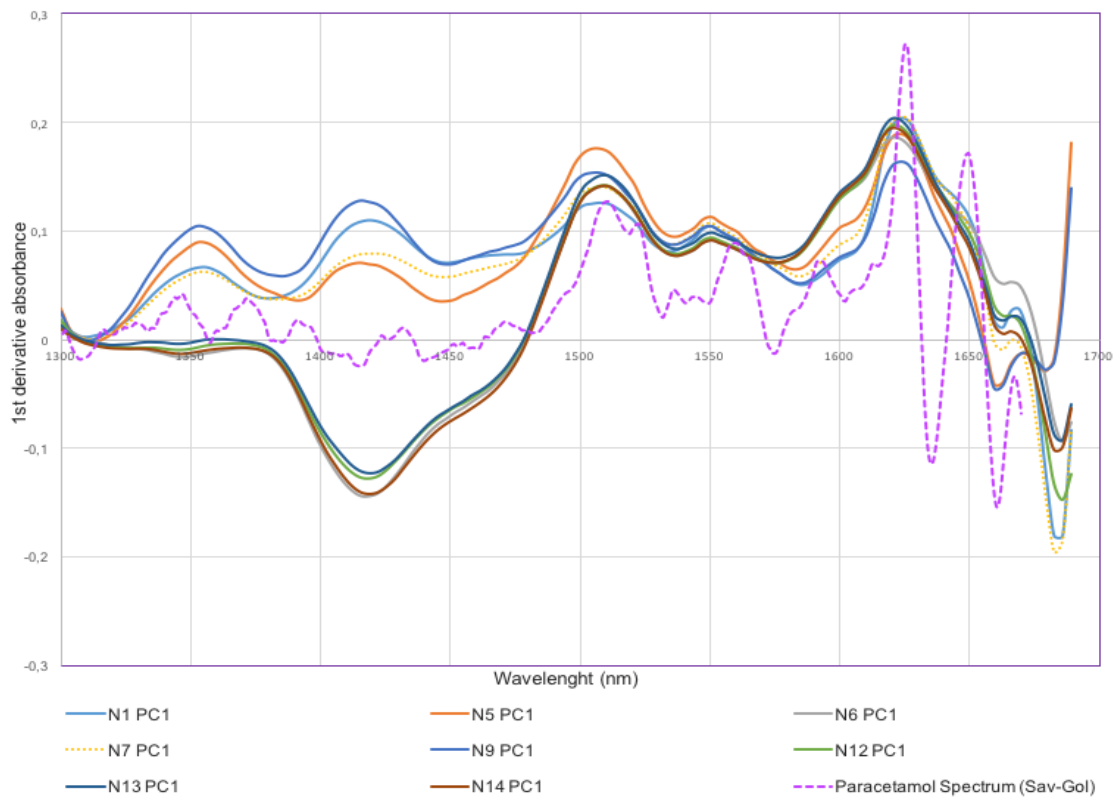


Figure 29 - Preprocessed (first derivative) and PCA PC1 loadings NIR spectra of paracetamol

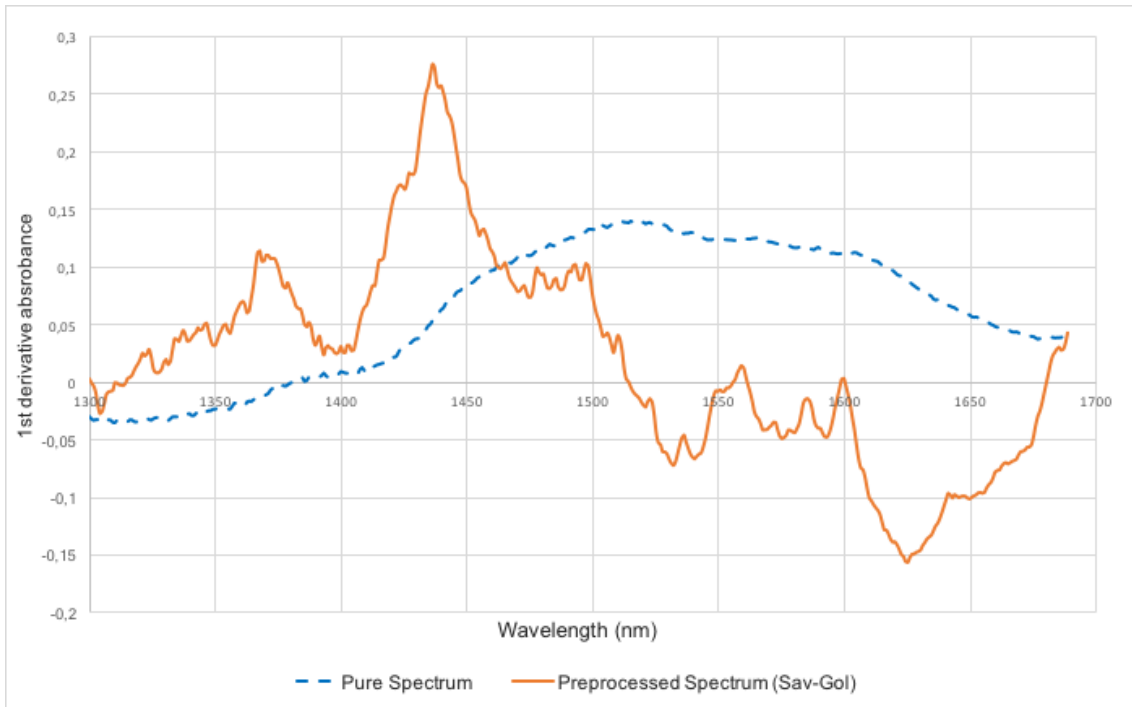


Figure 30 - Raw and preprocessed (first derivative) NIR spectra of MCC.

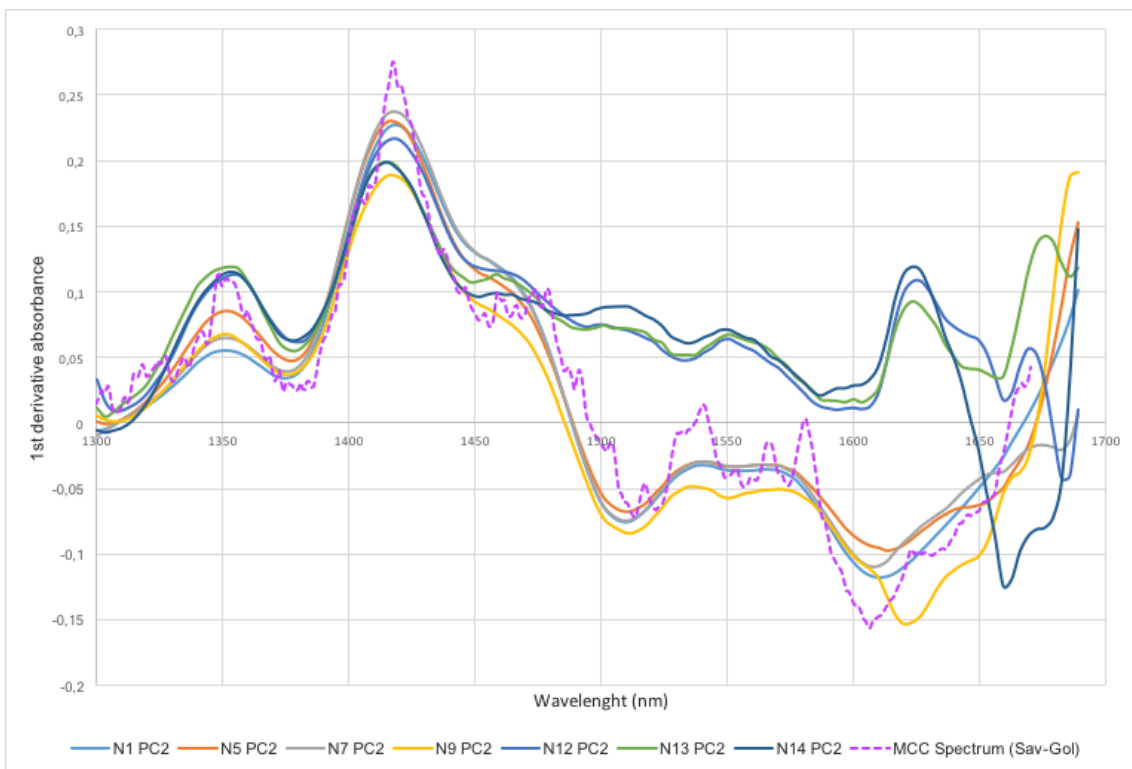


Figure 31 - Preprocessed (first derivative) and PCA PC2 loadings NIR spectra of MCC.

The reason why the pure substance spectrum has to be pre-processed too (Figure 28 and Figure 30) is because we are comparing the profiles of two sets of spectral data, and since one set of data was pre-processed for PCA, if the other is not processed in the same way the profiles will be extremely different and non-comparable.

As we can see from Figure 29, the PC1 loadings fit the preprocessed pure paracetamol spectrum quite nicely from 1500 nm to 1689 nm. This strongly suggests that the substance being monitored by that principal component is paracetamol. In a similar way we can observe in Figure 31 that the same happens between the PC2 loadings and the preprocessed MCC spectrum from 1300 nm to 1500 nm. This also points to the fact that the substance being monitored by the PC2 is MCC.

Finally, the reason why the loadings on both components don't always fit together throughout the range of wavelengths is because, as can be seen in Figure 32, MCC absorbance is stronger and only detectable from the 1300 nm to 1500 nm region, and from 1500 nm onwards paracetamol's absorbance is higher including MCC's signal. This causes the PCA to not always be able to generate chemically interpretable loadings for those regions causing them to diverge and split away from the preprocessed pure substance spectrum. These properties and characteristics are extremely important to take into account when doing a thorough analysis or when choosing which substances to include in the mix, if a continuous monitoring and control strategy is to be implemented.

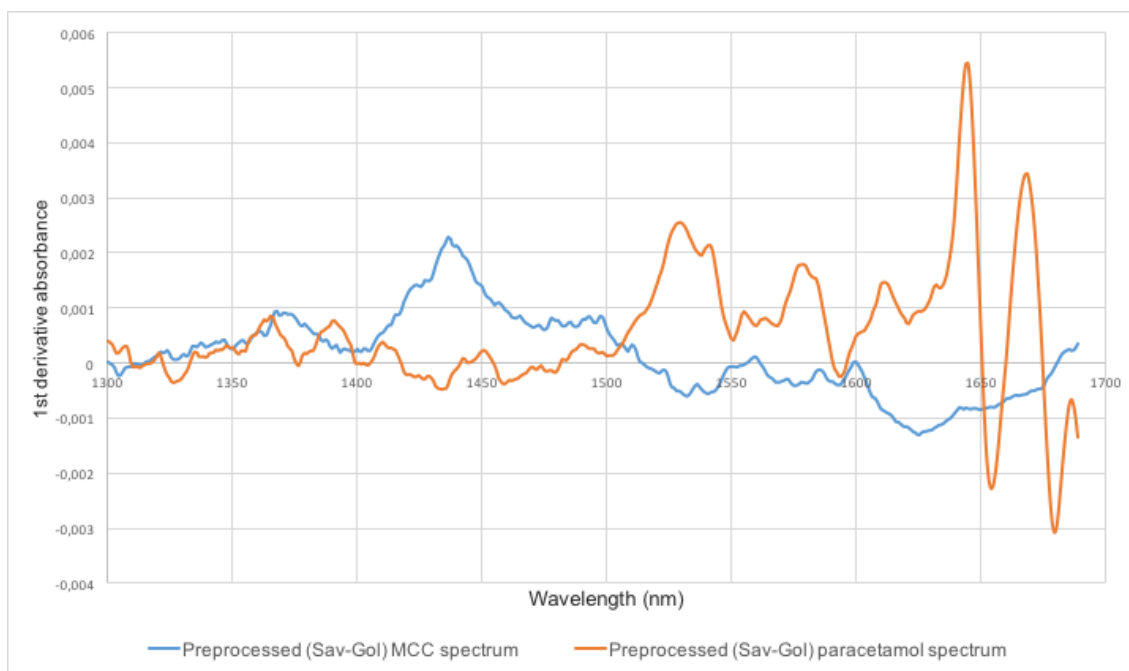


Figure 32 – Preprocessed (first derivative) paracetamol and MCC NIR spectra.

## 5.1.2 Multivariate curve resolution

In order to further explore the data obtained in the experiments another technique was implemented to determine API content in the powder mixture. This was done through MCR, which is defined as a group of techniques that help resolve mixtures by determining their number of constituents, their response profile (pure spectra) and their estimated concentrations, when no prior information is available about the nature and composition of the mixture. MCR decomposes the experimental data matrix  $D$ , using a constrained alternating least squares (ALS) algorithm, into the product of two smaller matrices  $C$  and  $S^T$ , with  $C$  being a matrix of concentration profiles for the modeled component in the system and  $S$  being the matrix of the corresponding pure spectra.

This method was done also in Matlab using the same initial NIR data matrices as those used for the PCA models, as well as a pure paracetamol absorbance spectra in the 1300–1689 nm region. All matrices containing paracetamol/MCC NIR data (N1, N5, N6, N7, N9, N12, N13 and N14) were concatenated into one big matrix and then applied a MSC preprocessing, in order to eliminate artificial baseline and scaling between runs. That together with the pure paracetamol NIR spectrum (forcing some  $S$  matrix rows) in the same spectral region was used.

In this case, and since the system was a binary mixture, the result was a clear separation between what was perceived as paracetamol and the other component (MCC) as seen in Figure 33.

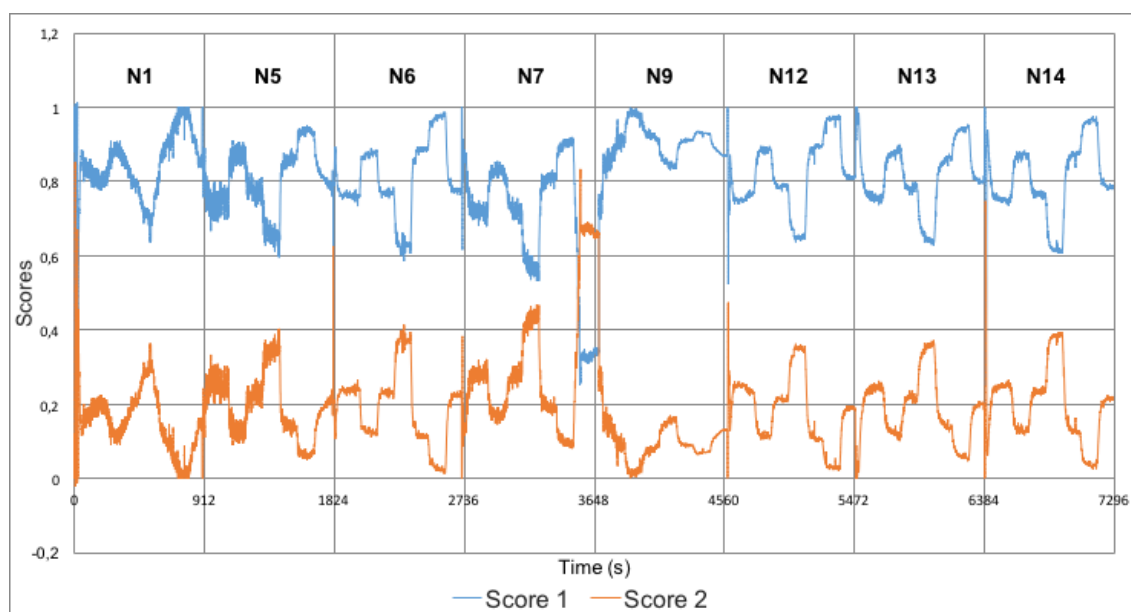


Figure 33 - Scores (first and second component) obtained from the MCR model for the eight runs containing MCC.

Each vertical line along the horizontal axis represents the end of a run and the beginning of another, or in other terms, the place where the matrices were concatenated, about every 912 seconds apart. The run order displayed in the graph is the same as listed above: N1, N5, N6, N7, N9, N12, N13 and N14.

The MCR values for the scores (the concentrations in an arbitrary scale) need to be normalized with a correction factor that should be additive but can also be multiplicative in order to reflect the real mass fractions (or concentrations) of the components of the binary mixture. A simple scale conversion equation correction was applied to both series of data (paracetamol and MCC). This will adjust the scores of the two components (related to the two substances in the binary mixture), in order for the sum of both at any given time to be constant and close to 1 or 100%.

Since the line equation is represented by:

$$y = mx + b$$

The multiplicative factor will be the slope  $m$  which will vertically stretch or shrink the data series profile, and the additive factor will be the y axis intercept  $b$  which will move the data series up or down the y axis. The line equations used as correction factors were the following.

$$\text{Paracetamol } y = 83.3x - 13$$

$$\text{MCC } y = 76.9x + 31$$

By applying the correction factors to the raw MCR scores, and plotting the paracetamol and MCC series on a 0 to 100% scale we obtain the following graph in Figure 34.

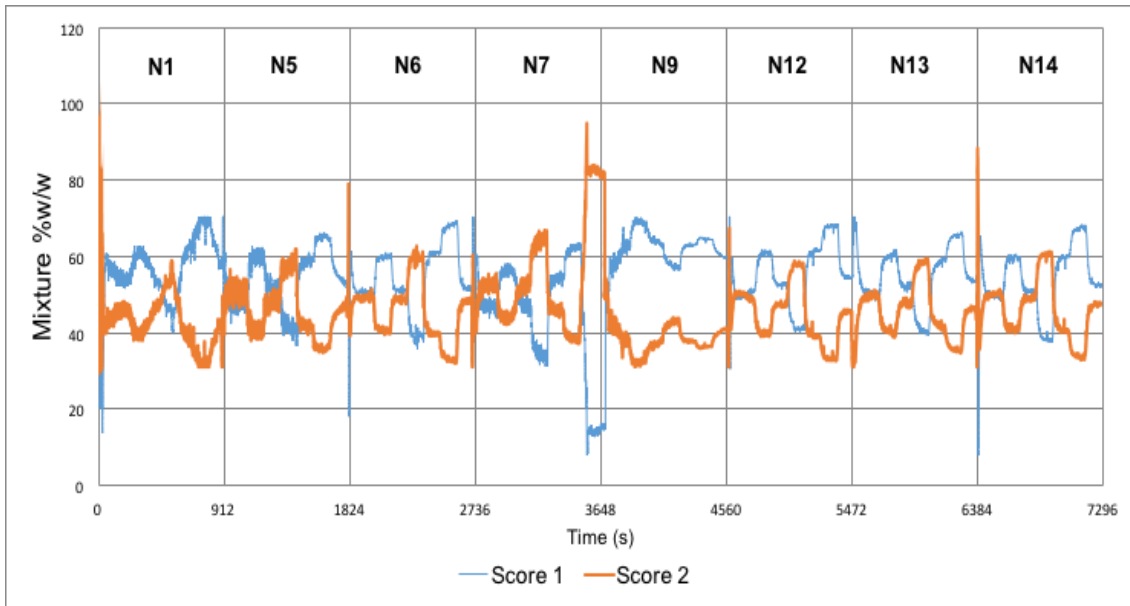


Figure 34 - Corrected scores (first and second component) obtained from the MCR model for the eight runs containing MCC

Since MCR allows us to determine the amount of paracetamol in a mixture in real time, it is useful and interesting to compare the profiles of each run obtained with the MCR technique to the ones obtained with PCA. Besides experiment N6 that has been used as an example, a few others will also be presented for the sake of diversity and accuracy.

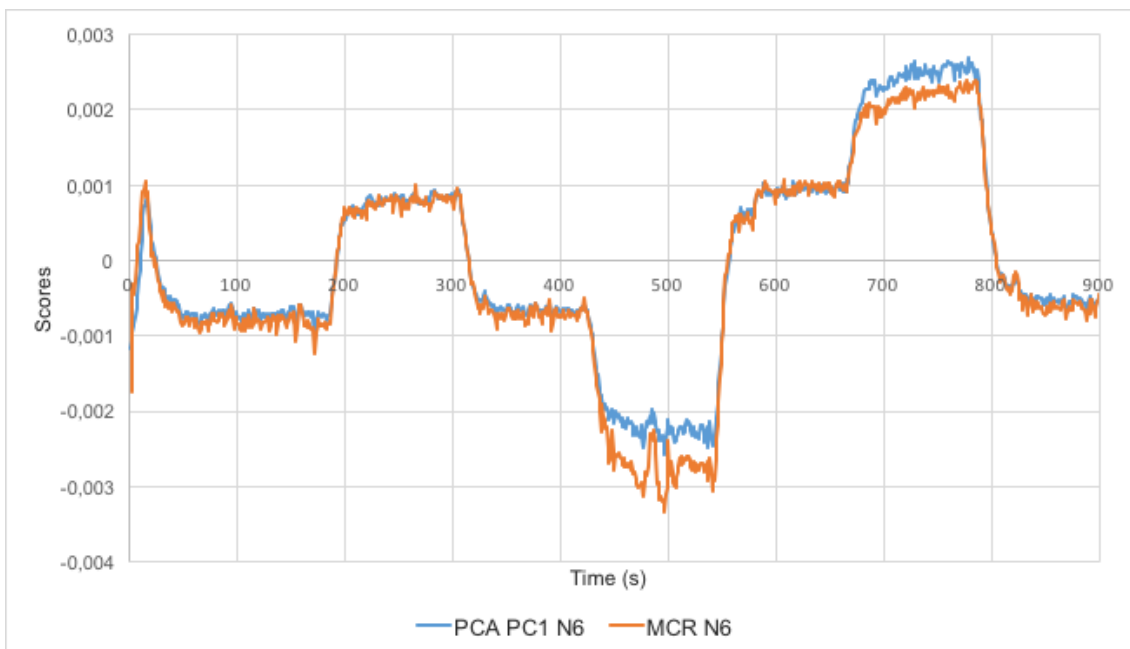


Figure 35 - Overlay of the first component profiles obtained for the PCA (blue) and MCR (orange) models for experiment N6.



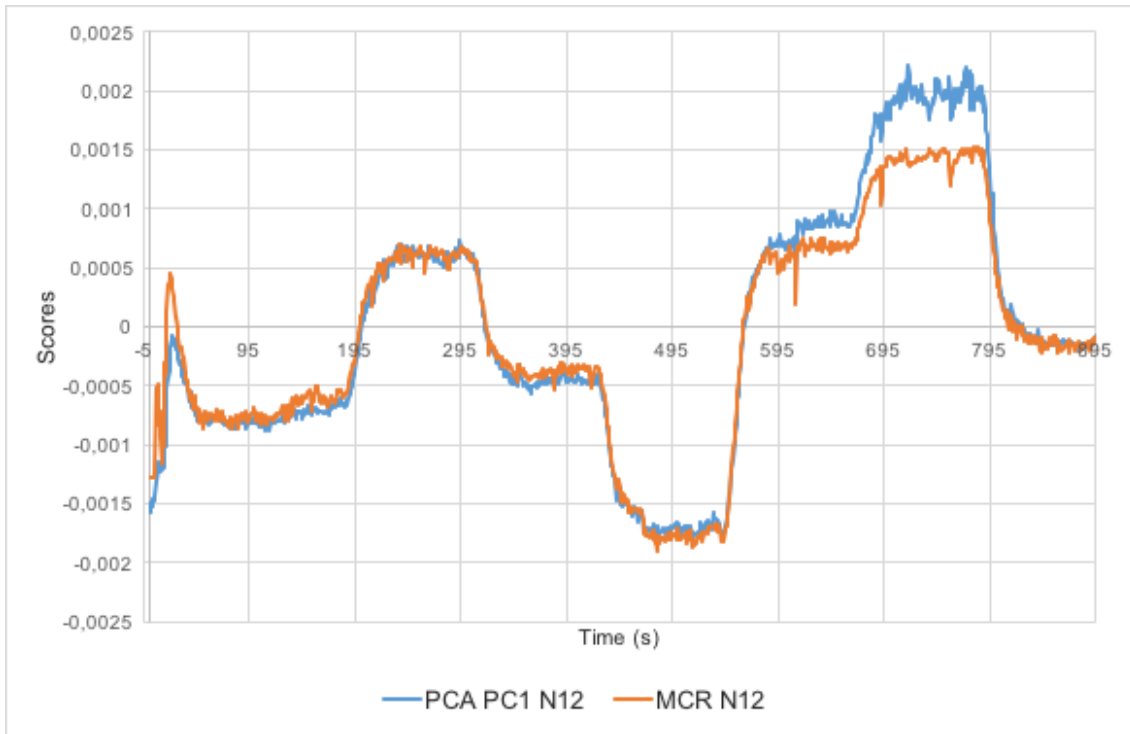


Figure 36 - Overlay of the first component profiles obtained for the PCA (blue) and MCR (orange) models for experiment N12.

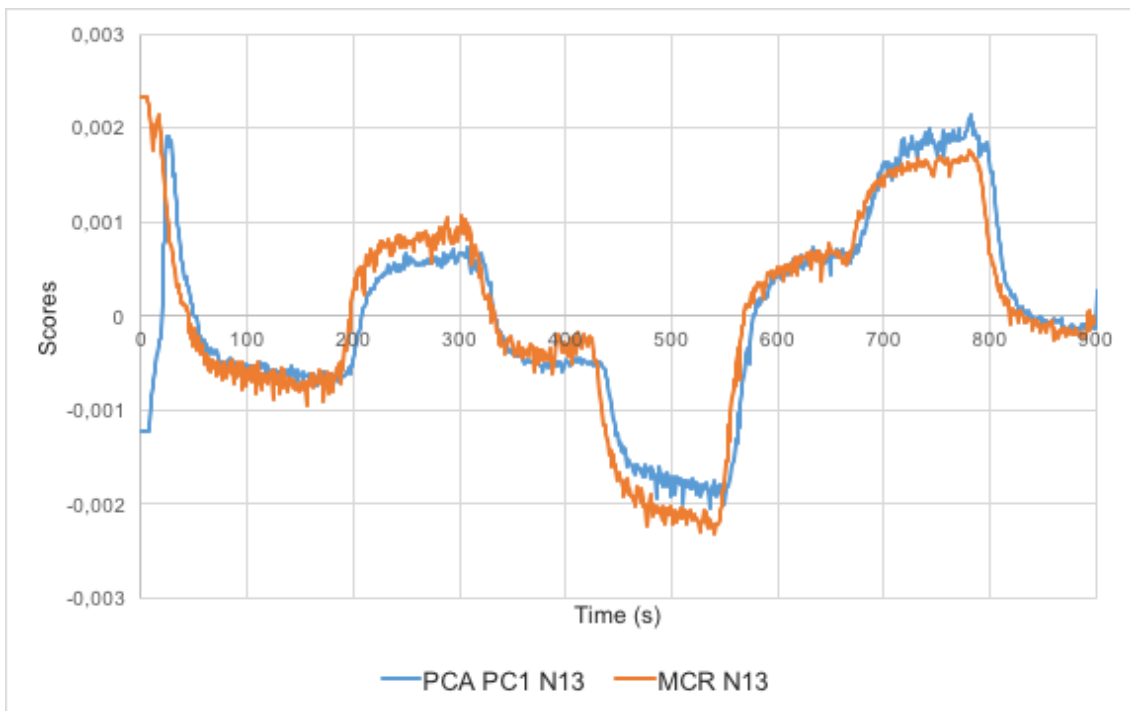


Figure 37 - Overlay of the first component profiles obtained for the PCA (blue) and MCR (orange) models for experiment N13.

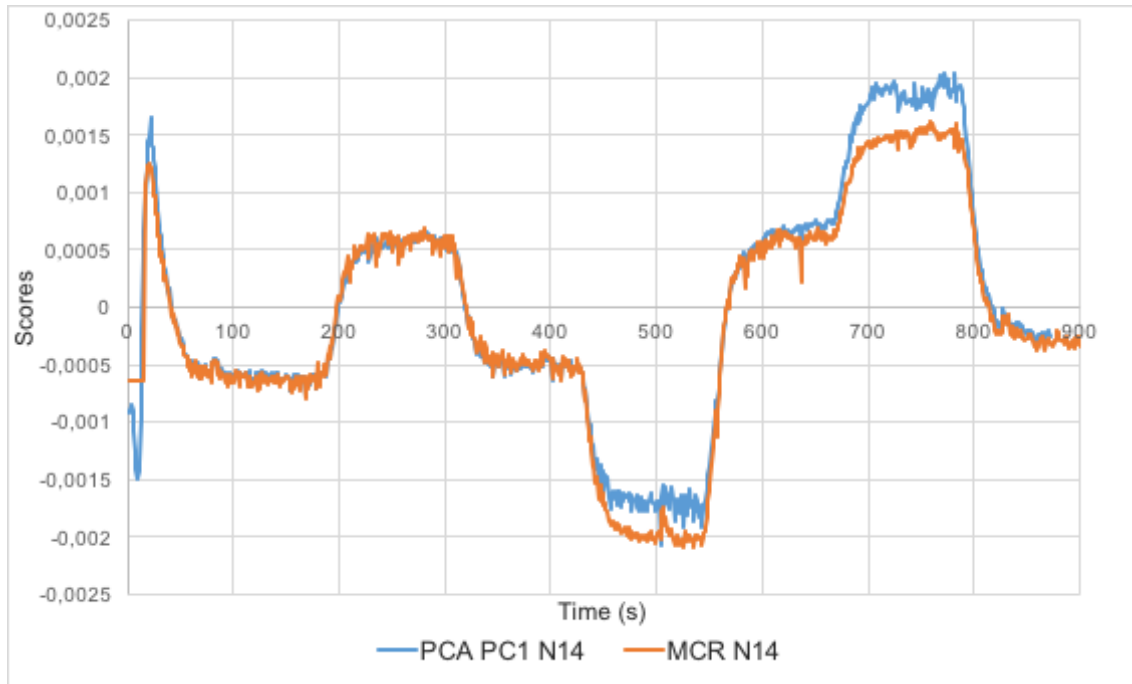


Figure 38 - Overlay of the first component profiles obtained for the PCA (blue) and MCR (orange) models for experiment N14.

As can be seen in Figure 35 to Figure 38 the profiles obtained with MCR resemble quite closely the ones obtained with PCA. It is interesting to verify that PCA manages to represent almost the same paracetamol step change profile in each experiment, even without being given the pure substance spectra. It can also be observed that the regions where PCA seems to deviate more noticeably from MCR are the extremes, namely the 40% and 70% step changes. The reasons for this are intrinsic to the techniques, since both used the same set of raw NIR data acquired in the same equipment.

Overall it is possible to say that the MCR results confirm and reinforce the PCA results most importantly in the first step change from the initial 50% to 60%, which is the step change used to calculate the RTD. In this region three out of the four experiments presented, had an almost perfect fit between the MCR and PCA profile, suggesting that the first step change data is the best choice for RTD calculation.

All results presented in the exploratory analysis correspond to experiments in which MCC was used. Unfortunately DCP NIR data did not allow for PCA or MCR implementation. This was due to the fact that DCP has a much lower absorbance across the whole NIR spectrum as can be observed in Figure 39. Because of this, the only signal detected by the spectral camera was that of paracetamol, making it impossible for the techniques used to distinguish one from the other.

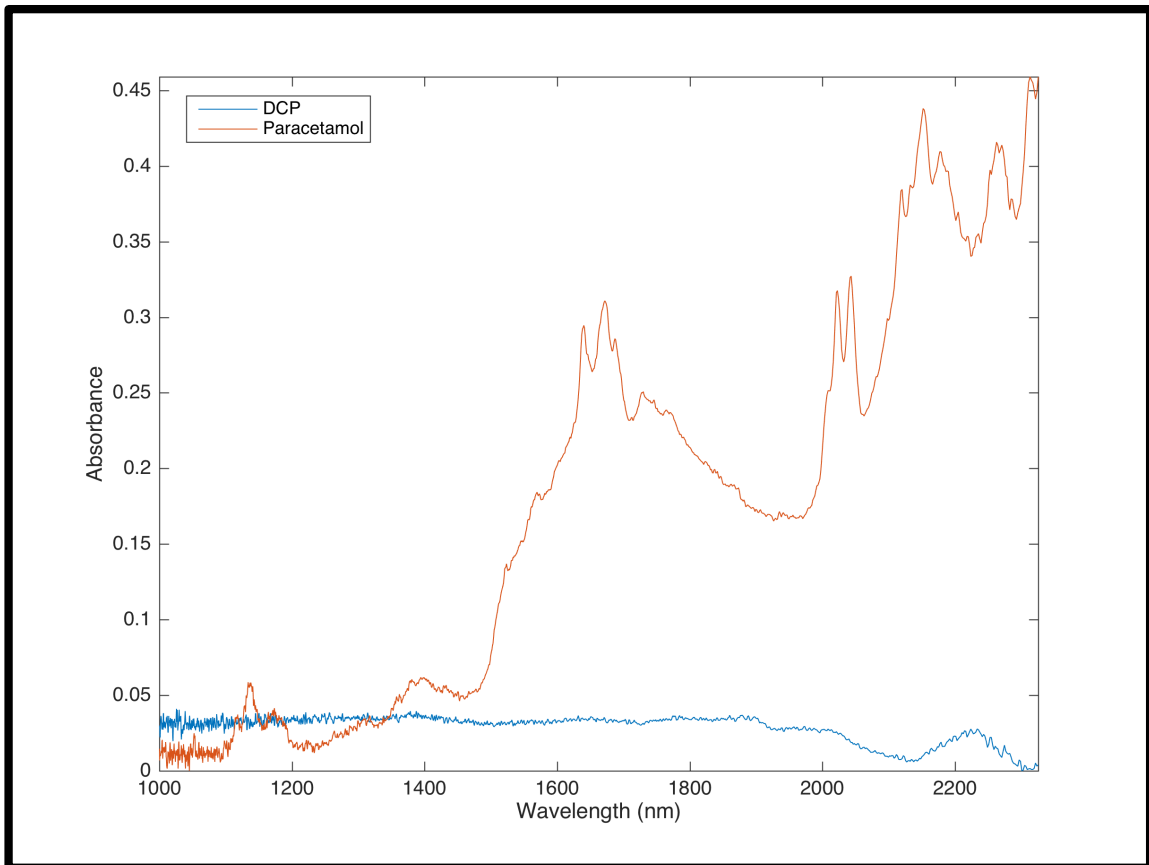


Figure 39 - DCP and paracetamol raw NIR spectra encompassing the region 1000–2500 nm

## 5.2 Residence time distribution calculation

For the curve fitting and function integration process, experiment N6 will be used as an example. As can be seen in Figure 40, the Weibull sigmoidal 5 parameter function fits the dataset of the 50% to 60% step change quite well.

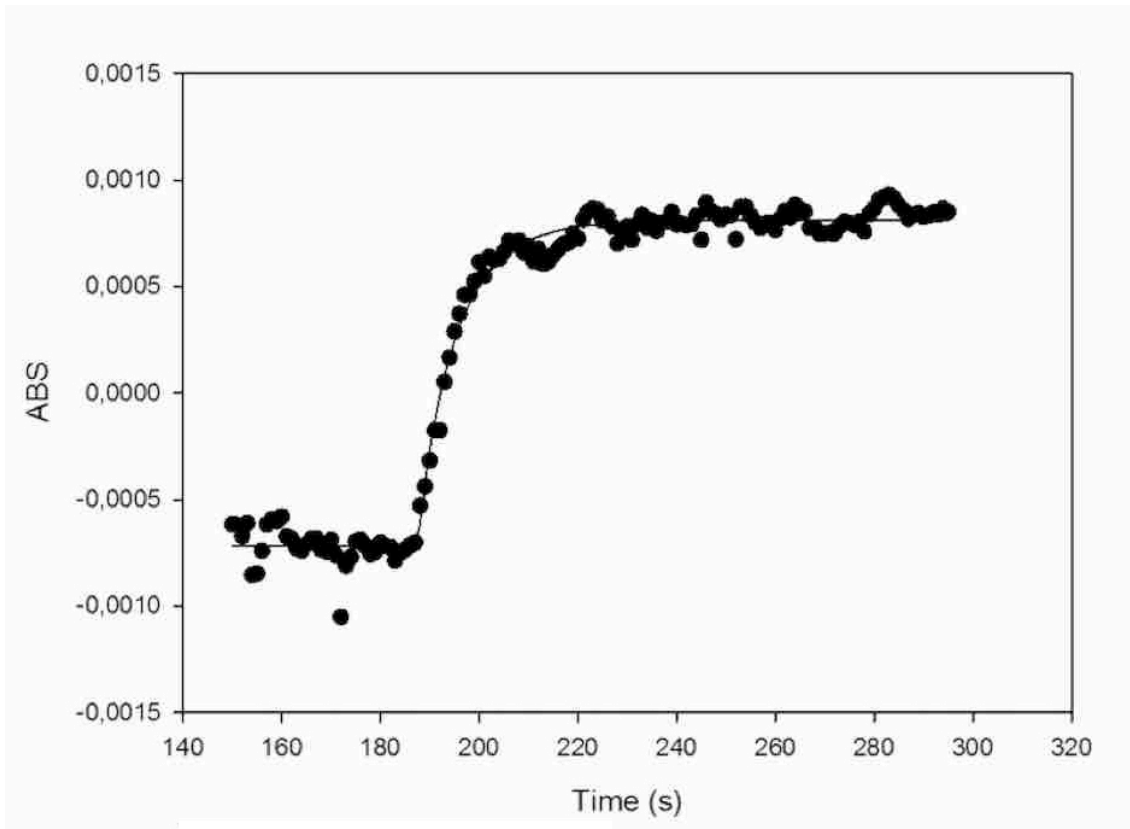


Figure 40 - Weibull Sigmoid function fitting for the 50% to 60% step change for experiment N6.

• Time (s) vs NIR PCA data; — Time (s) vs Fitted prediction

After fitting the Weibull function and determining and plotting its differential we obtain the residence time distribution in Figure 41. Then integrating  $t \cdot E(t)$  we obtain the mean residence time of  $\tau = 12,86s$ .

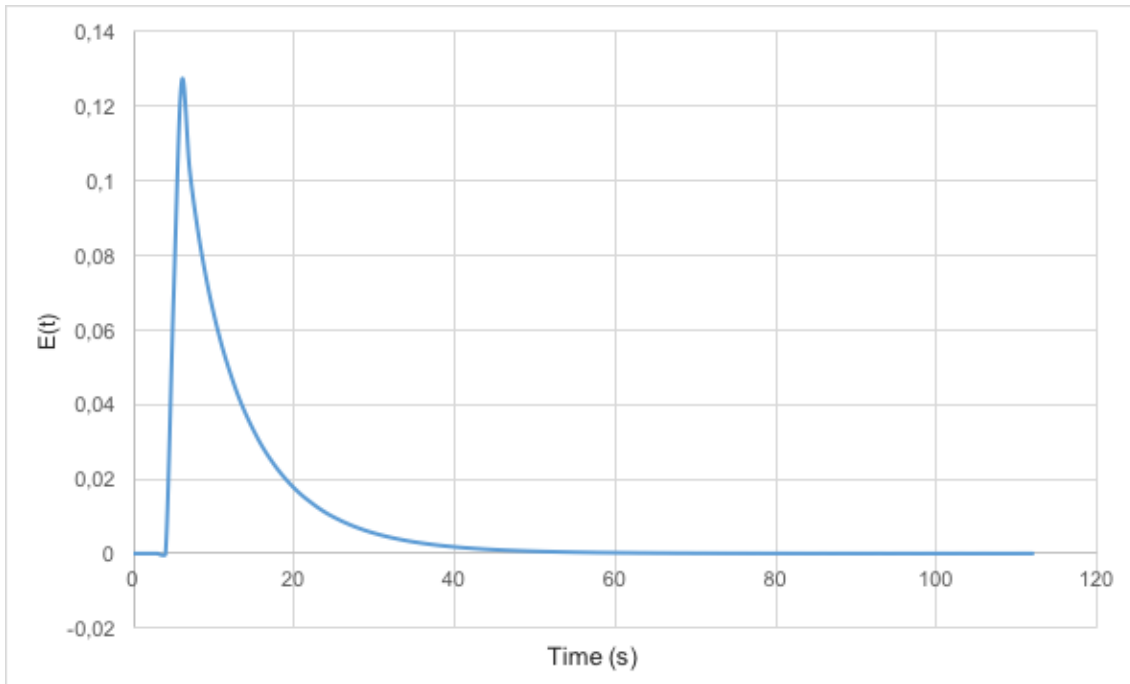


Figure 41 – Function  $E(t)$  representing the residence time distribution for experiment N6

Table 4 presents a summary of all the values calculated for this portion of the experimental work as well as the mass hold, and the bulk residence time for all experiments.

Table 4 - Mass hold and residence time for the produced experiments.

Exp.	Run Order	Total Feed rate (kg/h)	Mixer rpm	Port	Excipient	Mass hold after the run (g)	Bulk residence time (s)	Residence time from NIR data (s)	Variance $\sigma^2$	Standard Deviation $\sigma$
N12	1	10	900	A	MCC	42	15.12	19.63	165.30	12.86
N1	2	5	300	A	MCC	149	107.28	Poor resolution		
N10	3	5	1500	A	DCP	24	17.28	No NIR data		
N2	4	5	1500	B	DCP	25	18.00	No NIR data		
N11	5	5	300	B	DCP	219	157.68	No NIR data		
N9	6	5	1500	B	MCC	5	3.60	Poor resolution		
N5	7	15	1500	B	MCC	41	9.84	8.78	17.89	4.23
N7	8	15	300	B	MCC	142	34.08	10.80	68.08	8.25
N3	9	15	300	B	DCP	253	60.72	No NIR data		
N13	10	10	900	A	MCC	48	17.28	31.63	206.26	14.36
N6	11	15	1500	A	MCC	37	8,88	12.86	72.18	8.50
N4	12	15	1500	A	DCP	31	7.44	No NIR data		
N8	13	15	300	A	DCP	206	49.44	No NIR data		
N14	14	10	900	A	MCC	57	20.52	17.89	96.19	9.80

The experiments made with DCP had no usable NIR data, and some made with MCC (N1 and N9) had insufficient resolution on the sigmoid step change area to be able to determine the residence time from the NIR data.

The possible explanation for the poor resolution in N1 and N9 experiments is the slower 5 kg/h total feed rate which both share as a common setting. With that in mind both, N1 and N9 experiments were later repeated after this thesis experimental campaign was over, but with total feed rates of 7.5 kg/h and 10 kg/h. Those produced better results in relation to the NIR data with the 7.5 kg/h allowing to see the step changes albeit with some noise, and the 10 kg/h produced even better usable results. These results indicate that the total feed rate is indeed an important process parameter in regard to the NIR integration sphere performance, and that its minimum ideal set point for this process might be around 10 kg/h.

### 5.3 UV-Vis measurements

The results of the measurements taken to build the calibration curve are presented in Table 5 and Figure 42. The results indicate a good linear response in the range of concentrations measured. That is an assurance that the UV-Vis equipment is able to reliably measure the sample solutions allowing for an accurate determination of the amount of paracetamol in the sample, and thus determine sample homogeneity.

Table 5 - UV-Vis calibration curve measurement results

Paracetamol solution concentration ( $\mu\text{g/mL}$ )	Absorbance at $\lambda=242$ nm			
	Sample A	Sample B	Sample C	Abs average
1	0.066	0.071	0.069	0.069
5	0.314	0.322	0.324	0.320
10	0.653	0.658	0.656	0.656
15	0.911	0.964	0.966	0.947
20	1.296	1.295	1.311	1.301
25	1.548	1.615	1.617	1.593

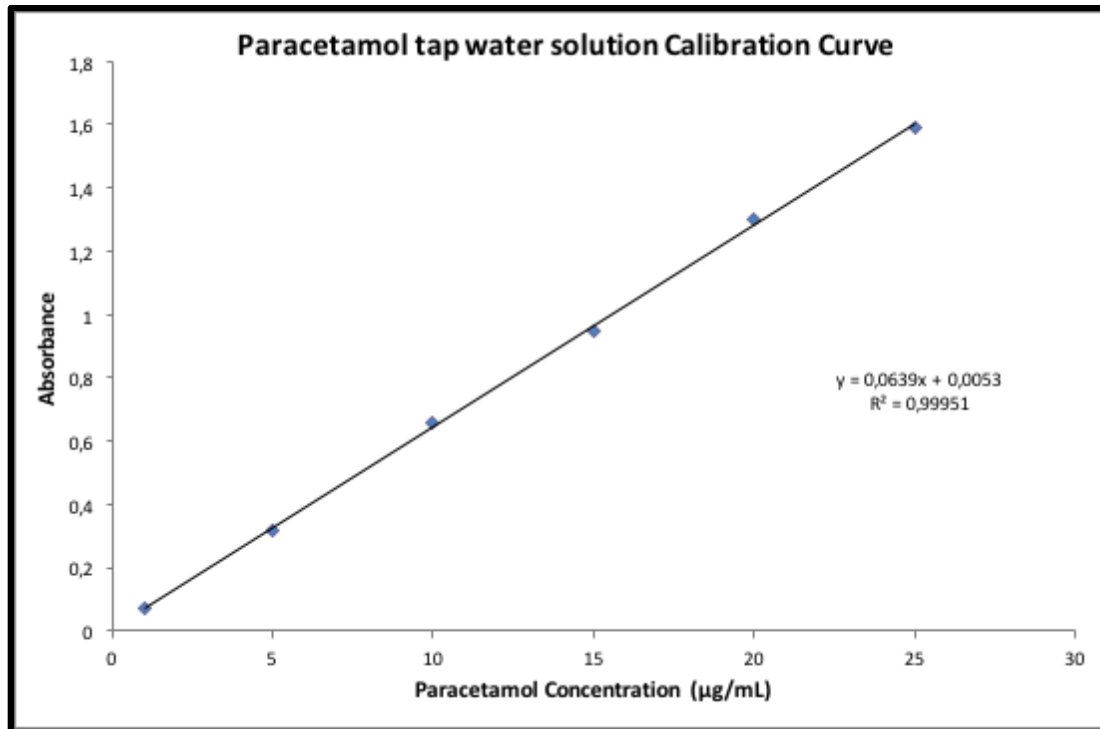


Figure 42 - UV-Vis Calibration Curve

After collecting all the UV-Vis data from the selected powder samples we proceeded by comparing the real UV-Vis measured values from the samples with the theoretical feeder data registry from the computer. The results were plotted in the following graphs from Figure 43 to Figure 56.

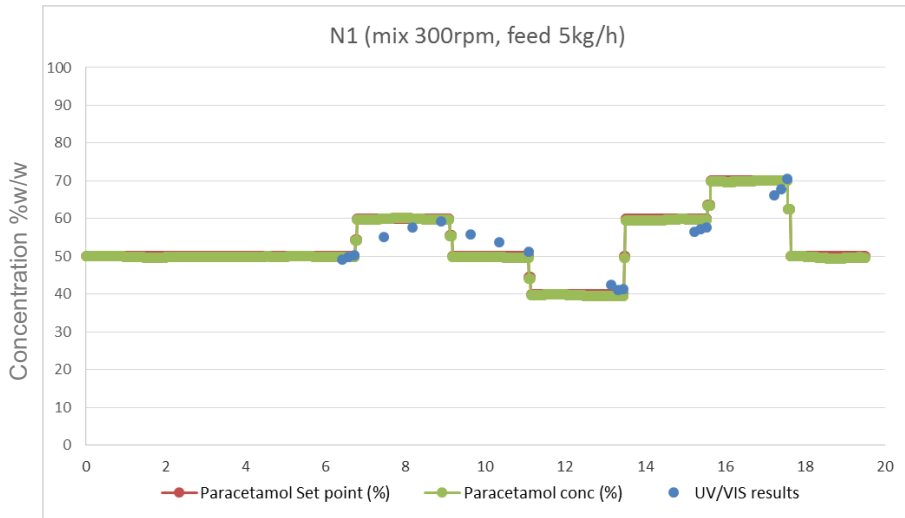


Figure 43 – Overlay of paracetamol feeder setpoint, real fed paracetamol concentration and UV-Vis measured results for experiment N1

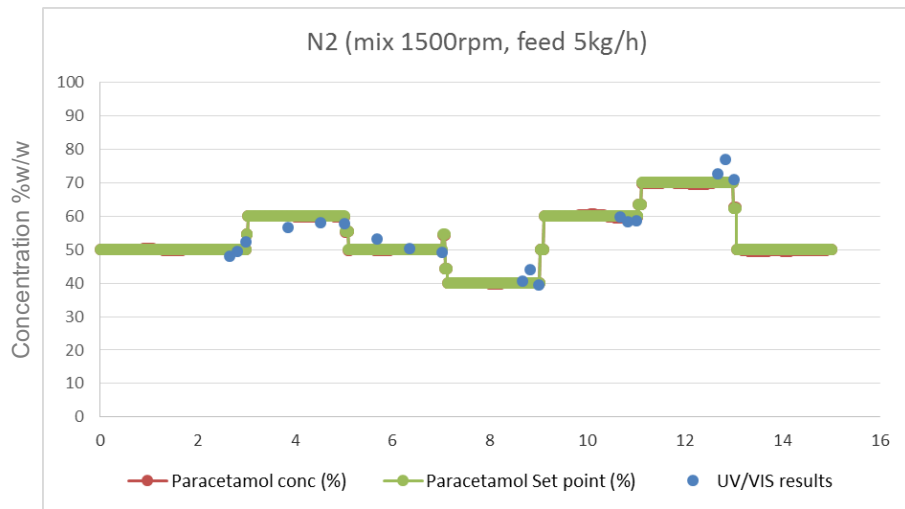


Figure 44 - Overlay of paracetamol feeder setpoint, real fed paracetamol concentration and UV-Vis measured results for experiment N2

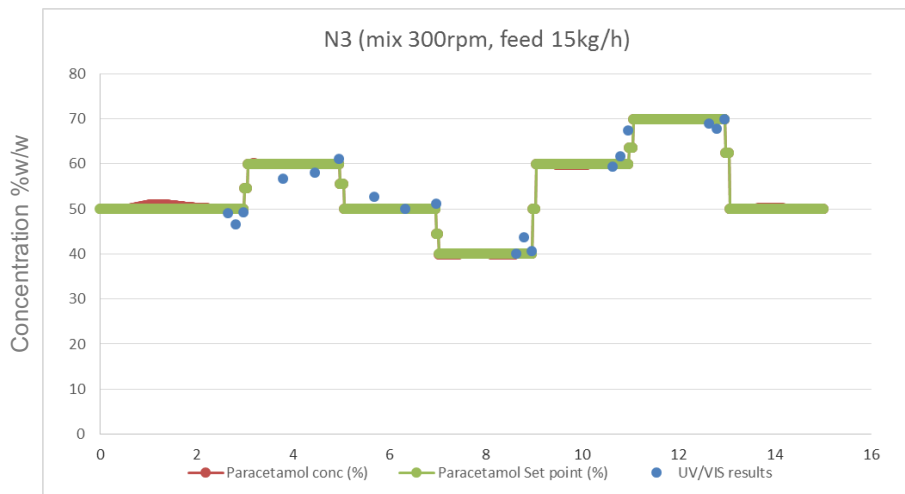


Figure 45 - Overlay of paracetamol feeder setpoint, real fed paracetamol concentration and UV-Vis measured results for experiment N3



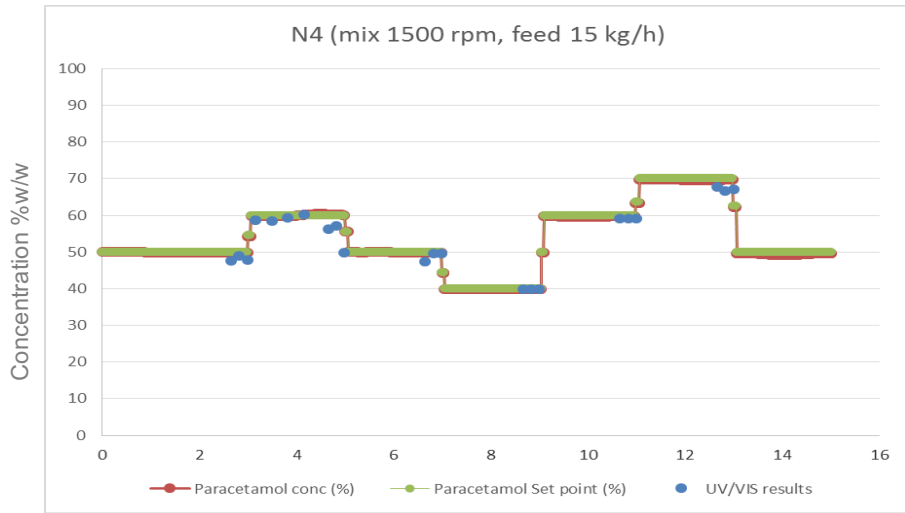


Figure 46 - Overlay of paracetamol feeder setpoint, real fed paracetamol concentration and UV-Vis measured results for experiment N4

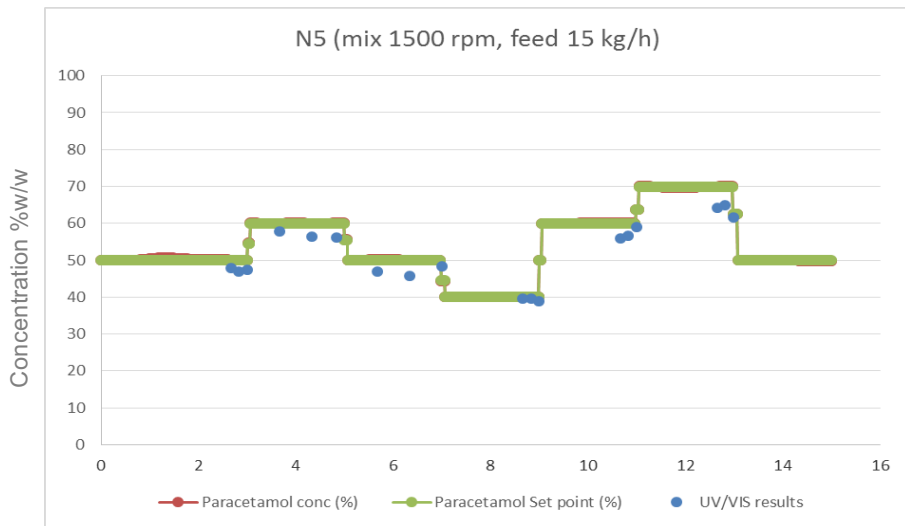


Figure 47 - Overlay of paracetamol feeder setpoint, real fed paracetamol concentration and UV-Vis measured results for experiment N5

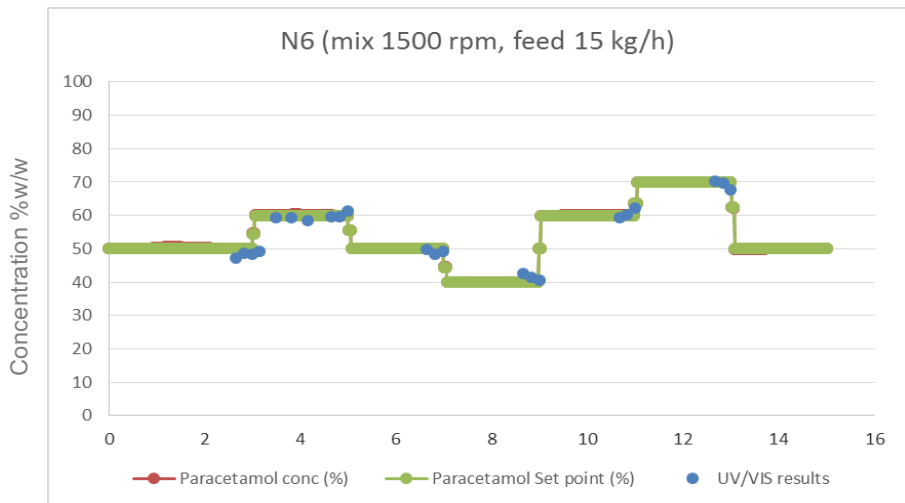


Figure 48 - Overlay of paracetamol feeder setpoint, real fed paracetamol concentration and UV-Vis measured results for experiment N6

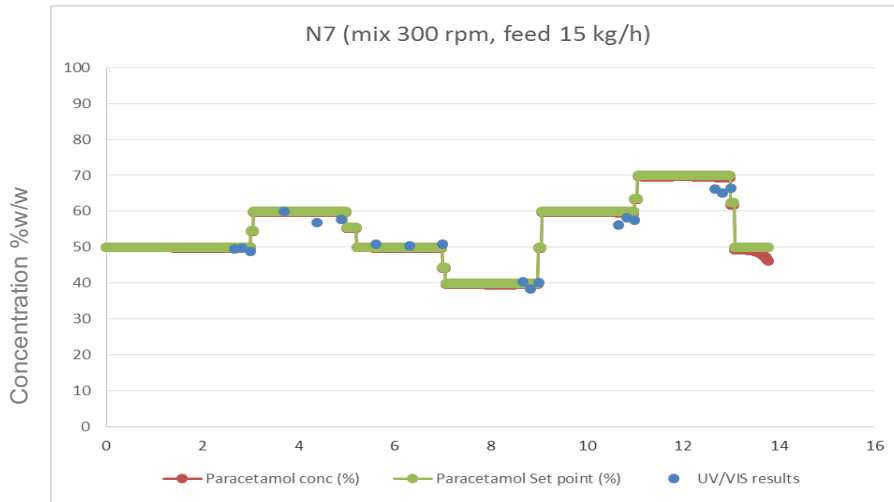


Figure 49 - Overlay of paracetamol feeder setpoint, real fed paracetamol concentration and UV-Vis measured results for experiment N7

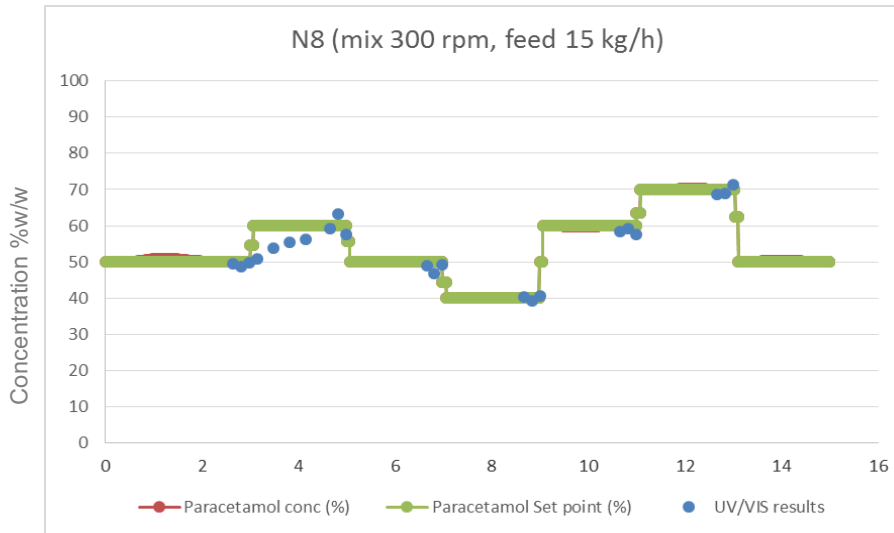


Figure 50 - Overlay of paracetamol feeder setpoint, real fed paracetamol concentration and UV-Vis measured results for experiment N8

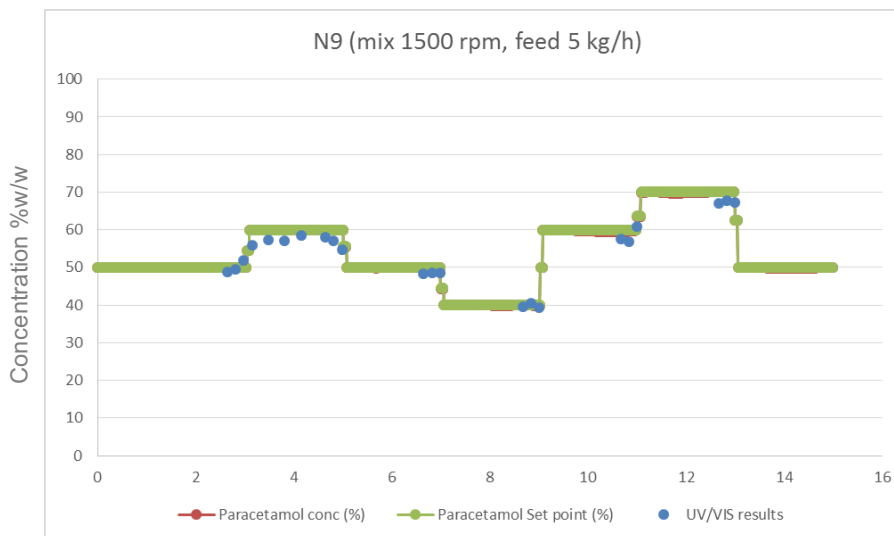


Figure 51 - Overlay of paracetamol feeder setpoint, real fed paracetamol concentration and UV-Vis measured results for experiment N9

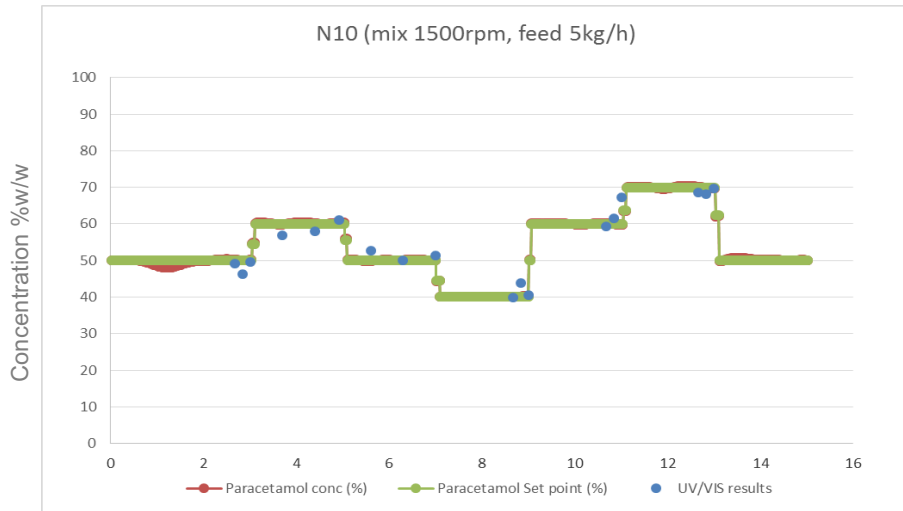


Figure 52 - Overlay of paracetamol feeder setpoint, real fed paracetamol concentration and UV-Vis measured results for experiment N10

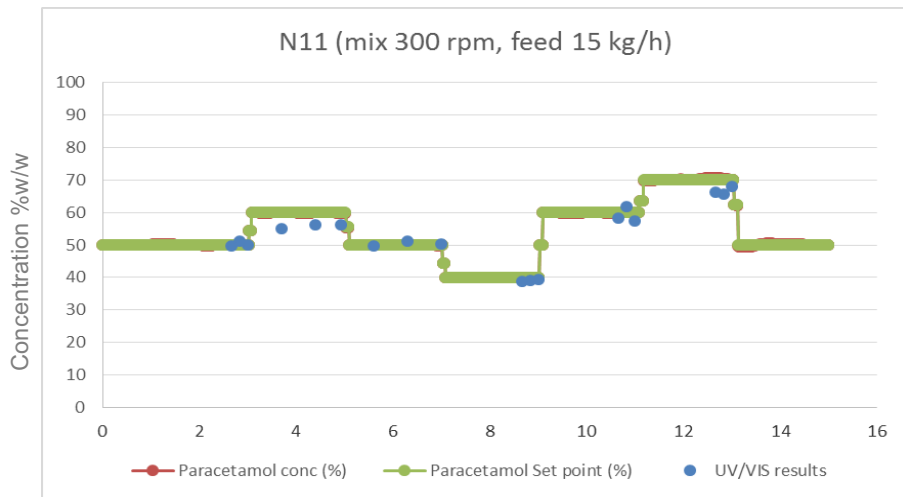


Figure 53 - Overlay of paracetamol feeder setpoint, real fed paracetamol concentration and UV-Vis measured results for experiment N11

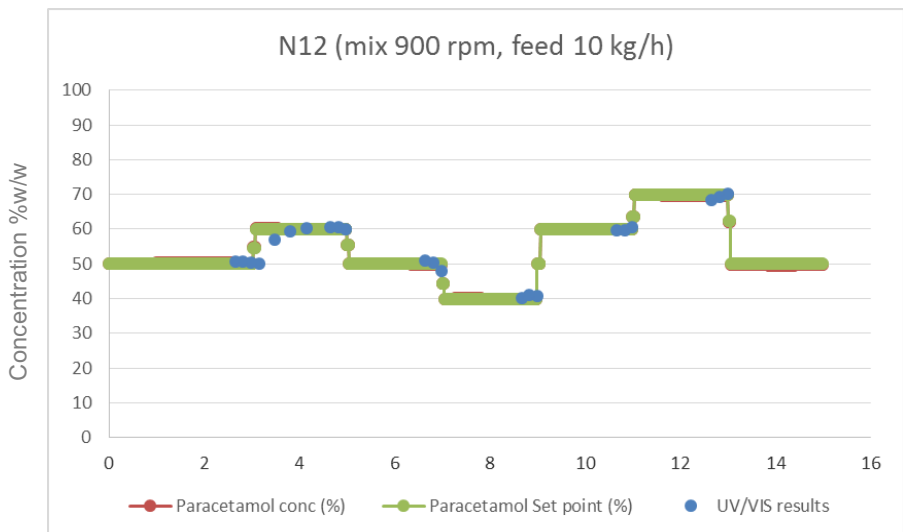


Figure 54 - Overlay of paracetamol feeder setpoint, real fed paracetamol concentration and UV-Vis measured results for experiment N12

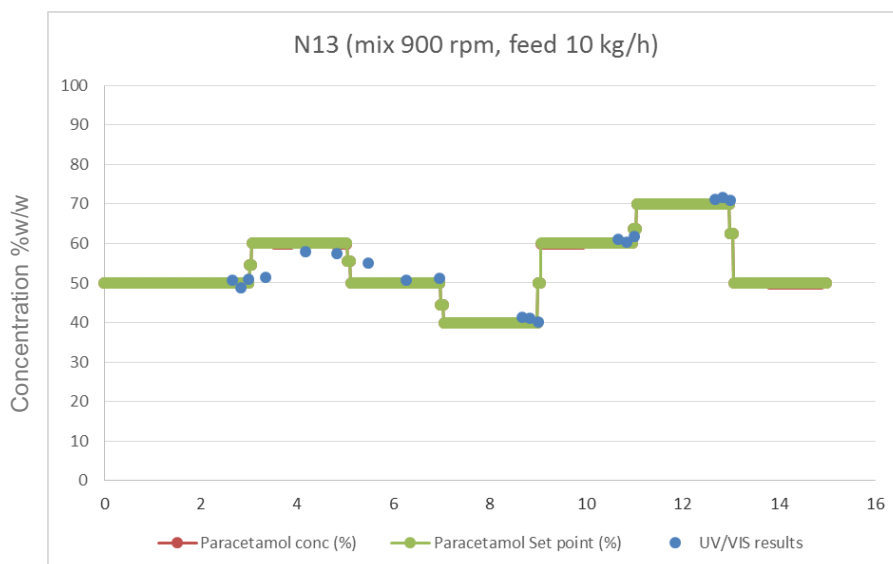


Figure 55 - Overlay of paracetamol feeder setpoint, real fed paracetamol concentration and UV-Vis measured results for experiment N13

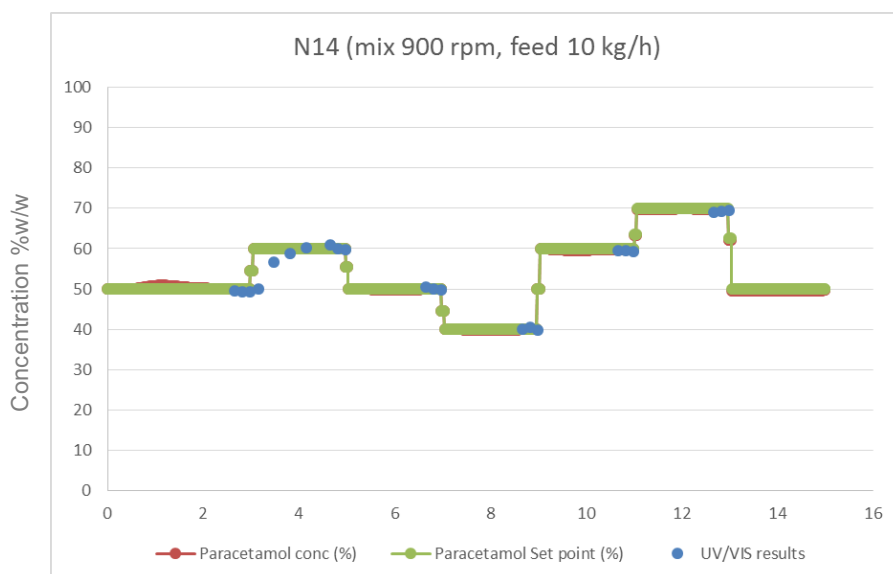


Figure 56 - Overlay of paracetamol feeder setpoint, real fed paracetamol concentration and UV-Vis measured results for experiment N14

Examining the profiles from Figure 43 to Figure 56 it is possible to say that overall the mixing performance of the experimental setup is quite good since the UV-Vis measurements are very close to the feeder data in terms of mixture homogeneity. Moreover it was also possible to calculate the relative standard deviation (RSD) between the UV-Vis measurements and the feeder registry data. These results, presented in Table 6 and Figure 57, allow for a much more detailed and methodical approach to homogeneity and mixing performance evaluation. All the experiments are well below the 5% limit according to industry guidelines, with only three experiments (N2, N3 and N10) having a RSD between 3% and 4%. This indicates that the mixing setup utilized in the

experimental work provided excellent mixing performance across a wide range of settings.

Table 6 - Relative standard deviation between UV-Vis results and feeder registry data.

Target %	RSD%													
	N1	N2	N3	N4	N5	N6	N7	N8	N9	N10	N11	N12	N13	N14
50	1.10	3.39	2.56	1.25	0.99	1.28	0.71	0.78	2.62	3.05	1.10	0.30	1.85	0.21
40	1.39	4.60	3.90	0.14	0.75	2.06	2.34	1.37	1.46	4.12	0.72	0.90	1.14	0.83
60	0.74	1.10	5.32	0.11	2.30	1.99	1.52	1.20	2.97	5.38	3.33	0.64	0.91	0.09
70	2.55	3.38	1.26	0.65	2.26	1.59	0.88	1.70	0.31	1.05	1.52	1.03	0.46	0.30
<b>Average RSD</b>	<b>1.24</b>	<b>3.39</b>	<b>3.23</b>	<b>0.39</b>	<b>1.63</b>	<b>1.79</b>	<b>1.20</b>	<b>1.28</b>	<b>2.04</b>	<b>3.59</b>	<b>1.31</b>	<b>0.77</b>	<b>1.02</b>	<b>0.26</b>

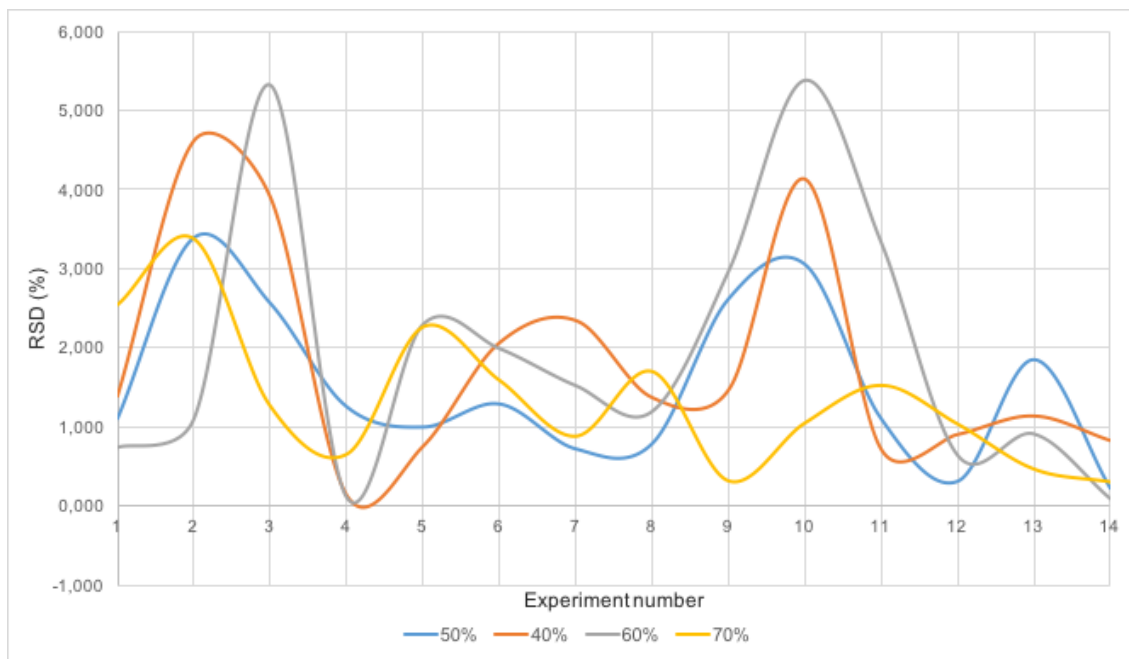


Figure 57 - RSD according to experiment number and concentration step

## 5.4 System variables influence over response parameters

Process data was introduced into the Modde software worksheet and used to build PLS models for the four response parameters presented in Table 7. Linear models without interactions were calibrated for the four parameters.

Table 7 – Data introduced into the Modde worksheet to build the PLS models. The input variables were: feed rate, mixer speed, port and excipient; and the responses were: bulk residence time, mass hold at the end of run, mass hold at 180s and RSD.

Exp Name	Run Order	Incl/Excl	Feed Rate	Mixer Speed	Port	Excipient	Bulk Residence Time	Mass Hold at End of Run	Mass Hold at 180s	RSD
N1	2	Incl	5	300	A	MCC	107,28	149	106,45	1,24
N2	4	Incl	5	1500	B	DCP	18	25	29,37	3,39
N3	9	Incl	15	300	B	DCP	60,72	253	192,724	3,23
N4	12	Incl	15	1500	A	DCP	7,44	31	8,2	0,39
N5	7	Incl	15	1500	B	MCC	9,84	41	52,74	1,63
N6	11	Incl	15	1500	A	MCC	8,88	37	17,58	1,79
N7	8	Incl	15	300	B	MCC	34,08	142	139,8	1,2
N8	13	Incl	15	300	A	DCP	49,44	206	206,63	1,28
N9	6	Incl	5	1500	B	MCC	3,6	5	30,72	2,04
N10	3	Incl	5	1500	A	DCP	17,28	24	78,49	3,59
N11	5	Incl	5	300	B	DCP	157,68	219	113,77	1,31
N12	1	Incl	10	900	A	MCC	15,12	42	49,94	0,77
N13	10	Incl	10	900	A	MCC	17,28	48	38,46	1,02
N14	14	Incl	10	900	A	MCC	20,52	57	64,2	0,26

We can look at the results of the linear models made by Modde regarding the bulk residence time (BRT) results (Figure 58). Not much can be said except that the mixer speed negatively affects the BRT, or in other words, a higher mixer speed causes a lower BRT due to the fact that particles are pushed faster and move more rapidly when a higher mixer speed is in place.

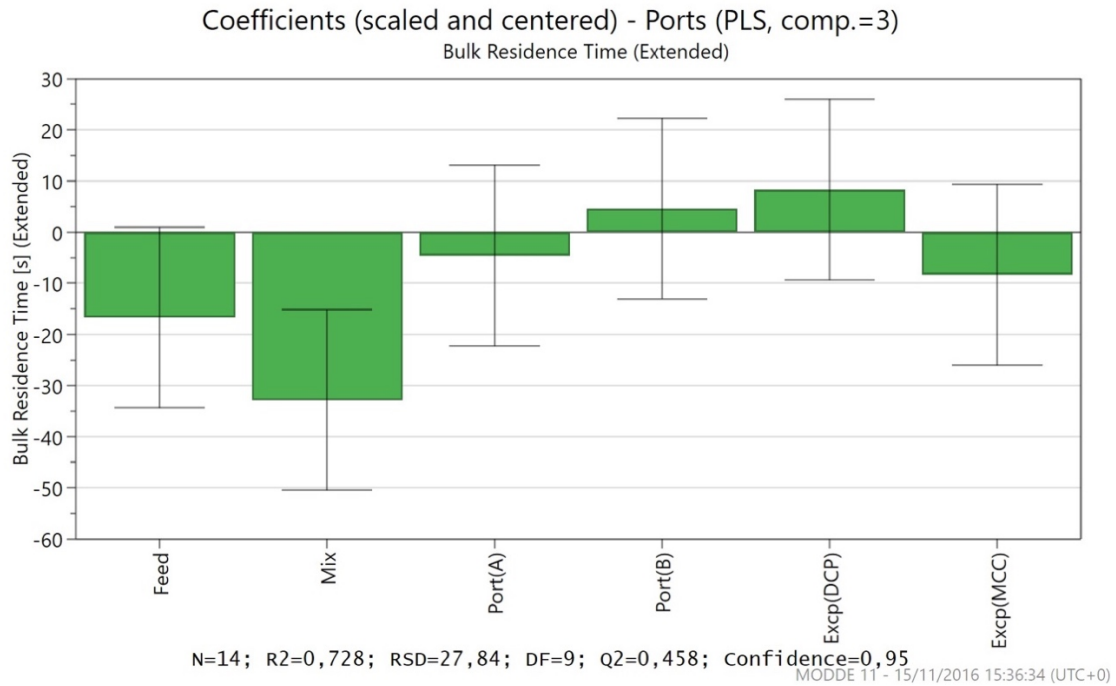


Figure 58 - Regression coefficients for the bulk residence time model developed including error bars for assessing coefficients significance.

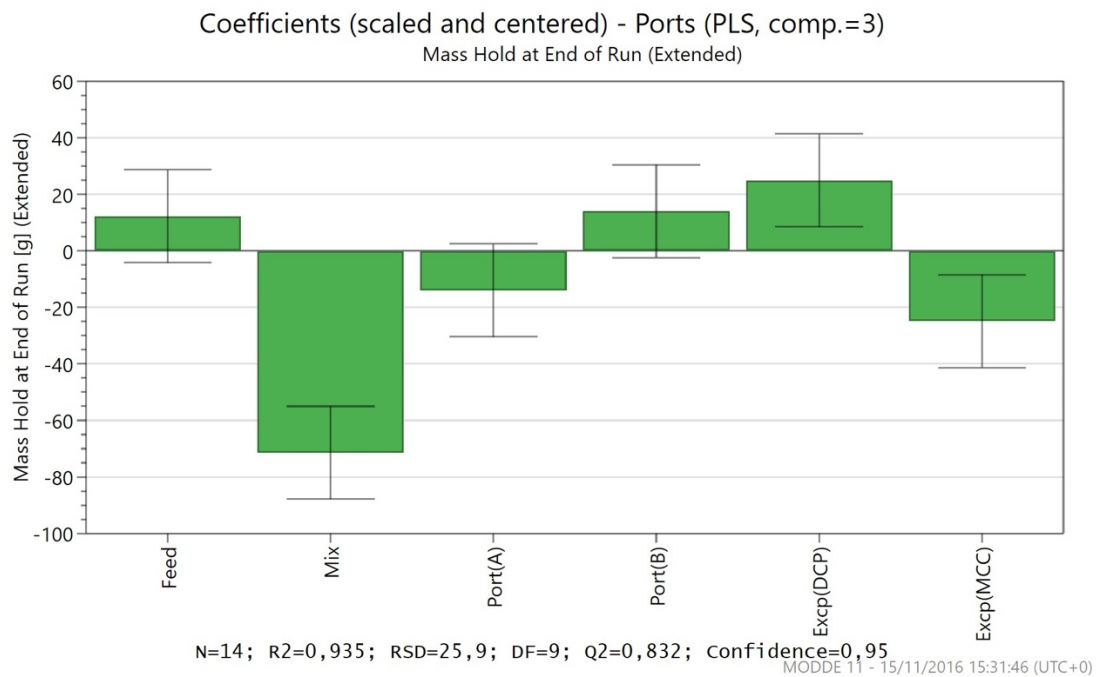


Figure 59 - Regression coefficients for the mass hold at the end of the run model developed including error bars for assessing coefficients significance.

Regarding the model for mass hold at the end of the run (Figure 59), it is possible to verify that both mixer speed and the use of MCC as an excipient contribute negatively to the mass hold. Once again this can be explained, because when the mixer speed is higher, less mass remains inside the mixer at the end of the experiment. MCC also

contributes negatively because of its inferior density compared to DCP. When occupying the same volume inside the mixer at the end of a run, DCP weights more than MCC and thus has more mass.

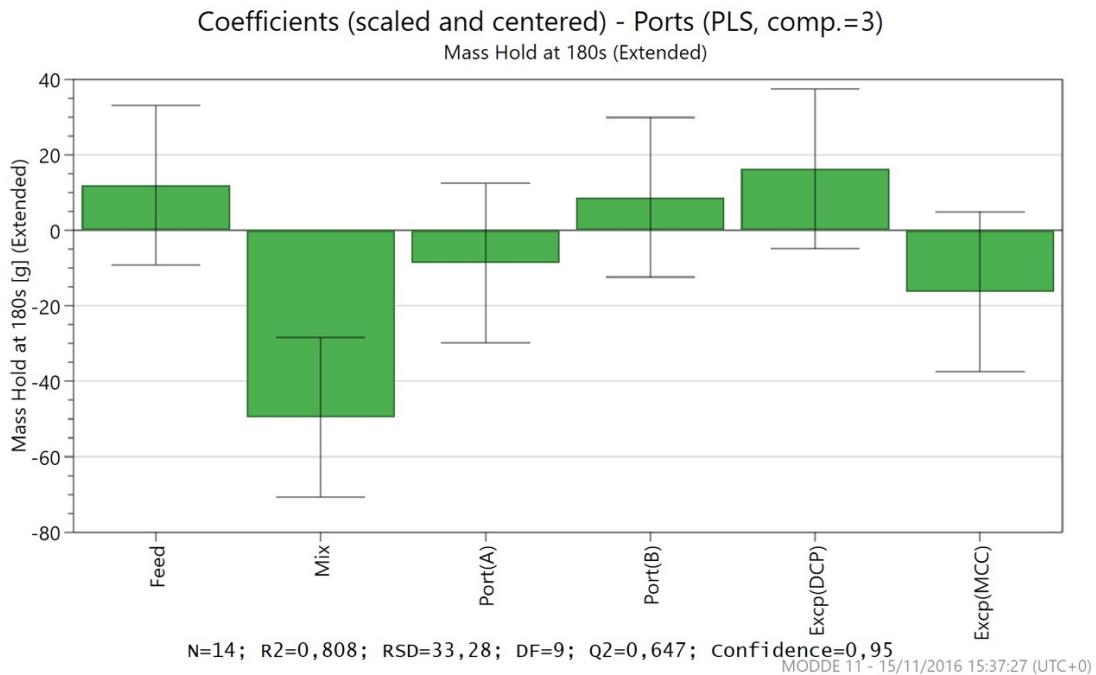


Figure 60 - Regression coefficients for the mass hold at 180s model developed including error bars for assessing coefficients significance.

The mass hold at 180 seconds coefficients (Figure 60) corroborate those at the end of the run, although with a higher uncertainty.

Finally, looking at the coefficients for the RSD model (Figure 61) it is difficult to extract any conclusions due to the high uncertainty, even though the UV-Vis measurements were quite accurate and the feeder registry data as well.

These results indicate that for the selected setpoint ranges, the RSD values between the feeder registry data and the UV-Vis measurements, are not significantly influenced by any of the system variables. This might also indicate that for almost every feeder and mixer setting the powder mixture is always very homogenous, thus instead of being related to process variables, the RSD values are more tightly related to the detection error of both techniques.



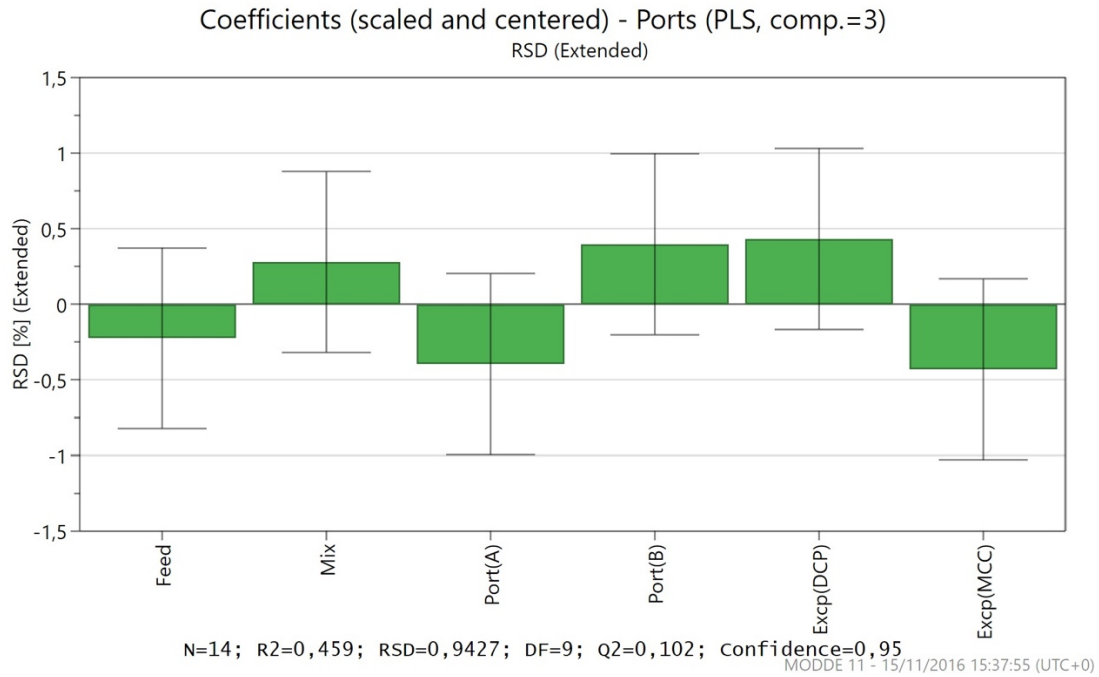


Figure 61 - Regression coefficients for the relative standard deviation developed model including error bars for assessing coefficients significance.

In order to see if the model results could be improved, another set of models were made without the inclusion of the inlet port qualitative variable, since this was the one that had the smallest statistical significance. The resulting models did not have a significant difference from the original ones and therefore were discarded.

Overall, the mixer speed variable seems to be the most important CPP.

## Chapter 6

### Conclusions

This work resourced on the definition of a set of experiments based on an experimental design to evaluate the performance of a continuous mixing process. The designed process variables' conditions involved varying the total feed rate (5 to 15 kg/h), mixer speed (300 to 1500 rpm), excipient (MCC and DCP), and inlet port of the mixer (A or B). The measured process responses were: bulk residence time, mass hold, and mixture relative standard deviation. NIR spectroscopy was used to evaluate in real-time the performance of the mixing process.

One of the biggest limitations of this experimental work derived from using DCP as one of the excipients especially when making the measurements with NIR spectroscopy as DCP is not active in the NIR range. This made it impossible to obtain good NIR data for all experiments including DCP and thus no PCA or MCR analysis was possible for almost half of the produced experiments.

The NIR spectral camera was able to operate, through the integration sphere's innovative design, with multi-point signal acquisition for a good representative analysis of the flowing powder. This allowed for the PCA models to clearly identify the imposed disturbances or steps in raw-materials concentrations, and to detect the time needed for the process to achieve steady state operating conditions.

PCA based on acquired NIR spectra proved to be able to capture paracetamol and MCC concentrations over time. With these results we can clearly state that PCA can distinguish and quantify binary mixtures, provided that both substances have characteristic and unique absorption peaks within the measured spectral region. These results were confirmed through MCR analysis of spectral data, imposing the pure component spectral profiles. Results confirmed that after roughly 3 minutes, the system achieved steady state conditions, therefore the first step change from 50% to 60% was the best region of the experiment to determine the residence time distribution and mean residence time.

The mean residence time calculated from the NIR data had significant deviations from the bulk residence time calculated from the feeder registry and powder sample data. The

interpretation of these results is quite limited since it was only possible to calculate the mean residence time from the NIR data for six out of fourteen experiments.

Monitoring the paracetamol blend content by UV/Vis spectroscopy (off-line method) revealed a close match against the feeder registry data. Experimental data for all runs showed that the produced blends were within the industry's guideline 5% RSD limit. Since the RSD serves as a benchmark for mixture homogeneity, this shows us that the CM setup utilized in the experimental work provided excellent mixing performance across a wide range of settings.

Regression models between process parameters and quality attributes indicated that the mixer speed was the major CPP, having a negative contribution to both bulk residence time and mass hold. MCC content also revealed to have a negative contribution to mass hold due to its lower density.

According to the Modde regression model for the RSD, the RSD is not significantly influenced by any of the system variables. This indicates that the mixture is always very homogenous regardless of the feeder and mixer settings used, therefore the RSD values are more tightly related to the detection error of the UV-Vis and LIW feeding techniques.

## Future Perspectives

One of the biggest limitations of this experimental work derived from using DCP as one of the excipients. Other excipients that present a more adequate absorption spectrum in the NIR region should be used in order to obtain a full DoE data set. That will undoubtedly contribute to a better understanding of the continuous feeder and mixer setup and also to better results.

The mean residence time study for this feeder and mixer configuration remains significantly unexplored. Further data obtained with a full set of experiments of a new DoE should allow for the correlation between process variable settings and residence time values.

Regarding the NIR spectral camera, it would be extremely beneficial for future studies if the imaging spectrograph could be upgraded to support a wider detection range, ideally up to 2500 nm. This would greatly improve the quality of the NIR data in respect to substances' chemical and physical properties analysis, and allow for a better implementation of multivariate process control.

Throughout the experiments, low total feed rates of 5 kg/h produced consistently bad NIR data. It would be pertinent to further analyse the adopted NIR sampling strategy and to verify flow limits that guarantee adequate NIRS performance.

When the feeder / mixer system has been properly characterized with new DoE data, the next logical step would be to build prediction models for CQA's such as the powder mixture RSD. That along with the integration of another unit process, like dry granulation or direct compression via a screw conveyor transport system, would represent the long term approach in this field of study.

## References

1. Muzzio FJ, Shinbrot T, Glasser BJ. Powder technology in the pharmaceutical industry: The need to catch up fast. *Powder Technol.* 2002;124(1–2):1–7.
2. FDA. Powder Blends and Finished Dosage Units – Stratified In-Process Dosage Unit Sampling and Assessment. Draft Guidance. [Internet]. Pharmaceutical cGMPs. 2003. Available from:  
<http://www.fda.gov/downloads/Drugs/GuidanceComplianceRegulatoryInformation/Guidances/ucm070312.pdf>
3. FDA USD of H and HS. Guidance for Industry PAT — A Framework for Innovative Pharmaceutical Development, Manufacturing, and Quality Assurance. FDA Off Doc [Internet]. 2004;(September):16. Available from:  
<http://www.fda.gov/downloads/Drugs/GuidanceComplianceRegulatoryInformation/Guidances/ucm070305.pdf>
4. ICH. Pharmaceutical Development Q8(R2): ICH Harmonised Tripartite Guideline. In: International Conference on Harmonisation of Technical Requirements for Registration of Pharmaceuticals for Human Use [Internet]. 2009. p. 1–24. Available from:  
[http://www.ich.org/fileadmin/Public\\_Web\\_Site/ICH\\_Products/Guidelines/Quality/Q8\\_R1/Step4/Q8\\_R2\\_Guideline.pdf](http://www.ich.org/fileadmin/Public_Web_Site/ICH_Products/Guidelines/Quality/Q8_R1/Step4/Q8_R2_Guideline.pdf)
5. USFDA. PHARMACEUTICAL CGMPs FOR THE 21ST CENTURY — A RISK-BASED APPROACH - Final Report. US Food Drug Adm. 2004;(September).
6. Boukouvala F, Chaudhury A, Sen M, Zhou R, Mioduszewski L, Ierapetritou MG, et al. Computer-aided flowsheet simulation of a pharmaceutical tablet manufacturing process incorporating wet granulation. *J Pharm Innov.* 2013;8(1):11–27.
7. Gernaey K V., Gani R. A model-based systems approach to pharmaceutical product-process design and analysis. *Chem Eng Sci.* 2010;65(21):5757–69.
8. Conway SL, Lekhal A, Khinast JG, Glasser BJ. Granular flow and segregation in a four-bladed mixer. *Chem Eng Sci.* 2005;60(24):7091–107.
9. Stewart RL, Bridgwater J, Parker DJ. Granular flow over a flat-bladed stirrer. *Chem Eng Sci.* 2001;56(14):4257–71.
10. Radl S, Kalvoda E, Glasser BJ, Khinast JG. Mixing characteristics of wet granular matter in a bladed mixer. *Powder Technol.* 2010;200(3):171–89.
11. Sato Y, Nakamura H, Watano S. Numerical analysis of agitation torque and particle motion in a high shear mixer. *Powder Technol.* 2008;186(2):130–6.

12. Remy B, Khinast JG, Glasser BJ. Discrete element simulation of free flowing grains in a four-bladed mixer. *AIChE J.* 2009;55(8):2035–48.
13. Zhou YC, Yu AB, Stewart RL, Bridgwater J. Microdynamic analysis of the particle flow in a cylindrical bladed mixer. *Chem Eng Sci.* 2004;59(6):1343–64.
14. Zhou YC, Yu AB, Bridgwater J. Segregation of binary mixture of particles in a bladed mixer. In: *Journal of Chemical Technology and Biotechnology.* 2003. p. 187–93.
15. Stewart RL, Bridgwater J, Zhou YC, Yu AB. Simulated and measured flow of granules in a bladed mixer- A detailed comparison. *Chem Eng Sci.* 2001;56(19):5457–71.
16. Muerza S, Berthiaux H, Massol-Chaudeur S, Thomas G. A dynamic study of static mixing using on-line image analysis. *Powder Technol [Internet].* 2002;128(2–3):195–204. Available from: [http://apps.isiknowledge.com/full\\_record.do?product=WOS&search\\_mode=GeneralSearch&qid=16&SID=X2MbhmHAhEnGKAIBjmF&page=4&doc=31](http://apps.isiknowledge.com/full_record.do?product=WOS&search_mode=GeneralSearch&qid=16&SID=X2MbhmHAhEnGKAIBjmF&page=4&doc=31)
17. Marikh K, Berthiaux H, Mizonov V, Barantseva E. Experimental study of the stirring conditions taking place in a pilot plant continuous mixer of particulate solids. In: *Powder Technology.* 2005. p. 138–43.
18. Allison G, Cain YT, Cooney C, Garcia T, Bizjak TG, Holte O, et al. Regulatory and quality considerations for continuous manufacturing May 20-21, 2014 continuous manufacturing symposium. Vol. 104, *Journal of Pharmaceutical Sciences.* 2015. p. 803–12.
19. Pernenkil L, Cooney CL. A review on the continuous blending of powders. Vol. 61, *Chemical Engineering Science.* 2006. p. 720–42.
20. Portillo PM, Muzzio FJ, Ierapetritou MG. Modeling and designing powder mixing processes utilizing compartment modeling. *Comput Aided Chem Eng.* 2006;21(C):1039–44.
21. Portillo PM, Ierapetritou MG, Muzzio FJ. Characterization of continuous convective powder mixing processes. *Powder Technol.* 2008;182(3):368–78.
22. Engisch WE, Muzzio FJ. Method for characterization of loss-in-weight feeder equipment. *Powder Technol.* 2012;228:395–403.
23. Fonteyne M, Vercruyse J, De Leersnyder F, Van Snick B, Vervaeke C, Remon JP, et al. Process Analytical Technology for continuous manufacturing of solid-dosage forms. Vol. 67, *TrAC - Trends in Analytical Chemistry.* 2015. p. 159–66.
24. Vanarase AU, Järvinen M, Paaso J, Muzzio FJ. Development of a methodology to estimate error in the on-line measurements of blend uniformity in a continuous powder mixing process. *Powder Technol [Internet].* 2013;241:263–71. Available

- from: <http://dx.doi.org/10.1016/j.powtec.2013.02.012>
25. Simonaho S-P, Ketolainen J, Ervasti T, Toiviainen M, Korhonen O. Continuous manufacturing of tablets with PROMIS-line – Introduction and case studies from continuous feeding, blending and tableting. *Eur J Pharm Sci* [Internet]. 2016;90:38–46. Available from: <http://www.sciencedirect.com/science/article/pii/S0928098716300367>
  26. Danckwerts P V. Continuous flow systems: Distribution of residence times. *Chem Eng Sci*. 1953;2:1–13.
  27. Gao Y, Muzzio FJ, Ierapetritou MG. A review of the Residence Time Distribution (RTD) applications in solid unit operations. *Powder Technol* [Internet]. 2012;228:416–23. Available from: <http://dx.doi.org/10.1016/j.powtec.2012.05.060>
  28. Muller FL, Latimer JM. Anticipation of scale up issues in pharmaceutical development. *Comput Chem Eng*. 2009;33(5):1051–5.
  29. Plumb K. Continuous Processing in the Pharmaceutical Industry: changing the mind set. *Chem Eng Res Des*. 2005;(June):730–8.
  30. Schaber SD, Gerogiorgis DI, Ramachandran R, Evans JMB, Barton PI, Trout BL. Economic analysis of integrated continuous and batch pharmaceutical manufacturing: A case study. Vol. 50, *Industrial and Engineering Chemistry Research*. 2011. p. 10083–92.
  31. Berthiaux H, Marikh K, Gatumel C. Continuous mixing of powder mixtures with pharmaceutical process constraints. *Chem Eng Process Process Intensif*. 2008;47(12):2315–22.
  32. Portillo PM, Ierapetritou MG, Muzzio FJ. Effects of rotation rate, mixing angle, and cohesion in two continuous powder mixers-A statistical approach. *Powder Technol* [Internet]. 2009;194(3):217–27. Available from: <http://dx.doi.org/10.1016/j.powtec.2009.04.010>
  33. Harwood CF, Walanski K, Luebcke E, Swanstrom C. The performance of continuous mixers for dry powders. *Powder Technol*. 1975;11(3):289–96.
  34. Marikh K, Berthiaux H, Gatumel C, Mizonov V, Barantseva E. Influence of stirrer type on mixture homogeneity in continuous powder mixing: A model case and a pharmaceutical case. *Chem Eng Res Des*. 2008;86(9):1027–37.
  35. Muzzio FJ, Robinson P, Wightman C, Dean Brone. Sampling practices in powder blending. Vol. 155, *International Journal of Pharmaceutics*. 1997. p. 153–78.
  36. Berman J, Schoeneman A, Shelton JT. Unit Dose Sampling: A Tale of two Thieves. *Drug Dev Ind Pharm* [Internet]. 1996;22(11):1121–32. Available from:

- <http://www.informaworld.com/10.3109/03639049609065948>
37. Hausman DS, Cambron RT, Sakr A. Application of Raman spectroscopy for on-line monitoring of low dose blend uniformity. *Int J Pharm.* 2005;298(1):80–90.
  38. Tomuță I, Iovanov R, Bodoki E, Leucuța SE. Quantification of meloxicam and excipients on intact tablets by near infrared spectrometry and chemometry. *Farmacia.* 2010;58(5):559–71.
  39. Saerens L, Dierickx L, Lenain B, Vervaet C, Remon JP, Beer T De. Raman spectroscopy for the in-line polymer-drug quantification and solid state characterization during a pharmaceutical hot-melt extrusion process. *Eur J Pharm Biopharm.* 2011;77(1):158–63.
  40. Wahl PR, Fruhmann G, Sacher S, Straka G, Sowinski S, Khinast JG. PAT for tableting: Inline monitoring of API and excipients via NIR spectroscopy. *Eur J Pharm Biopharm.* 2014;87(2):271–8.
  41. Liew C V., Karande AD, Heng PWS. In-line quantification of drug and excipients in cohesive powder blends by near infrared spectroscopy. *Int J Pharm.* 2010;386(1–2):138–48.
  42. Lai CK, Cooney CC. Application of a Fluorescence Sensor for Miniscale On-line Monitoring of Powder Mixing Kinetics. *J Pharm Sci.* 2004;93(1):60–70.
  43. Fonteyne M, Soares S, Vercruyssen J, Peeters E, Burggraeve A, Vervaet C, et al. Prediction of quality attributes of continuously produced granules using complementary pat tools. *Eur J Pharm Biopharm.* 2012;82(2):429–36.
  44. Roggo Y, Chalou P, Maurer L, Lema-Martinez C, Edmond A, Jent N. A review of near infrared spectroscopy and chemometrics in pharmaceutical technologies. Vol. 44, *Journal of Pharmaceutical and Biomedical Analysis.* 2007. p. 683–700.
  45. Wang I-C, Lee M-J, Seo D-Y, Lee H-E, Choi Y, Kim W-S, et al. Polymorph transformation in paracetamol monitored by in-line NIR spectroscopy during a cooling crystallization process. *AAPS PharmSciTech* [Internet]. 2011;12(2):764–70. Available from:  
<http://www.ncbi.nlm.nih.gov/pubmed/21671200>  
<http://www.pubmedcentral.nih.gov/articlerender.fcgi?artid=PMC3134639>
  46. Rantanen J, Jørgensen a, Räsänen E, Luukkonen P, Airaksinen S, Raiman J, et al. Process analysis of fluidized bed granulation. *AAPS PharmSciTech.* 2001;2(4):21.
  47. Rosas JG, de Waard H, De Beer T, Vervaet C, Remon JP, Hinrichs WLJ, et al. NIR spectroscopy for the in-line monitoring of a multicomponent formulation during the entire freeze-drying process. *J Pharm Biomed Anal.* 2014;97:39–46.
  48. Berntsson O, Danielsson LG, Lagerholm B, Folestad S. Quantitative in-line



- monitoring of powder blending by near infrared reflection spectroscopy. *Powder Technol.* 2002;123(2–3):185–93.
49. Sekulic SS, Wakeman J, Doherty P, Hailey PA. Automated system for the on-line monitoring of powder blending processes using near-infrared spectroscopy. Part II. Qualitative approaches to blend evaluation. Vol. 17, *Journal of Pharmaceutical and Biomedical Analysis*. 1998. p. 1285–309.
  50. Sekulic SS, Ward HW, Brannegan DR, Stanley ED, Evans CL, Sciavolino ST, et al. On-line monitoring of powder blend homogeneity by near-infrared spectroscopy. *Anal Chem.* 1996;68(3):509–13.
  51. Rowe, Raymond C; Sheskey, Paul J; Cook, Walter G; Fenton ME. *Handbook of Pharmaceutical Excipients*. Seventh Ed. Pharmaceutical Press; 2012.
  52. Kruse J, Abraham M, Amelung W, Baum C, Bol R, Kühn O, et al. Innovative methods in soil phosphorus research: A review. Vol. 178, *Journal of Plant Nutrition and Soil Science*. 2015. p. 43–88.
  53. Abdi D, Tremblay GF, Ziadi N, Belanger G, Parent LE. Predicting Soil Phosphorus-Related Properties Using Near-Infrared Reflectance Spectroscopy. *Soil Sci Soc Am J.* 2012;76(6):2318–26.
  54. Malley DF, Yesmin L, Wray D, Edwards S. Application of near-infrared spectroscopy in analysis of soil mineral nutrients. *Commun Soil Sci Plant Anal.* 1999;30(7–8):999–1012.
  55. Chang C-W, Laird DA, Mausbach MJ, Hurburgh CR. Near-Infrared Reflectance Spectroscopy–Principal Components Regression Analyses of Soil Properties. *Soil Sci Soc Am J.* 2001;65:480–90.
  56. Pandolfini C, Bonati M. A literature review on off-label drug use in children. Vol. 164, *European Journal of Pediatrics*. 2005. p. 552–8.
  57. Coperion K-Tron Website. 2016; Available from: <http://www.ktron.pt/process-equipment/feeders/technology/batch-feeding.cfm>
  58. Coperion K-Tron Website. 2016; Available from: <http://www.ktron.pt/process-equipment/feeders/catalog/feeder-specs/T20-Twin-Screw-Loss-in-weight-Feeder.cfm>
  59. Hosokawa Micron B.V. website. 2016; Available from: <http://www.hosokawa-micron-bv.com/technologies/mixing-equipment/continuous-mixing-solutions/modulomix-continuous-modular-mixer.html>